EFFECT OF PROCESS PARAMETERS ON MECHANICAL PROPERTIES OF HIGH PRESSURE DIE CAST MAGNESIUM AZ91 COMPONENTS

A THESIS SUBMITTED TO
THE GRADUATE SCHOOL OF NATURAL AND APPLIED SCIENCES
OF
MIDDLE EAST TECHNICAL UNIVERSITY

BY

IŞIK YILMAZ OKCU

IN PARTIAL FULFILLMENT OF THE REQUIREMENTS
FOR
THE DEGREE OF MASTER OF SCIENCE
IN
METALLURGICAL AND MATERIALS ENGINEERING

OCTOBER 2011

Approval of the thesis:

EFFECT OF PROCESS PARAMETERS ON MECHANICAL PROPERTIES OF HIGH PRESSURE DIE CAST MAGNESIUM AZ91 COMPONENTS

submitted by **IŞIK YILMAZ OKCU** in partial fulfillment of the requirements for the degree of **Master of Science in Department of Metallurgical and Materials Engineering, Middle East Technical University** by,

Prof. Dr. Canan Özgen _____
Dean, Graduate School of **Natural and Applied Sciences**

Prof. Dr. Tayfur Öztürk _____
Head of Department, **Metallurgical and Materials Engineering**

Prof. Dr. Ali Kalkanlı _____
Supervisor, **Metallurgical and Materials Engineering Dept., METU**

Examining Committee Members:

Prof. Dr. Ekrem Selçuk _____
Metallurgical and Materials Engineering Dept., METU

Prof. Dr. Ali Kalkanlı _____
Metallurgical and Materials Engineering Dept., METU

Prof. Dr. Rıza Gürbüz _____
Metallurgical and Materials Engineering Dept., METU

Assoc. Prof. Dr. Arcan Dericioğlu _____
Metallurgical and Materials Engineering Dept., METU

Assoc. Prof. Dr. Nuri Durlu _____
Mechanial Engineering Dept., TOBB University of Economics and Technology

Date: 25.10.2011

I hereby declare that all information in this document has been obtained and presented in accordance with academic rules and ethical conduct. I also declare that, as required by these rules and conduct, I have fully cited and referenced all material and results that are not original to this work.

Name, Last name: Işık Yılmaz OKCU

Signature:

ABSTRACT

EFFECT OF PROCESS PARAMETERS ON MECHANICAL PROPERTIES OF HIGH PRESSURE DIE CAST MAGNESIUM AZ91 COMPONENTS

Okcu, Işık Yılmaz

M.Sc., Department of Metallurgical and Materials Engineering

Supervisor: Prof. Dr. Ali Kalkanlı

October 2011, 107 pages

Before beginning the experimental work of this study, a magnesium high pressure die casting facility is set up to manufacture magnesium cast parts for defence industry. In this thesis two components are cold chamber high pressure die casted using magnesium alloy AZ91 as raw material, and one component was manufactured using both aluminium alloy A.413, and magnesium alloy AZ91.

Mechanical properties of high pressure die casting parts depend on various parameters such as, thickness of the cast part, position of the cast part in the cavity, molten metal temperature, die temperature, piston speeds, and injection pressure. The aim of this study is to investigate the effects of section thickness of the cast part, position of the cast part in the die cavity, piston speeds, and molten metal temperature on mechanical properties of magnesium die cast parts. Tensile properties of products from Al A.413 and Mg AZ91 alloys are also compared.

Casting analysis software is used to simulate filling and temperature evolution of three different casting components. Piston speeds are first calculated from equations in the literature and then verified by using the software. Specimens for microstructural investigation, and mechanical tests are machined directly from the mass produced parts. Optical microscopy, and scanning electron microscopy investigations are carried out for grain size and porosity determination. Tensile tests are conducted for yield strength, ultimate tensile strength, and % elongation values. The results of casting analysis software simulations, grains size investigations, porosity investigations, and tensile tests are correlated to each other.

Optimum piston speeds, optimum molten metal temperatures are observed, effect of grain size and porosity concentrations on the effect of mechanical properties are

compared. Weight of cast parts produced from Mg AZ91 are 35 % lower than that of Al A.413 parts. However, ultimate tensile strength of the cast parts produced from Mg AZ91 are found to be similar to the aluminium parts.

Keywords: High pressure die casting, Mg AZ91 alloy, section thickness, melt tempertaure, mechanical properties

ÖZ

YÜKSEK BASINÇLI DÖKÜM YÖNTEMİYLE MAGNEZYUM AZ91 ALAŞIMINDAN ÜRETİLMİŞ PARÇALARDA PROSES PARAMETRELERİNİN MEKANİK ÖZELLİKLERE ETKİSİ

Okcu, Işık Yılmaz

Yüksek Lisans, Metalurji ve Malzeme Mühendisliği Bölümü

Tez Yöneticisi: Prof. Dr. Ali Kalkanlı

Ekim 2011, 107 sayfa

Çalışmanın deneysel kısmı başlamadan önce, savunma sanayine yönelik üretim yapacak bir magnezyum basınçlı döküm üretim tesisi kurulmuştur. Bu tezde iki ürün soğuk kamara yüksek basınçlı döküm yöntemi kullanılarak magnezyum AZ91 alaşımından, bir ürün ise hem aluminyum A.413 alaşımından hem magnezyum AZ91 alaşımından üretilmiştir.

Yüksek basınçlı döküm yöntemiyle üretilmiş parçaların mekanik özellikleri parçanın cidar kalınlığı, parçanın kalıp boşluğu içerisindeki pozisyonu, eriyik metal sıcaklığı, kalıp sıcaklığı, piston hızları ve enjeksiyon basıncı gibi çeşitli parametrelere bağlıdır. Bu çalışmanın amacı cidar kalınlığının, parçanın kalıp boşluğu içerisindeki pozisyonunun, piston hızlarının ve eriyik metal sıcaklığının magnezyumdan yüksek basınçlı döküm tekniğiyle üretilmiş parçaların mekanik özelliklerine etkisini incelemektir. Al A.413 ve Mg AZ91 alaşımlarından üretilmiş parçaların çekme özellikleri ayrıca karşılaştırılmıştır.

Üç döküm parçanın dolum ve sıcaklık analizleri döküm analizi yazılımı kullanılarak simüle edilmiştir. Piston hızları önce literatürdeki denklemler yardımıyla hesaplanmış daha sonra yazılımda doğrulanmıştır. Mikroyapı ve mekanik test numuneleri doğrudan seri üretilmiş parçalar üzerinden alınmıştır. Tane boyutu ve döküm boşluğu çalışmaları optik mikroskop ve taramalı elektron mikroskobu ile yapılmıştır. Akma mukavemeti, kopma mukavemeti ve % uzama değerleri için çekme testleri yapılmıştır. Döküm analizi simülasyonu, tane boyutu incelemeleri, döküm boşluğu incelemeleri ve çekme testi sonuçları birbirleriyle ilişkilendirilmiştir.

Optimum piston hızları, optimum eriyik metal sıcaklıkları bulunmuş, tane boyutu ve döküm boşluğu yüzdesinin mekanik özelliklere etkisi karşılaştırılmıştır. Mg AZ91 alaşımından üretilmiş döküm parçalarının ağırlıkları, Al A.413 alaşımından üretilmiş parçadan % 35 düşüktür. Buna rağmen Mg AZ91 alaşımından üretilmiş ürünlerin kopma mukavemeti yalnızca aluminyum ürünlerinkine yakındır.

Anahtar kelimeler : Yüksek basınçlı döküm, Mg AZ91 alaşımı, cidar kalınlığı, eriyik sıcaklığı, mekanik özellikler

ACKNOWLEDGEMENTS

First of all, the author would like to express his deep appreciation to his supervisor, Prof. Dr. Ali Kalkanlı for his encouragement, guidance, and support during the study.

The author is grateful to the owners of Rutaş Die Casting Mold and Machinery Co., Ltd. , Ruhi Taşkesen, and Deniz Taşkesen, who offered invaluable guidance throughout the manufacturing process. He is also thankful to the employees of Rutaş Die Casting Mold and Machinery Co., Ltd.

The author would like to express his deepest gratitude to his parents Yusuf Okcu, Zühal Okcu, his brother Ilgaz Doğa Okcu, and Esra Uyar for their unconditional support in any condition.

Also, special thanks to Murat Kamberoğlu, and Onur Demirel for their friendship, help and support.

This research was carried out within the scope of the TÜBİTAK KOBİ AR-GE BAŞLANGIÇ DESTEK PROGRAMI. The author would like to acknowledge TUBITAK for the financial support.

TABLE OF CONTENTS

LIST OF TABLES

TABLES

LIST OF FIGURES

FIGURES

CHAPTER 1

INTRODUCTION

There is a growing need of light materials in automotive, aerospace, defence, and electronics industries due to environmental effects and limitations of the industry. By reducing weight, fuel consumption of the automobiles are decreased, minimizing green house gas emissions. Reduction of weight of the military equipment increases device carrying capacity of soldiers or military vehicles. Consumer electronics, such as cameras, laptops, and mobile phones create new markets by innovative design possibilities.

Using magnesium alloys in exchange of aluminium alloys which are recently used, makes the products 30-40% lighter without expensing mechanical properties. In recent years magnesium high pressure die cast products are widely used mainly because of their low density, comparable mechanical properties with respect to aluminium and ease of production. Die casting of magnesium alloys offer economical advantages that other production techniques cannot. As densities of magnesium die casting alloys are much lower than that of aluminium alloys, with same weight of raw materials more magnesium products can be manufactured. Magnesium die casting is a suitable process for mass production as it is easily automated. Differences in thermal properties of aluminium and magnesium alloys yield high cooling rate formagnesium alloys which makes the cast part to be cooled fast, therefore higher rate of production is available.

Despite high pressure die casting seem to be a straightforward production method, there are many factors affecting the product quality and mechanical properties of the cast parts. That factors are closely related to part- die design such as section thickness and positon of the cast part in the die cavity . But the key factors affecting the product quality is process paramaters. Process parameters are molten metal temperature, die temperature, cavity fill time, piston speed, and intensification

pressure [1]. The aim of this study is to investigate the effects of section thicknes of the cast part, position of the cast part in the die cavity, piston speeds, and molten metal temperature on mechanical properties of magnesium die cast parts.

High pressure die casting of magnesium alloys is a high technology production method which is used for decades. However, no attempt was made ever before to die cast magnesium alloys as mass production in Turkey. In order to increase the productivity and quality of Turkish industry, production methods involving high technology should be supported. An investment is made to an aluminium high pressure die casting foundry in Ankara, Turkey to cast magnesium alloys within the scope of this thesis. The samples investigated in the experiments are machined from the mass production parts manufactured in the facility.

CHAPTER 2

THEORY and LITERATURE SURVEY

2.1 High Pressure Die Casting

High pressure die casting (hpdc) is the dominant production method in industry for Mg alloys. Magnesium market share can be seen in figure 2.1 and magnesium consumption as hpdc raw material can be seen in figure 2.2. High pressure die casting is a near-net shape casting process for the manufacturing of high fluidity and low melting point materials like Al, Mg, and Zn alloys [2]. In the process, hpdc machines are used, which consists of several components. The main components of hpdc machines are shot sleeve, shot cylinder, toggle clamps, hydraulic system, moving and stationary platens [3]. A die casting mold having two die halves is machined and placed in between the moving and stationary platens. The mold does not only operate as a casting cavity but also dissipiates superheat of the molten metal, absorbs the injection stress, provide a vent for trapped air, and eases the removal of the cast part[4]. Hot work tool steels are used as mold materials because of their heat resistance, high temperature toughness, and high temperature wear resistance [5]. During a cold chamber hpdc cycle, initially two pre-heated die halves are closed, liquid metal is poured into the shot sleeve and injected into the die cavity at very high velocity and under very high pressures. After a short cooling period in the vicinity of seconds, die halves are opened by the help of toggle clamps and casting product is taken out of the mold, then mold is cleaned and lubricated for the other casting cycle. Cycling time of a casting process depends on product geometry, but mostly high pressure die casting cycles last shorter than a minute. Because of this high productivity rate, hpdc is suggested as the shortest distance between raw material and casting produc[3]. Casting period is very short but it includes very complex issues. The piston of the shot cylinder initially moves slowly

until the molten metal fills the runner, after the runner is filled and molten metal reaches the gate of the casting cavity, piston speeds up. Velocity of the melt at the entering point of die cavity is maximum, filling of the cavity continues with constant velocity. When the cavity is filled, an intesification pressure is applied on the molten metal to improve soundness and quality of the castings[2]. Another issue is the air left in casting cavity and shot sleeve. Obviously there will be some amount of air in the shot sleeve when the metal is poured and also some amount of air is left in the mold when die halves are closed. Entrapment of air in the cast part is impossible to be avoided but air can be drawn into specific grooves of the casting cavity which are called overflows by theory of fluids knowledge and proper die design [6]. There are also casting softwares used for simulating filling process .

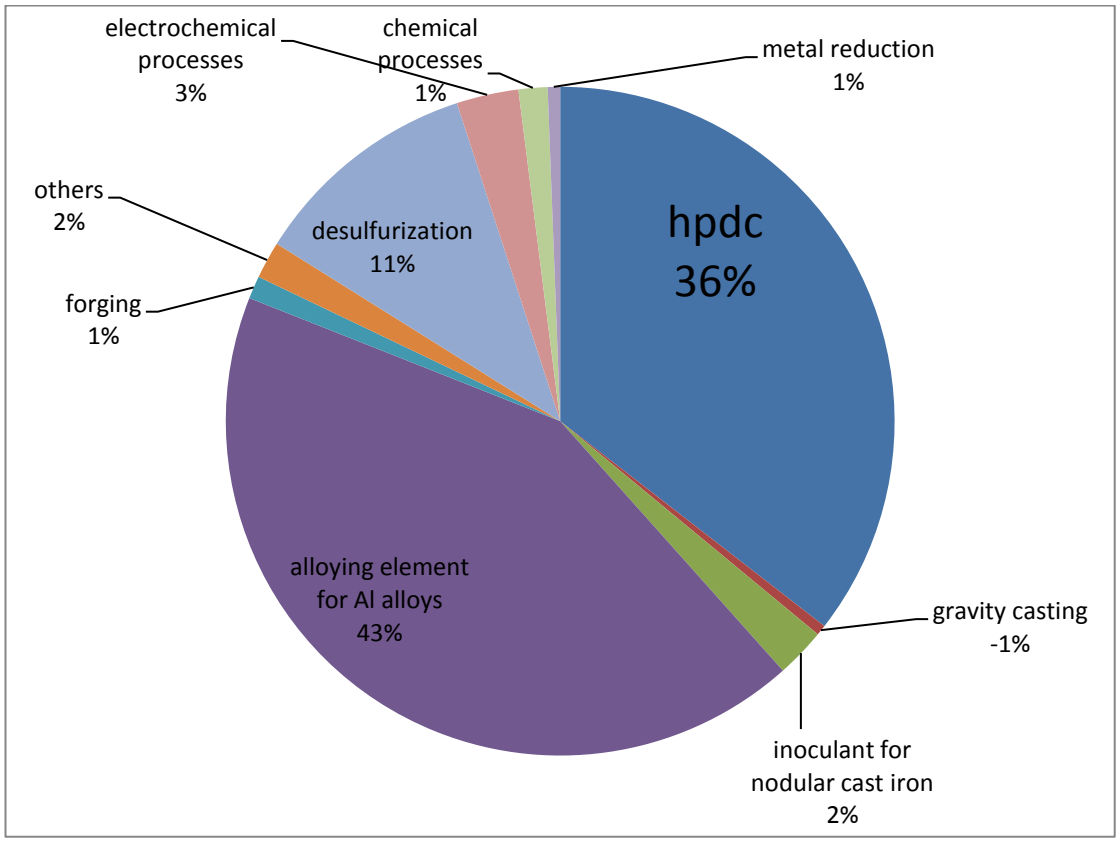

Figure 2.1 : Market share of magnesium in the year 2000 [6]

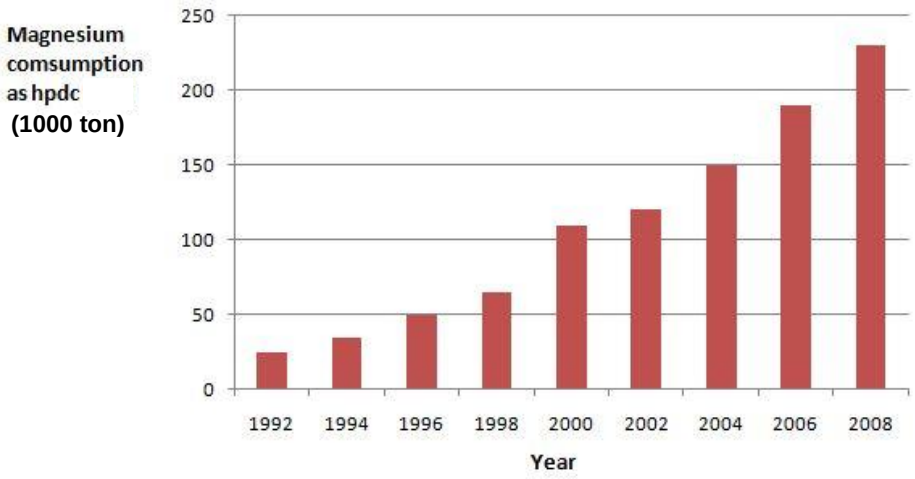

Figure 2.2 : Worldwide magnesium consumption as high pressure die casting raw material [6]

2.2 Comparison of Hpdc with Other Casting Processes

High pressure die casting is a sophisticated casting method. It offers low cost for high volumes of casting parts, high quality of products both in visual and microstructural point of view. The process also have limitations. The advantages and disadvantages of hpdc over other casting methods are given below .

2.2.1 Advantages of hpdc process

- High production rate
- High production amount with single die
- Low cost for a single product in high production volumes
- High precision, good dimensional accuracy and casting tolerances
- High surface quality
- Fine microstructure due to fast cooling
- Possibility of designing thin sections and complex parts
- Avoided secondary machining [7]

2.2.2 Disadvantages of hpdc process

- Limited range of alloys
- Gas pores because of entrained air
- Impossible heat treatment because of gas pores
- Limited size of casting parts
- Thick walls castable only to a limited degree
- High tooling costs [7]

2.3 Process

High pressure die casting is simply a casting process, letting liquid metal to solidify in a shaped cavity. Different aspects of high pressure die casting process from other processes are the high speed of liquid metal, and the high pressure exerted on molten metal when it is in the die. Speed - pressure diagram of hpdc can be seen in figure 2.3 which shows speed of the piston and pressure exerted on the cast part during filling.

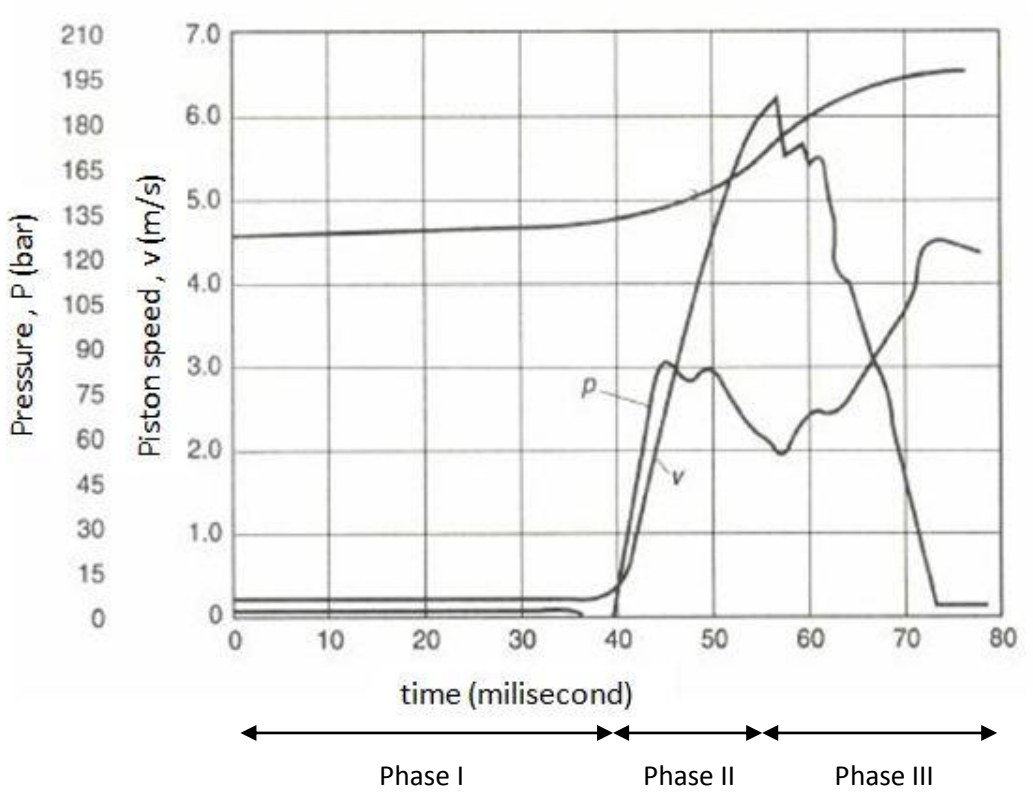

Figure 2.3 : Speed – pressure diagram of high pressure die casting process [3]

This aspects offer some advantages and also have some drawbacks. High pressure die casting offers very high production rate, most high pressure die casting cycles last no more than a minute. Cycle time mainly depends on product geometry. High pressure die casting can be investigated under two basic processes: hot chamber and the cold chamber processes[3]. In hot chamber die casting process some portion of the metal injection machine is immersed into the liquid metal througout the process, this is an advantage for keeping the cycle time to a minimum as travel distance of the liquid metal is very short. But close contact of the molten metal with the casting machine also have a drawback, degradataion of the injection system[3]. In cold chamber die casting process molten metal is ladled or dosed into the shot sleeve for each cycle so only shot sleeve of the die casting machine is affected by the high temperatures. The procedure of casting is same in both processes, first liquid metal is metered into the shot sleeve, which is injected into the die through a runner system under high pressure. To achieve quality high pressure is maintained during solidification. After the alloy is solidified, die halves are opened and the product is ejected from the die . Product removal can be manual or automated. Before closing the die for the next cycle, dies are air blasted for cleaning, and lubricated to facilitate ejection. Excess metal such as gating and overflows are trimmed and melted for recyling[4].

2.4 Injection of Liquid Metal

Injection of liquid metal is an important consideration for the quality of castings. In die casting process, shot sleeve is partially filled to avoid splashing liquid outside of shot sleeve. Then the piston (plunger) moves relatively slow not to form waves and/or entrap air. The movement is called the first phase (pre-filling phase). The low velocity of the piston enables air to escape via overflows and air vents. In the second phase (mold filling phase), the piston rapidly accelerates the liquid up to proper gate velocity. Second phase is usually shorter than the first phase, and venting of die cavity is not possible in this time interval. The third phase (final pressure phase) starts at the time just after the entry of liquid into the cavity. In that phase high pressure is applied on the solidifying metal called intensification pressure to obtain sound cast parts[8][9]. Phase times can be seen in Figure 2.3.

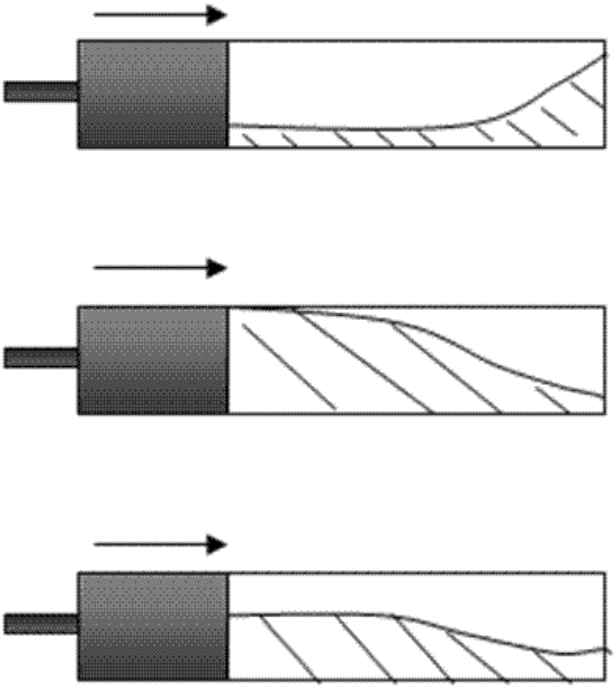

Figure 2.4 : Entrapment of air with a- high, b- low, and c- optimum first phase velocities [10]

Filing time of magnesium alloys is in the vicinity of miliseconds and formulized as :

$$t_f = 0.03409\, t\, [(T_m - T_f + 2.5S)/(T_f - T_d)] \tag{2.1}$$

Where t_f is the die filling time in seconds. t is the average thickness of the cast part in mm. T_m , T_d, and T_f are the melting, die, and fluidity temperatures of the casting alloys respectively. T_f is the fluidty temperature of the alloy which can be approximated as 500 ºC for Mg AZ91 alloy. S is the fraction of solid entering into the die. Fraction of solids are mentioned as externally solidified crystals. This phenomena will be explained in chapter 2.15. Pre-filling phase velocity is also named as V_1, while mold filling phase velocity is abbreviated as V_2 . They are calculated by using the below equations:

$$V_1 = K\,(1 - f_{shotsleeve})\,\sqrt{\emptyset_{piston}} \tag{2.2}$$

Where K is a proportionality constant with 3,634 $m^{1/2}$ / s value, $f_{shotsleeve}$ is the fraction of the shot sleeve filling, and $\emptyset_{piston}$ is the diameter of the piston in meters.

$$V_2 = (4v_{casting})/\emptyset_{piston}^2 t_f \pi \tag{2.3}$$

Where $v_{casting}$ is the total volume of the cast part in m^3 , t_f is the filling time obtained from equation 2.1, and $\emptyset_{piston}$ is the diameter of the piston in meters[1].

2.5 High Pressure Die Casting Machines

Die casting machines are usually rated by their die closing force capacity. Generally unit of tonnes for clamping forces is used. Two types of die casting machines are widely used today: hot chamber and cold chamber. Both machines are horizontally oriented. Experiments in this thesis were carried out with cold chamber die casting machines so, details will be given only for cold chamber hpdc machines. Both machines are really a clamp on one end to support and move the dies, and an injection unit on the other hand to supply liquid metal to the die. This is why hot chamber and cold chamber machines have the same components with slight differences. The components which will be mentioned are: machine base, the platens, tie bars, toggle linkage system, power units, hydraulic pumps and shot end.

Machine base supports the structure of the machine. It must be leveled to the ground precisely to avoid moving of the machine. Before leveling the machine base a concrete platform is build and machine is fastened onto the platform. The base is mainly a steel structure to serve as a frame for all components and also a tank for hyraulic fluid. The base must be strong to avoid bending, and rigid to avoid twisting under high pressures applied on it during the casting cycle.

There are three platens on die casting machines, which are basically steel plates supporting the mold mounted on them. Stationary platen is directly attached to base

of the machine and located between the shot end and the die. Movable platen is in the middle of the machine opening and closing the by sliding between rear and stationary platens, also hold the ejector pins. Rear platen is assembled at the clamp end of the machine. The toggle linkage system is mounted on one side of rear platen which is closer to the shot end, the other side of rear platen is occupied with hydraulic closing cyclinder. Rear platen also moves as movable platen but displaces little just to raise or lower the clamping force of the die casting machine. Platens are the most vulnerable sections of the machine because they are heated up and clamped under high pressures during casting cycles. Although the platens are vulnerable, they are the most dangerous part to human extremities as they are clamping the dies.

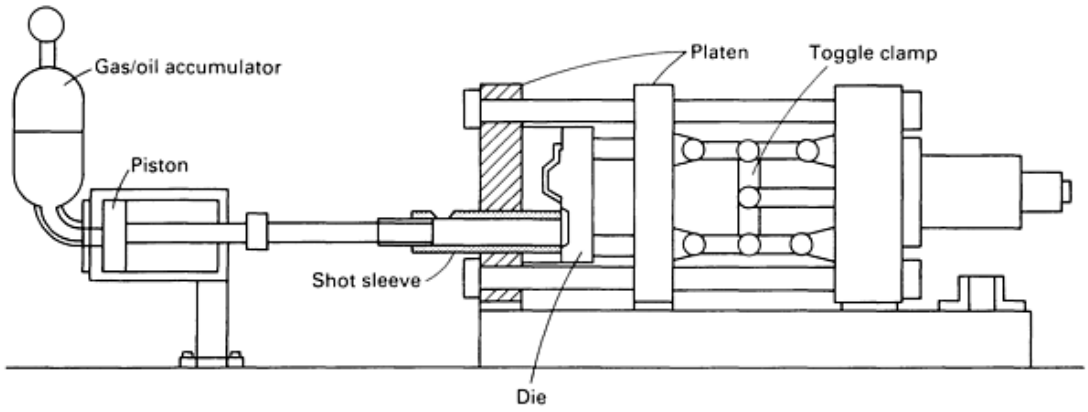

Figure 2.5 : Schematic view of a cold chamber die casting machine [2]

Tie bars are responsible for the true position of the platens. Moving plates slide along the tie bars during cycles. Their length determines the locking capacity of die casting machines. There are usually four tie bars assembled on die casting machines symmetrically. Center of tie bars is an important factor regarding die casting design, Moment of inertia of a die casting product including runners and overflows should be as close as possible to the center of tie bars, so that the pressure applied distributed equally.

Toggle linkage system is connected to the movable and rear platens for opening and closing the die halves. When the toggle linkage retracts, die halves are opened and when the toggle linkage extends, die halves are opened. It is a simple lever

mechanism to increase the work done with respect to the force applied. As the required force decreases, power and size of the die closing cylinder decreases.

Power of modern high pressure die casting machines generally supplied by electric motors. Hydraulic fluid is moved and converted into energy by valves on the machine. One electric motor is enough for low locking force machines, however for high locking capacity machines more than one electric motor is needed. Power units are sine quo non of high pressure die casting machines, because of this reason they should be kept clean all the time.

There are at least two hydraulic pumps on a die casting machine. Hydraulic pumps pressurizes the hydraulic fluid travelling inside the machine to drive the necessary parts. The flow of fluid from the reservoir tank to the pipes is controlled by valves. Cleanliness of the hydraulic fluid is also important as it is travelling all around the machine.

Shot end of the machine injects the molten alloy to the die casting cavity, shot end is the only component different in hot chamber and cold chamber machines. In hot chamber machines, there is a mechanism called gooseneck which resposible for injection of the liquid metal. The mechanism is immersed in the melt all the time so, the molten metal should not be corrosive to the gooseneck. The piston is directed downward to the ground on the metal bath, when the piston moves up, liquid metal enters into the gooseneck from an inlet, then piston pressurizes the molten metal and flows it through the nozzle to the die cavity[3] .

Hot chamber die casting machines are heated up easily because metal bath is always very close to the machine. This offers advantages of very short casting cycles and no heat loss. Hot chamber process need less pressure but limited to the metals which do not corrode the gooseneck. Altough, process cycles are shorter for hot chamber machines, cycles of cold chamber process can easily be automated by use of robot arms which reduces cycle times and labour cost. Cold chamber machines can cast more complex and heavier products than hot chamber machines. Today there are hpdc machines in the industry with clamping forces above 2500 tonnes. For casting of BMW Al-Mg composite crankcase 4000 tonnes hpdc machines are used [10].

2.6 Hpdc Dies

Die construction is the key factor of product quality in high pressure die casting. Beside operating as a casting cavity, dies also dissipiate superheat of the melt, absorbs injection stress, provide a vent for trapped air, and eases the removal of the cast part [4]. The dies are usually machined from hot work tool steel blocks. Machining of these materials are expensive because of the high hardness values. Rough machining operation is carried out on prehardened blocks which are hardened to about 30 rockwell C value (HRC). Before the finishing machining operation dies are heat treated to relieve their stresses arised from machining. Finishing operation is done after stress relieving and dies are heat treated to 50 – 55 HRC for long service life[5][11].

2.6.1 Die construction

A complete die set can be seen in figure 2.6 which contains two die halves: cover die half (stationary die half) , and ejector die half (movable die half) . Negative of product shape is machined on two steel blocks after deciding parting plane of the die. Than that two cavity blocks are assembled to the retainer blocks which holds the die and some other components. Ejector plate contains the runners and gates which is the route of molten metal to the cavity, and holds the ejector pins to ease product removal from the die after each casting cycle. Dies also include channels for coolant liquid, and leader pins to fix the two halves when closing.

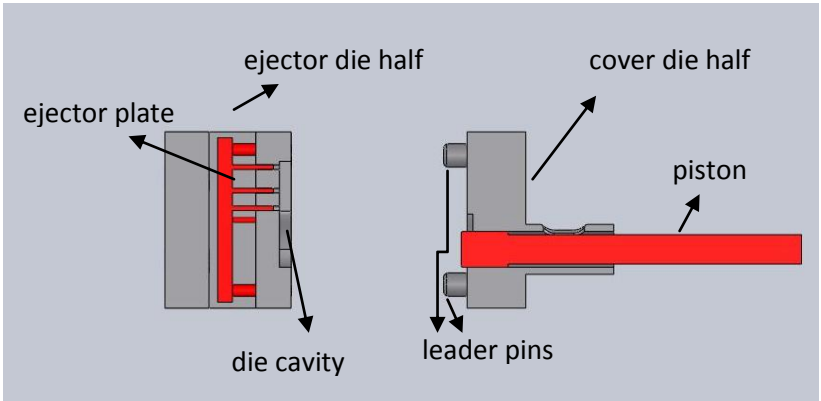

Figure 2.6 : Schematic view of a die set

Design of a die set depends on various parameters such as number of cavities, production amount, product geometry, capacity of hpdc machine, need for cores, mold parting line, location of ejector pins, and overlows. The materials for cavity

blocks, retainer blocks, ejector pins, shot sleeve and some other components are given in the table 2.1.

Table 2.1 : Materials and final hardness values of die components [2]

die component	material	hardness
cavity block	SAE 2344	45 HRC
cores	SAE 2344	45 HRC
retainer block	SAE 4140	30 HRC
ejector pins	SAE 1020	case harden
leader pins	SAE 1020	case harden
shot sleeve	SAE 2344	45 HRC

2.6.2 Die design

The most important factor of a quality die casting is proper die design. There are lots of parameters to design a die cavity. As Hpdc dies consist of two die halves, parting line of the mold should be considered first. Generally flat planes are selected as the mold parting lines, this facilitates the machining operation and thus decreases the cost. But complex parts of today's industry needs do not let such a simple mold parting line. There is a simple limit in designing of a die casting part. The details perpendicular to the mold parting line cannot be casted without steel cores. These steel cores can be mechanically or hydraulicaly movable. When die halves are closed, cores are in their position, melt is injected into the cavity, and after solidification cores are drawn back leaving the detail on the part. Another consideration is number of cavities. A die can be of single cavity or multiple cavity. This choice is mainly affected by production amount and core need of the product design. Identical or different cast parts can be drawn from multiple cavitiy dies. A die with two identical cavities can be seen in figure 2.7.

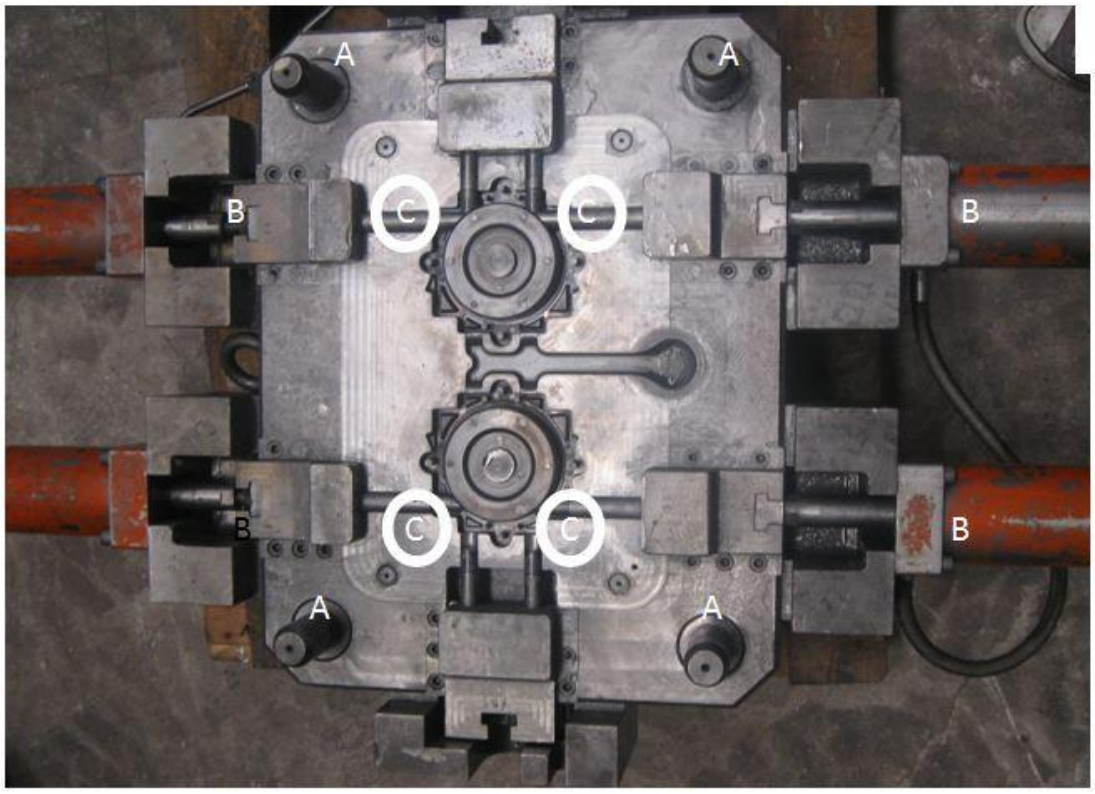

Figure 2.7 : Multiple cavity die showing a – leader pins, b –hydraulic pumps, c- cores

Drawing of a part from the die should be favoured by draft angles. 1 to 5º angles are given to all walls parallel to parting direction depending on geometry. Angle of inside surfaces must be twice of the outer surfaces of walls because the casting alloy reduces in volume during solidification. Another design limit of hpdc is undercuts, which is to be avoided at all cost because during opening of the die halves undercuts are impossible to be ejected. When designing of a hpdc die, location of ejector pins is an important criteria because they leave ejector pin marks on the casting part. If part to be produced is a decorative component, care must be taken about location of ejector pins.

2.7 Developments of High Pressure Die Casting

The processes semisolid casting, sequeeze casting, and low pressure die casting are generally evaluated as modifications on hpdc. But in this text they are treated as seperate methods of casting, because extensive differences with respect to hpdc are developed during the years in service. On the other hand vacuum assisted die casting just uses vacuum assistance on hpdc.

2.7.1 Vacuum assisted hpdc

Porosity is one of the most difficult defects to avoid in hpdc process. Voids are formed inside the casting parts due to shrinkage or air entrainment. Shrinkage porosity is minimized by application of pressure when the melt is solidifying in high pressure die casting process. Gas porosities however, cannot be removeed completely by conventional methods. The industry try to move porosity to different location in casting parts rather than eliminating it [6]. Gas porosity in die casting parts reduces mechanical properties dramatically. Also porosity leads to blistering during heat treatment, thus applications of die casting parts are limited to non-structural components which do not heat treatment [12]. Scientists develop vacuum die casting process recently. In the process, pressure lower than atmospheric pressure is created in the injection chamber and die cavity, reducing the air entrained by melt flow during molten metal injection. This enchancement in the conventional hpdc gives rise to production of larger castings with thin sections and availability of heat treatment to such part[12].

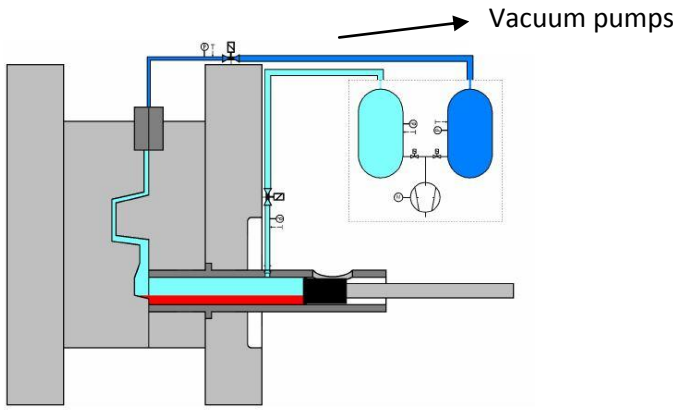

Figure 2.8 : Vacuum assisted die casting processes

2.8 HPDC defects

High Pressure die casting mainly differs from other casting methods by high flow rate of liquid, high cooling rate, and high pressures exerted on liquid metal during solidification. So other than regular casting defects there are some unique defects encountered in hpdc process. In this section casting defects will be clarified.

2.8.1 Gas related defects

This type of defects form voids in casting parts. The main reason of gas porosity is the air entrapped in die cavity during closing of the dies. Hydrogen and other gasses dissolved in melt also appear as gas porosity in high pressure die cast parts. In addition wrong selection of die lubricants may produce gas pores [13][14]. Dominating reason is the air entrapment in the die cavity so “gas pores” term will define pores resulted from air entrapment in this text. Gas pores have spherical shapes and are in micron level diameters [13].

2.8.2 Shrinkage defects

Volume of liquid metal decreases when solidifying, this is called shrinkage. Shrinkage occurs in regions where feeding of liquid metal is insufficient. This regions are the last solidifying regions locally, and they can be internal or on the surface of the cast part. Internal defects are intedendritic porosities, and blowholes. Interdendritic porosity forms between the dendrite arms, have crack like shapes, and are in micron levels. In hpdc liquid metal is pressurized during solidification however, complete removal of shrinkage pores is not possible [13][15]. Blowholes are relatively large depending on the volume of improper filled region. Sinks are the shrinkage defect that occurs on the surface of casting parts. Due to locally high rate of cooling, some areas shrink and leave sinks on the surface[14][16] .

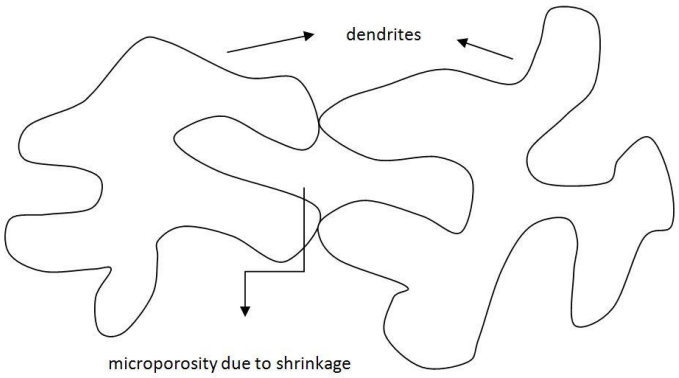

Figure 2.9 : Microporosity formation due to shrinkage between dendrite arms

2.8.3 Thermal contraction defects

Thermal contraction defects form during cooling and solidification of the molten metal because of the contraction stresses higher than UTS of the alloy. Cracks occur at low temperatures after ejection of the product from the die due to greater contraction of casting alloys with respect to die materials. Hot tears occurs in the solid portions of solidifying alloy when the local UTS is exceeded. Both cracks and hot tears usually occur in regions of concentrated stresses. Geometry of the cast part, for example perpendicular thin walls are stress concentration factors [14].

2.8.4 Filling defects

During filling of the liquid to the cavity, liquid or partially solidified metal flows can come into contact because of design related flaws, and cause metallurgical inhomogenities. Flow defects, lamination, and cold shut are major filling related defects. When a warmer liquid flow encounter with a partially solidified region, it try to flow around it. This flow defect results in a wrinkled surface on cast part[14][16].

2.8.5 Die – metal interaction defects

These type of defects generally depends on irregularities on the die due to long service life without maintanence. Thermal fatigue marks on the die , corrosion, and erosion of the die are such kind of defects. Die soldering is also a problem related to die. For hpdc of mangesium alloys, die soldering is not considered to be a major problem as reaction of magnesium alloys with steel dies is limited. Another problem is ejection marks on the cast part surface. Die designers should overcome this problem when desiging the product and locating the ejector pins [17] .

2.8.6 Undesired phases

Undesired phases in the cast part developed because of low quality raw materials or improper dross removal. Also liquid metal interaction with environment (e.g. die lubricant) can be a reason[14]. This type of problems can be eliminated by quality assurance, and continuous quality control of the ingots to be melted.

2.9 Set-up of a magnesium alloy hpdc foundry

High pressure die casting foundries have numerous casting machines of different sizes, melting furnaces, molten metal transport appliances, tools for machining dies (die construction can also be outsourced) and various other devices [18]. Hpdc foundries are easy to automate Robots can be used to transport molten metal, to eject the product out of die casting cavity, and to remove overflows. Devices other than the ones come in contact with molten magnesium are common for all hpdc foundries.

Fire is the greatest risk in magnesium foundaries because of higher reactivity of molten Mg with oxygen. To overcome fire problem, some reducing gas atmoshpere should be used. Usually that atmosphere is created inside of the magnesium melting furnaces[19]. Cover gases are contained in industrial type tubes and should not be located close to heat sources. A furnace such as in the figure 2.10 shown is located near the die casting machine. The furnace does operate as melting furnace, holding furnace and, dosing pump. It doses molten magnesium at the desired volume to the shot sleeve of hpdc machine. After dosing, piston immediately moves and injects the

melt in to the die cavity to let the melt to solidify. This immediate cycle prevents ignition of liquid magnesium.

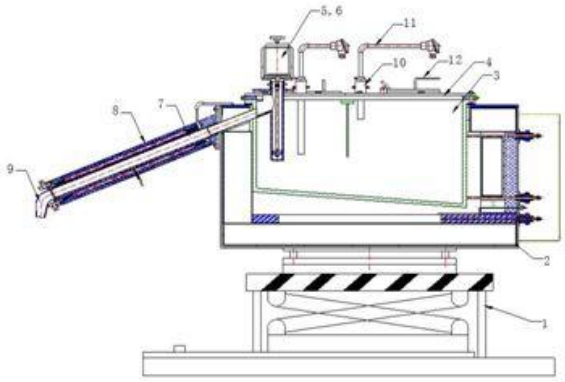

1. lifting platform
2. encapsulating sheet steel
3. melting pot
4. cover gas pipes
5-6. propeller and dosing pump
7. cover gas pipes
8. transfer tube
9. nozzle
10. thermocouple fittings
11. thermocouple
12. cover of the furnace

Figure 2.10 : Schematic view of a magnesium melting furnace

Before each casting cycle the die is air blasted and lubricated. Air compressors and pipe system should be installed near casting machines. Compressed air is also needed to operate the covers hpdc machines. Operators working on hpdc machines must be experienced due to the risks involved .

Machining centers are needed for a complete hpdc facility to machine the dies. A complete die set consists of many machined steel blocks, which may need maintanece or revision during service. Weight of die sets range between 200 to 5000 kg. So a crane or a forklift is needed to lift die sets and fix them to hpdc machine.

2.10 High Pressure die casting of magnesium alloys

Hpdc is the dominant processing technique to produce magnesium alloy products. There are various magnesium casting alloys used in the industry for different production methods. The Mg – Al alloys are cheap solutions compared with other magnesium casting alloys. In addition to cost effective good mechanical properties, they can be casted into long and thin sections by hpdc process [20]. Also the alloy must satisfy castability requirements such as, high fluity, good feeding characteristics and, low hot tearing tendency [21]. Although there are various types

of magnesium casting alloys, scientists are trying to develop new casting alloys. This is mainly because of the limitations of conventional Mg alloys, such as low ductility, low corrosion resistance, and poor high temperature mechanical properties [22][23]. The cast parts investigated in this thesis work will be used as electronic box covers and cases.Therefore, cheap alloys with reasonable strength and good castability is needed. Mg AZ91 alloy is selected because of these reasons. *Mordike et. al.* suggests that Mg alloy AZ91 accounts for more than 50 % of all hpdc castings due to its good strength, ductility and castability [7]. Physical properties and mechanical properties of Mg alloy AZ91 can be seen in the table 2.2. The magnesium alloys are designated by a code, the first two letters of which describes two major alloy constituents and the numbers shows their respective amounts. If present the last letter refers to the composition ranges. As in AZ91 which consists of nearly 9 % Al and 1% Zinc. In this chapter microstructure of hpdc Mg AZ91 alloy, and the process variables effecting on microstructure and mechanical properties will be investigated.

Table 2.2 : Physical and mechanical properties of Mg AZ91 alloy from raw material supplier

Physical properties				Mechanical properties		
density (g/cm^3)	thermal expansion coefficient 10^{-6} K^{-1} (20-200 °C)	thermal conductivity $Wm^{-1}K^{-1}$ (20°C)	specific heat $Jkg^{-1}K^{-1}$ (20-100C°)	tensile yield strength MPa	ultimate tensile strength MPa	elongation %
1.81	25	72	1050	150	230	5

2.11 Mg – Al binary phase diagram and Mg – Al – Zn ternary phase diagram

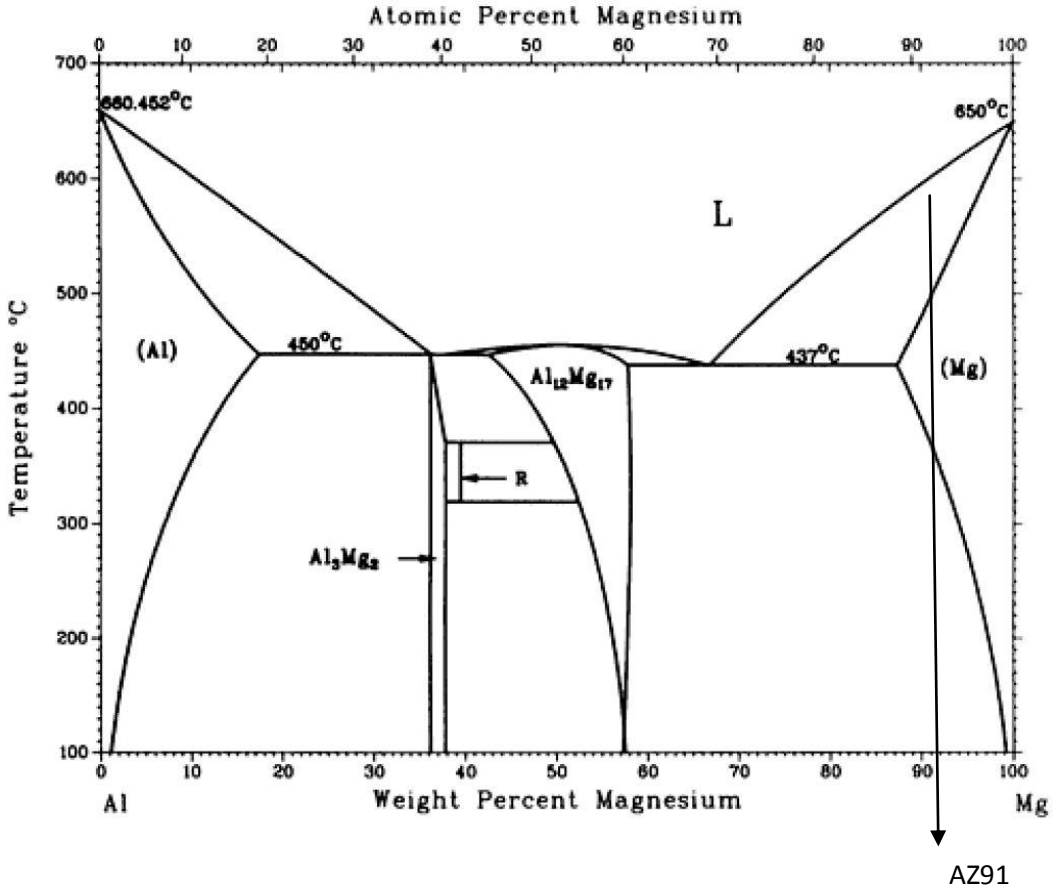

Figure 2.11 : Al – Mg binary phase diagram

The solidification process in hpdc is a non equilibrium crystallization process due to high cooling rates. This phenomena will be explained in chapter 2.12.2. However it will be explanatory to start with equilibrium phase diagrams. The alloy used in this study is Magnesium AZ91 alloy having ~9 wt% Al and ~1wt% Zn. The Mg-Al-Zn ternary phase diagram is not completely known as suggested in “The Alloy Phase Diagrams, vol 3” [24] .

The Magnesium – Aluminium binary system is the most commonly used magnesium casting alloy system. Figure 2.11 shows the binary Mg-Al phase diagram with the location of AZ91 alloy. The maximum solibility of Al in Mg is 2.1 wt% at 25 °C, 12.6 wt% at the eutectic temperature 437 °C. The eutectic between Al and Mg is $Mg_{17}Al_{12}$ with the composition of 32.3 wt% Mg [25]. Generally magnesium casting alloys

contain less than 12.6 wt % aluminium, and that alloys solidify with primary α – Mg phase, also non-equilibrium , metastable eutectic phase forms during cooling[20]. The phase diagram signals a precipitation heat treatable alloy, however precipitation heat treating is not an effective method to enhance the mechanical properties of magnesium alloys, as eutectic phase is metastable in Mg-Al casting alloys, therefore complete dissolution of β - $Mg_{17}Al_{12}$ occurs[25][26]. Wide freezing range can also be seen from the phase diagram. Magnesium alloy AZ91 has a freezing range of 160ºC. In casting of Mg – Al alloys, various defects can be seen because of this wide freezing range[20]. Similar defects can be seen in Al – Si alloys, it is documented in the literature that by casting Al A.413 alloy in exchange of Al A.380 shrinkage porosity is reduced. A380 shows a freezing range about 100 ºC, however Al A.413 has lower freezing range in the vicinity of 20 ºC limiting the possiblity of volumetric shrinkage [3].

Table 2.3 : Composition of Al alloys A.380 and A.413

Aluminium A.380	
elements	%
Si	7.5-9.5
Fe	2.0 max
Cu	3.0 -4.0
Zn	3.0 max
Mn	0.5 max
Mg	0.2 max
Ni	0.1 max
Sn	0.35 max
others	0.25 total
Al	balance

Aluminium A.413	
elements	%
Si	10.5 – 13.5
Fe	1.0 max
Cu	1.0 max
Zn	0.2 max
Mn	0.5 max
Mg	0.2 max
Ni	0.1 max
Sn	0.1 max
others	0.25 total
Al	balance

The binary Mg- Al system is the mostly used magnesium casting alloy system as mentioned before. But these alloys are not only binary alloys, but also ternary or quarternary alloys such as AM or AZ magnesium casting alloys. That two systems constitute manganese and zinc as the second alloying element respectively. These additions improve mechanical properties of alloys and also improve their casting behaviour, also because of these additions solidification behaviour of magnesium casting alloys are very complex[4][20].

2.12 Solidification theory of alloys

Casting of metals is one of the oldest processes to manufacture a metal component. Hundreds of articles and scientific works cover solidification theory of alloys[27][28]. In this text, a brief introduction about physcial fundamentals of solidification of alloys will be given and, principle mechanisms of hpdc solidification will explained.

2.12.1 Heterogenous nucleation

At a fixed temperature, the lowest free energy (G) having state is the thermodynamically stable state. For solidification to occur a driving force is needed. Driving force for nucleation is thermal undercooling (ΔT). Driving force for solidification can be formulized by the difference between free enery of solid state (G_s) and free energy of liquid state (G_l).

$$\Delta \mathrm{G} = G_s - G_l \tag{2.4}$$

The undercooling should be large enough to form new interfaces. ΔG have two competing terms, energy for forming a new interface and, free energy per volume of the solidifying mater. For formulation simply a sphere with radius "r" is taken into account.

$$\Delta G = \left(4\pi r^2 \gamma_{sl} + \frac{4}{3}\pi r^3 \Delta G_v \right) \left(\frac{2 - 3cos\theta + cos^3\theta}{4} \right) \tag{2.5}$$

Where γ_{sl} is the interfacial energy and, ΔG_v is the volumetric free energy.When ΔG is negative, nucleation is favoured. The second term in the equation 2.5 is a factor called shape factor $f(\theta)$. The wetting angle between the nucleus and substrate is θ . If θ is small, good wetting betweeen nucleus and substrate occurs. The wetting can be improved by adding appropriate inoculants to the melt to decrease θ .

As explained, solidification starts in the alloys when crystals are nucleated on substrates at a required amount of undercooling. This substrates are inoculants for most of the casting processes. But for hpdc which has very high cooling rates, inoculant addition is unnecessary. In the next section, two accepted explanations on nucleation in hpdc process will be summarized.

In hpdc, filling of the shot sleeve is very similar to the filling of a permanet mould. Liquid layer which comes into contact with the relatively cold mould cools below the liquidus temperature, T_{liq}, of the alloy. In the first theory, which is presented by Ohno [29], Southin[30], and Chalmers [31] the melt near the die wall is suggested to be thermally undercooled because of the heat loss by radiation at the melt surface. The thermal undercooling, ΔT_t, is sufficient to overcome the nucleation undercooling , ΔT_n. A schematic diagram can be seen in figure 2.12.

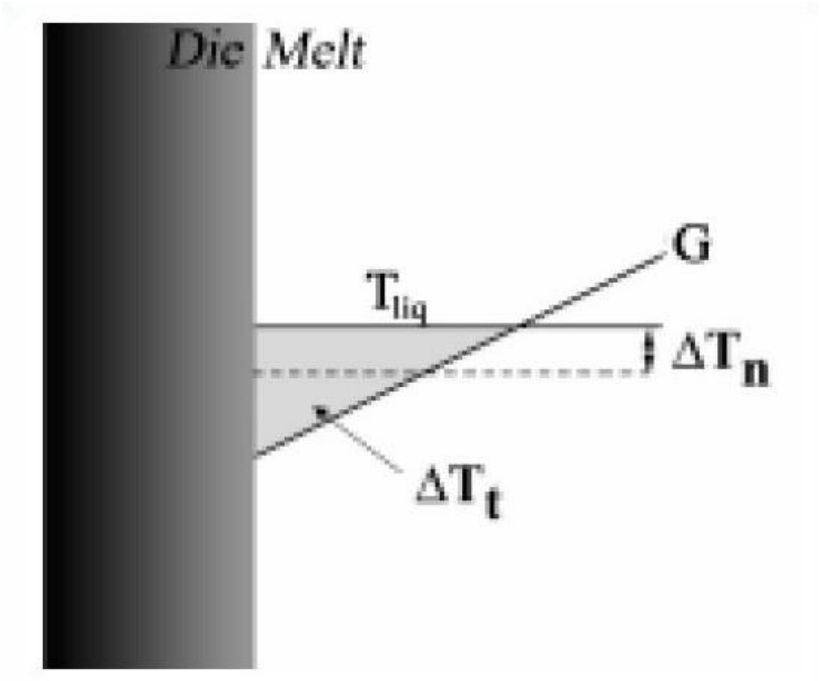

Figure 2.12 : Thermal undercooling, ΔT_t, exceeding the required nucleation undercooling, ΔT_n . [32]

The second theory suggests a growing solid layer from the die wall. In Mg-Al or Al-Si alloys which show eutectic solidification, solute is rejected from the interface creating a solute enriched zone. In the layer, solute concentration , c_l, decreases by

increasing distance from the die wall, so the liquidus temprautere, T_{liq}, is changing by distance. T_m is the actual melting temperature of the alloy. A constitutionally undercooled zone can identified clearly which is very suitable for nucleating of crystals. This theory is presented by Winegard et.al [33].

2.12.2 Solidification behaviour of magnesium alloys

As cast microstructure of Mg-Al alloys depends on mechanisms of nucleation and growth of primary grains and eutectic[34]. Solidification of Mg – Al alloys starts near 650 °C according to the composition of alloy with the formation of primary (α) magnesium grains. After primary grains, eutectic phase forms below 437 °C theoretically [20]. Nucleation and growth characteristics depend on several factors such as grain refiners, alloying elements and cooling rate. Nucleation is highly affected by use of grain refiners, and growth is dependent on aluminium content and cooling rate [35][36].

A widely used grain refiner is not applicable for magnesium casting alloys. Nevertheless experiments of this thesis work only includes high pressure die casting, in which the cooling rates are extremely high. In their work Nave et.al. suggests that high pressure die casting of magnesium alloys reveal cooling rates of 400 – 500 K/s [2][37]. On the other hand, Avedesian et. al. say in their article that, short filling time of the die and thin sections of cast parts brings out high cooling rates, typically 100 – 1000 K/s [4][21]. High cooling rates introduces high driving forces for nucleation, and yields large amount of primary grains. Because of this reason hpdc of magnesium process do not need further grain refinement.

Morphology of primary Mg grains are globular when the Al content is as low as 1 wt%, up to 9 wt% of Al content globular structure changes to a dendritic structure. Also at high cooling rates the primary morpholgy is again dendritic. As soon as the primary phase starts to solidify,dendrites nucleate and grow. Nave et.al. found that primary grain morphology and formation of eutectics is related. The size and shapes of primary grains affect the size and shape of eutectics. When the primaries are dendritic, eutectic morphology is divorced eutectic [36]. In addition, formation of

eutectic phase is important because size, shape, and distribution of the brittle $Mg_{17}Al_{12}$ phase affects ductility of the cast part [20].

2.13 Microstructure and second phases of hpdc Mg alloys

High pressure die casting yields finer and more complex microstructures when compared to other casting processes. The filling rate in hpdc is very high making the metal flow turbulent. High flow rate of metal may also atomize the liquid during cavity fill. On the other hand the pressure applied during solidification makes the accepted solidification theory inapplicable. S. Otarawanna et. al. bring out in their article in 2009 that development of microstructure in high pressure die casting is not completely understood currently [21][38]. G. Song et. al. suggest in their article that, microstructure of the hpdc Mg alloys can be different in different parts of the same cast product [39]. Grain size in hpdc is very small when compared with other casting processes. The number of grains per unit area is approximated with the formula :

$$Z_s = 1.1\,(\frac{\dot{N}}{\dot{G}})^{1/2} \tag{2.6}$$

where $\dot{N}$ is the nucleation rate, and $\dot{G}$ is the growth rate. From the formula it can be seen that higher nucleation rate or lower growth rate influences smaller grains. Cooling rate is the driving force for nucleation. High pressure die casting, yielding very high cooling rates produces very fine grains because high nucleation rates let crystals to grow in a limited area. More dendritic morphology is formed until impingement of neighboring crystals [21].

The dendrite cores, which contain low Al solidify first. The concentration of Al is increasing towards the interdendritic regions. Al is rejected when the primary α – Mg is growing, therefore interdendritic regions become supersaturated. SEM pictures can be seen in figures 2.13: (a-b). In the picture grey regions are the primary α – Mg phase. Grain size measurement are conducted on that phase.

Table 2.4 : Grain sizes of hpdc AZ91 alloy reported in the literature

reference	T_m (°C)	T_{die} (°C)	thickness (mm)	Grain size (µm)
[24]	650-670	150-200	1.5	3.6
	650-670	150-200	3	4.7
	650-670	150-200	6	5.1
	650-670	150-200	9	8.4
[40]	630±20	280	1.5	4.8
	630±20	280	3	13.6
	630±20	280	4,5	12.2
[41]	680	230	10	5.91
	680	230	10	8.82
[42]	-	-	5	3.9
	-	-	10	7.72

In the figure 2.13 the darkest areas are high Al content eutectic α –Mg and the lightest areas are β - $Mg_{17}Al_{12}$. Grey regions are the primary magnesium grains.

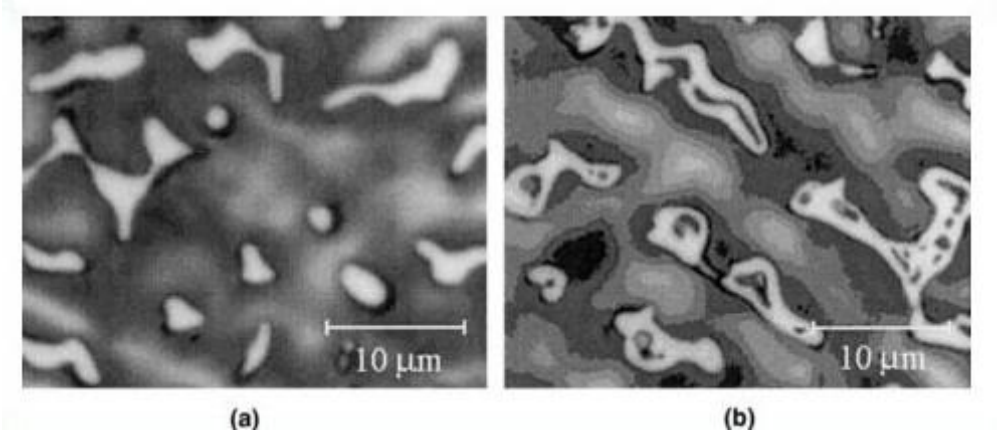

Figure 2.13 : a- fully divorced microstructure, b- partially divorced microstructure in Mg-Al die casting alloys [20]

As mentioned before hpdc Mg alloys generally exhibit partially or fully divorced morphology. Islands of eutectic Mg inside of the β - $Mg_{17}Al_{12}$ region surrounded by the bulk of α – Mg , is the accepted partially divorced morphology. On the other hand, fully divorced morphology consists of completely separate eutectic phases. Eutectic Mg surrounds single β - $Mg_{17}Al_{12}$ particles. Eutectic Mg grows from the primary dendrites [20][40].

According the phase diagram, β - $Mg_{17}Al_{12}$ is expected to form when the concentration of Al is above 13 wt% but because of the non-equilibrium cooling conditions in hpdc eutectic appears in alloys containing Al as low as 2 wt%.[41] Formation of β - $Mg_{17}Al_{12}$ reveals that during solidification local Al concentration in the liquid reaches high enough values to start eutectic crystallization [40]. The morphology becoming partially or fully divorced depends of various factors, such as aluminium content, zinc content and cooling rate. A fully divorced structure occurs with low Al contents, high Zn contents and relatively low cooling rate. Details about that subject can be found by the articles of Nave et.al [36][42].

Aluminium is the main alloying element in Mg-Al casting alloys. Variation in the distribution of Al in the same region, α – Mg regions or β - $Mg_{17}Al_{12}$ region can be seen. In the literature there are several EDS results. One research states that Al concentration at primary α – Mg regions near to the boundry of β - $Mg_{17}Al_{12}$ is high and decreasing through the primary α – Mg zone. Aluminium content is 6 to 8 wt % at the α phase 35 wt % at the β phase [43] .

Zinc is the second alloying element in Magnesium AZ91 with 0.45 to 0.90 wt%. In binary phase diagram of Mg- Zn it can be seen that the solubility of Zn in Mg is 6.2 wt % at 340 ºC. Zinc concentration is an important parameter for corrosion behaviour of magnesium alloys therefore, research on this topic generally covers zinc concentration of Magnesium hpdc alloys. Ambat et. al. measure concentration of Zn by using EDS and suggest that zinc concentration at α – Mg regions near to β - $Mg_{17}Al_{12}$ is high but decreasing with the increasing distance from the β - $Mg_{17}Al_{12}$ phase [39][43].

Magnesium AZ91 alloy have Mn as the third alloying element with 0.15 to 0.30 wt% . Therefore one expected to see Mn having phases in the microstructure. In the literature, it is suggested by V.Y. Gertsman that [40] inclusions are present in hpdc AM50 and AM60 alloys, which are very similar to AZ91 in compostion having lower Al, higher Mn content. That inclusions contain Al, and Mn. Several researchers have studied on Al – Mn intermetallics in die casting Mg alloys. But they are not in an agreement about the stoichometry of the intermetallic. In their work Sohn et. al. do not give a composition only states that inclusion containing Al-Mn present in the microstructure [44]. While in another research, Al_6Mn phase is detected by X ray diffraction analysis [45]. More recent studies states that the inclusions are Al_8Mn_5

intermetallics having polyhedral shapes. EDS analysis of the same studies indicates that inclusions contain 58.4±7 at % Al, 41.6±7 at % Mn. The stoichometry of Al_8Mn_5 composed of 61.5 at % Al, 38.5 at % Mn [40].

2.14 Skin effect

A very definite characteristic of hpdc microstructure is the skin effect. Metallic dies results in rapid cooling of the melt and produces a thin surface layer with very fine grain size and very good soundness [46]. Figure 2.14 shows two sections of an AM50 high-pressure die casting, one near the surface and one near the center of the section. The extremely fine grain size of the skin can be clearly detected.

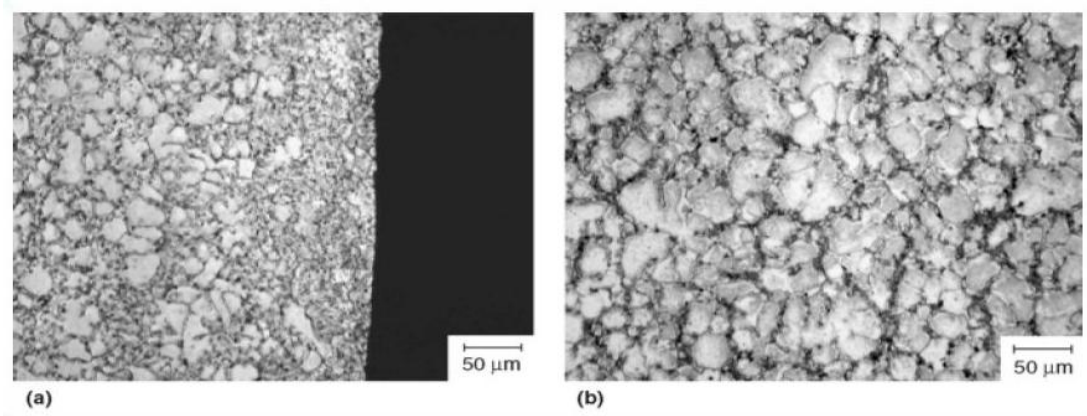

Figure 2.14 : High pressure die cast AM50 alloy, a – skin region near the surface, b – core of the specimen [46]

Although researchers do not agree on a definition, the skin is thought to be several hundred of microns in thickness [47]. Sequeira et.al. define the skin for AZ91 alloy as the depth where the microhardness decrease below 82 Hv. However in the same study, it is suggested that the skin depth decreases with increasing thickness of casting section [48]. In a different study Bowles et. al. define skin as the porosity free layer from the surface of the casting. This definition can be opposed in a similar direction that, when the casting thickness increases skin depth also increases [49]. Another explanation is presented by Chen for hpdc of aluminium alloys. No detailed formation mechanism of skin is presented in the study but it is suggested that, a surface layer is formed at the die surface during the pressure intensification phase. A thickness formulation is given where S is the skin thickness in milimeters, h_i is the

heat transfer coefficient of the interface, t_s is the solidification time, and ΔH_f is the latent heat of fusion [50].

$$S = h_i t_s \left[\frac{T_m - T_{die}}{\rho \Delta H_f}\right] \tag{2.7}$$

The skin effect is mainly because of different cooling rates of the outer and interior regions of the cast parts. The local heat extration from the melt near die surface can create a solid layer on the die wall. When that surface layer reaches a critical thickness, liquid adjacent to that solid layer do not extract suffiecient heat to solidify and continue flowing [51]. N. A. El-Mahallawy et. al. study thermal conditions in hpdc by measuring the cooling rate at various distances from the die, in the article it is published that solidification rate is 62.5 K/s near the die, 44.1 K/s 0.5 mm from the die. 35.7 and 34.1 K/s at 3.5 and 5.5 from the die surface respectively. These results are reasonable with the explanation of skin layer [52]. Fine grain size of α and β - $Mg_{17}Al_{12}$ particles present in the surface of the castings due to high cooling rate, course grains and β - $Mg_{17}Al_{12}$ particles formed at the interior because of relatively low cooling rate, and the externally solidified crystals which are explained in the chapter 2.15 [38].

2.15 Externally Solidified Crystals

As mentioned in chapter 2.3, cold chamber high pressure die casting process starts with pouring the melt into a shot sleeve made of steel. Therefore a heat transfer from the liquid to the shot sleeve occurs, which start solidification prior to injection of the melt into the die. According to Chen et.al all the superheat of the melt is dissipiated at that stage [53]. Solidification of the melt in shot sleeve forms a thin solid layer at the shot sleeve wall, and equaxed dendritic crystals in liquid. That solidified primary crystals are termed as floating crystals, presolidified crystals, or externally solidified crystals (ESC) [8]. Formation mechanisms of ESC in hpdc of aluminium and magnesium alloys are reported in literature. Equiaxed dendritic crystals are formed at the shot sleeve in the thermally undercooled zone near the

wall. Crystals grow into dendrites into the melt opposite and parallel to the direction of heat flow. During solid growth at the wall, a solute enriched zone is created by solute rejection at the crystal interface. Therefore regions with lower T_{liq} then that of the melt forms. Extracted heat from the growing solid establishes a thermal gradient and potential nucleation sites for substrates are formed at that constitutionally undercooled zone [8][34]. Another mechanism presented by Southin, suggest that a thermally undercooled zone is created near the melt surface due to radiation of heat [30]. Crystals growing from the shot sleeve walls are detached by the injection movement of the piston and together with the crystals formed in the shot sleeve, they are injected into the die.

ESCs have deteriorating effect for the mechnanical properties of magnesium hpdc products. Because they are larger than the grains formed in the die cavity. Otarawanna et.al. find two populations of primary grains in their research specimens that, one are crystals formed in die cavity with 10 μm size, the others are ESCs solidified in shot sleeve with 200 μm size[21]. There is a distinctive bi-modal grain size distribution in high pressure die casting due to ESCs. Because of that size difference externally solidified crystals are easily detected by optical microscopes.

There are different findings in the literature about the ratio of ESCs in the microstructure. In one research it is suggested that injecting liquid into the die consists 20 % presolidified liquid [54]. Another research states that ESCs occupies 20 % volume in aluminium hpdc products, 40 % volume in magnesium hpdc products [55].

Two phase flow in industrial applications are similar to flowing of ESCs inside of the melt. But it is not precisely true to directly interpret the that mechanism in hpdc context. The major volume of the ESC are thought to occupy the central regions of the casting. A high amount is present near the gating of the die and lower fractions are distributed far from the gate [32]. Also when the superheat of the melt is large and the shot sleeve is relatively cold, formation of ESCs are favored and ESCs occupy larger ratio in microstructre of hpdc magnesium alloys [8]. ESC fraction is suggested to be controlled by altering the casting temperature or shot delay time, and by heating or insulating the shot shot chamber [55].

2.16 Porosity

The microstructure of a high pressure die casting part contains significant amount of porosity. Formation of porosity is one of the major problems faced in hpdc of magnesium process. Porosity and its distribution are very decisive factors when evaluating quality of casting products. When load carrying capacity is considered, internal casting defects such as porosity have very pronounced effects on tensile properties. The ultimate tensile strength (UTS) and elongation of the products depends on porosity concentration and distribution [56][57]. Prakash et. al. suggests in their article that, initiation and growth of cracks from shrinkage pores are major microstructural failure modes of hpdc Mg alloys. In the same article it is added that gas pores are the additional contributors to that failure mode [58]. In various studies it is explained that microporosity detoriates the fracture related mechanical properties such as ductility, toughness, and fatigue resistance of Mg – Al casting alloys [52][59][60][61]. Porosity also have an effect of altering the stress field to initiate and propagate fracture. Before initiation of fracture, pores plays the role of stress concentrators when a tensile load is applied to a brittle alloy. After crack formation, pores leads to crack propagation as they are thought to be pre-existing crack elements.

Porosity in hpdc magnesium alloys can be divided into two types according to the reason of their occurence. Shrinkage related pores, and gas related pores. Shrinkage porosity occurs because of the volume contraction of solidifying liquid metal. Shrinkage voids generally occur at two places. Shrinkage pores are seen at sections where high volume / low surface area ratio is satisfied, because at this regions heat extraction could not be enough to solidfy high volume of liquid encapsulated by relatively low surface area. Shrinkage pores can also be seen at the last places to solidify in the absence of possible feeders. Contraction allowance of magnesim alloys for sand casting is given at the range of 1.3% - 1.43& in [18]. For hpdc process, because of high cooling rates contraction allowance is 0.06 % - 0.07%.

On the other hand, gas related voids are basically air bubbles encapsulated by the soldified metal. There are several sources for gas related porosity. Gas pores can grow because of entrapped air during liquid metal injection in the runner, over

lubricating the die, gas formed in liquid metal or turbulence in the die cavity during metal flow [3].

Two types of pores can be identified easily by macroscopic or microscopic examination techniques. Shrinkage pores are generally located between the dendrite arms and they are elongated features characterized by sharp edges and corners. Shrinkage pores are microporosity and show a size range of 1- 300 μm according to Prakash et. al [58]. Shrinkage pores can be detected easily by optical microscopy techniques. Location of gas related pores can be detected prior to casting by use of casting simulation softwares, casting simulation softwares are mentioned in chapter 2.20. Gas related pores are seen at the thick sections of the casting parts occupying the middle one-third of the plate thickness. Gas porosity in skin sections are very limited because during the solidification of the skin, gas pores are pushed into interior sections of the cast part [59]. Gas pores are spherical and usually larger than the shrinkage pores.

An interesting finding about the distribution of pores are documented in S.G.Lee et. al.. It is suggested that the gas voids are usually surrounded by the smaller shrinkage porosity, but the shrinkage porosity are not always located near the gas pores [59]. In the an article, a microscopic sample is said to contain 0.23 area % of gas pores and 0.56 area % of shrinkage pores [58]. Generally it is accepted that 1/3 of total porosity is gas pores, and 2/3 of total porosity is shrinkage pores [64][65]. In the literature shrinkage porosity and gas porosity fractions can be reported seperately. Generally total porosity content of the cast parts is reported. In some articles total porosity content is given without reporting any process variables, some articles report porosity content depending on casting parameters.

In an article not reporting casting parameters, five microscopic samples of Mg AM60 alloys are said to contain 0.1, 0.2, 0.7, 1.3 and, 0.2 volume % respectively [57]. In another research of which processing conditions are not reported, total porosity fraction is given as 0.3 – 0.88 area % in thin casting parts, 1.0 – 1.18 area % in thick casting parts of Mg AZ91 alloy [63].

Several parameters are affecting porosity amount and distribution in high pressure die casting parts such as melt temperature, die filling time, gate velocity, intesification pressure, die temperature and section thickness[48][64]. Huang et. al. measure total porosity in casting parts not seperating shrinkage and gas porosity.

As shrinkage and gas porosity have different origins, they may depend on different process parameters. Also they recommend observing samples for porosity in as-polished condition becuase etching can degradate the pores and leads to overestimation of porosity content [62]. Sequeira et. al. observe the effects of gate velocity on porosity content and conclude that the high gate velocity increases the surface quality but at the same time increases porosity levels [48].

S. G. Lee et.al. investigate the effects of intensification pressure, gate velocity, and casting temperature on porosity distribution of AM series magnesium alloys. The porosity distribution is investigated at different distances from the gate of the die. Five square plates are casted in this experiment to obseve volume fraction of gas pores, volume fraction of shrinkage pores, and volume fraction of total porosity. It is documented that intensification pressure decreases the gas related porosity and total porosity concentration whereas, there is no significant dependence of shrinkage porosity on intensification pressure. As the gate velocity increases gas porosity and total porosity increases in cast parts, due to the turbulence caused by high speed of melt flow. It is found that gate velocity do not affect the amount of shrinkage pores significantly. On the other hand, higher melt temperature means higher amount of gas porosity and total porosity because increasing melt temperature increases the amount of dissolved gases in magnesium melt. Shrinkage porosity is again seem not to be affected [59]. Their findings are tabulated in figure 2.15.

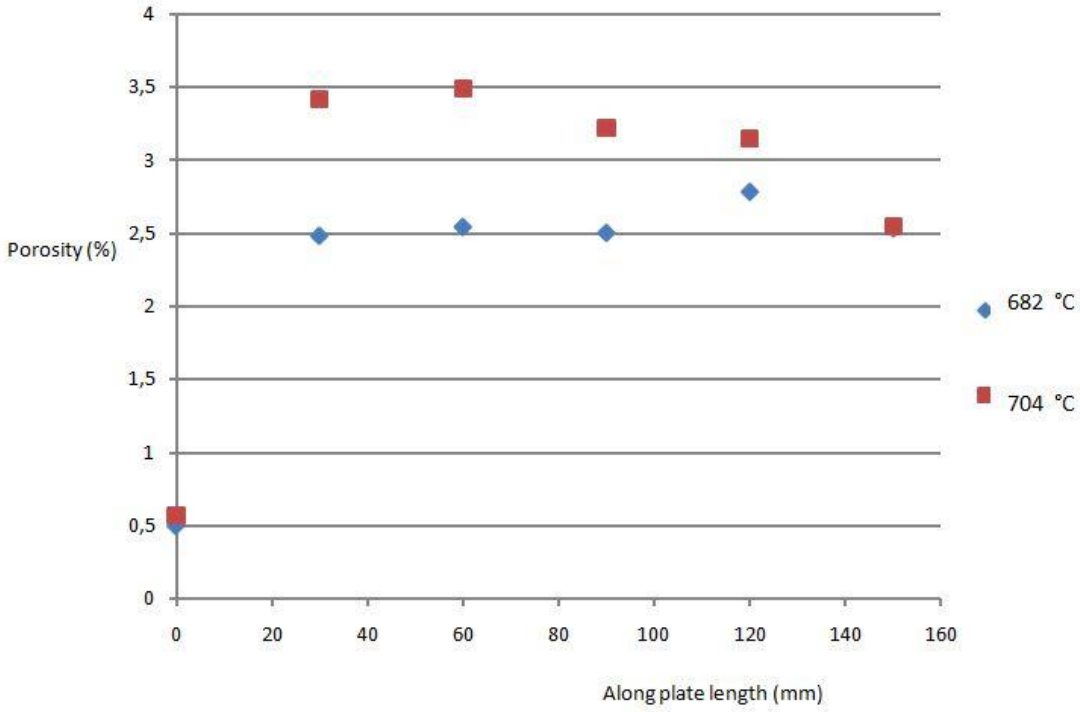

Figure 2.15 : Porosity concentration of a die cast AM50 plate casted at different temperatures [59]

Similar results about total porosity can be found in the literature. In an article publishing density values as an indication of total porosity, it is said that the average density of the cast parts increases with increasing intensification pressure. Also in the same article it is suggested on the contrary to S. G. Lee that gate velocity do not affect porosity content. All experiments of this research reveals highest porosity content at he far end of cast parts due to entrapped gas [52].

2.17 Banded defects

There is a very dynamic environment for solidification in hpdc. As metioned before, solidification begins in the shot sleeve before injection of the melt into the die cavity. While the liquid with some ratio of presolidified grains enters the cavity at high velocity, solidification is progressing at the same time. This coupled filling and solidification behaviours of hpdc creates distinct defect characteristics such as banded defects. Defect bands can occur in different forms such as cracks, band of gas or shrinkage pores. These defects show similarities however, there is no clear

indication that they form by same mechanism or multiple mechanism involved in their formation. Further research on this topic are needed to fully understand the banded defects.

Generally, banded defects occur parallel to the casting surface. Sometimes defect bands can be observed in the cast part starting from the runners continuing throughout the cast part up to overflows. In some observations more that one bands in the same region of casting part are seen. According to Dahle et.al. solid phase inside of the flowing liquid migrates towards the center and at the same time, heat extraction through the die increases solid fraction near the die surface [55]. As a result a highly liquid region is left in between high solid fraction layers. As flow and solidification continues, center and surface layers develops some mechanical strength. As a consequence localization of shearing in the high liquid fraction region occurs. Central region has a lower solute content that the outer region by this mechanism [65]. Mao explains a different mechanism about formation of bands. In the article, bands are though to contain only gas pores, and the gas pores occurs due to a sudden drop in pressure becuse of the back movement of the plunger tip during intensification phase [66]. Another mechanism is suggested in the context of freezing range. As discussed before Mg AZ91 has a freezing range of 160 ºC which is five times larger than the conventional Al-Si die casting alloy A356. This wide freezing range allows longer times for the alloy to solidify. In this extra time primary magnesium grains are rearranged and a band of liquid is formed to lubricate the flow of the partially solidifed melt into the die cavity. This band flows until the temperature is dropped below eutectic temperature [34]. Dahle et. al claims in their article that unidirectional flow or sudden changes in cross section favors more definite defect bands. Also in the same article it is suggested that defects band consists only shrinkage pores not the gas pores which is contrary to Mao [34].

There are various research in the literature about the effect of process parameters on defect bands. The findings are generally qualitative. One research point out that pouring temperature and second phase velocity have more pronounced effect in the position of defect bands. By increasing melt tempratue and decreasing second phase velocity, the defect band occurs further from the surface of the cast part. Effect of intensification pressure is investigated by several researches. The researches found out that intensification pressure has very little effect on position of

the defect band. However same articles suggest that increasing intensification pressure results in more distinct bands with lower level of porosity [55][67].

2.18 Strengthening mechanisms in AZ91

According to Caceres et.al, five strengtening mechanisms can be applied to AZ91 casting alloy. Solid solution strengthening, grain boundary strengthening, dispersion strengthening, Orowan looping, and general dislocation hardening are all sum up to give overall flow stress [68].

$$\sigma_f = \sigma_{ss} + \sigma_{gb} + \sigma_{disp} + \sigma_{or} + \sigma_{disl} \tag{2.8}$$

Orowan looping and general dislocation hardening are not relevant to hpdc cast parts. For high pressure die cast AZ91 alloys overall flow stress is defined as :

$$\sigma_f = \sigma_{ss} + \sigma_{gb} + \sigma_{disp} \tag{2.9}$$

2.18.1 Solid solution strenghtening

Magnesium dissolves large amounts of aluminium in solution, also zinc is in the solution. Solution strengthening effects of Al and Zn are significant. Contribution of solid solution strengthening to the overall is given in various articles as :

$$\sigma_{ss} \cong k_s c^{2/3} \tag{2.10}$$

Where k_s is a constant, and c is the concentration of atoms. Contribuiton of σ_{ss} to the overall of solution heat treated gravity cast AZ91 is estimated as 80 MPa [68]. Only 67% of aluminium atoms dissolve into magnesium in hpdc AZ91 alloys [49] whereas 33% are in the β phase. σ_{ss} contribution should be lower in the case of

hpdc than that of sand casting. Two different experiments estimates that the contribution is nearly 60 MPa [68].

2.18.2 Grain boundary strengthening

Grain boundary strengthening is usually designated by the famous Hall – Petch equation. Hall and, Petch suggests that crystalline metallic materials with grain size d, and yield strength σ_y follow the below equation :

$$\sigma_{gb} = \sigma_o + k\, d^{-1/2} \tag{2.11}$$

Where σ_o, and k are constants reported in various articles. The grain size of hpdc AZ91 is in 5 – 10 μm range. Contribution of σ_{gb} to overall is estimated to be 63 Mpa[69], and 84 Mpa [68]. However there are some raesons for discrepancies generally about the grain size of the materials. The grain size range is very wide in hpdc parts because of mentioned skin region and ESCs. Variation of grain size because of this reasons can effect the contribution of grain boundary strengthening.

2.18.3 Dispersion strengthening

Dispersion strengthening in hpdc AZ91 alloy is due to the elastic $Mg_{17}Al_{12}$ particles in plastic Mg-Al matrix. Dispersion hardening effect is calculated by the equation below:

$$\Delta\sigma_{disp} = 4\varphi\gamma\mu f\varepsilon^* \tag{2.12}$$

γ is an accomodation factor in the equation 2.12, φ follow the equation 2.13 :

$$\varphi = \mu^*/[\mu^* - \gamma(\mu^* - \mu)] \tag{2.13}$$

where μ is the shear modulus of matrix , and μ^* is the shear modulus of dispersed particles which are $Mg_{17}Al_{12}$ in this case. f is the volume fraction of the dispered

phase in the matrix and $\varepsilon^*$is the unrelaxed plastic strain. $\Delta\sigma_{disp}$ is estimated as 5.4 MPa in hpdc AZ91 alloy in the literature. Caceres et.al. add all the terms in the equation and estimate the yield strength of hpdc AZ91 specimens as 150 MPa. This estimation is very close to the values in the literature [68][69]. However processing parameters and macro factors effecting mechanical properties are more important in manufacturing. In the next sections these depencies are explained.

2.19 Variables effecting microstructures and mechanical properties of hpdc Mg alloys

Microstructure of the hpdc Mg AZ91 alloy is affected by several parameters such as casting temperature, thickness of the casting part, distance of the part from the gate, velocity of the melt at the gate, and intensification pressure. Mechanical properties are highly influenced by the microstructure. Therefore, control of process parameters improves the quality of the casting part. However, relationship between microstructure and mechanical properties of hpdc AZ91 alloy are still do not known completely [60]. There are several research in the literature conducted on these topics. But most of these research are conducted in laboratory environments therefore, real conditions of a manufacturing cannot be observed.

Microporosity and β phase are the major microstructural inhomogenities affecting to the mechanical behaviour of hpdc Mg AZ91 alloy. Microporosity and β phase involve in fracture process of the cast part. Various research are present in the literature on crack initiation from α - β interfaces and grain boundaries. Crack initiation at microporosity is investigated several times. It is published that the arrangement of shrinkage pores and β phase particles in grain boundary area speeds up failure. The effect of shrinkage pores and β particles are mainly due to their sharp radiuses acting as stress concentrators [70].

Small grain size favors higher mechanical properties in all crystalline materials according to Hall – Petch equation as mentioned in 2.18.2. Also it is reported by Prakash et. al. that small grain size obtained in hpdc process provides a large grain boundary area inhibiting slip across the boundaries [63]. Key advantage of hpdc prosesses is the high cooling rate obtained which influences small grains. Wei et.al.

conclude their article by suggesting that the mechanical properties of the die cast parts depends on the grain size of α – Mg phase [60].

Low ductility of magnesium alloys is due to the lack of slip systems present in HCP structure. Mg alloys do not have a significant yield point , 0.2 % proof strength ($\sigma_{0.2}$) is taken as an indication of yield strength (σ_y) in the literature [58]. Also Lee et. al add that ductility and UTS of hpdc Mg cast parts follows a nonlinear inverse parabolic depence upon microporosity level [56].

Skin effect which is explained in chapter 2.14 is also an important factor determining the mechanical properties of the hpdc parts. Sequeira et. al. removes 1 mm from flat die casting parts and obtain a 0.2 % proof strength decrease from 185 to 159 MPa. That expriment reveals the importance of the skin region for the mechanical properties of hpdc magnesium alloys [48][54].

2.19.1 Effect of melt temperature

The melt temperature is chosen to be 30 to 90 ºC above the theoretical melt temperature of the alloys according to NADCA [1]. Effect of melt temperature on microstructure and mechanical properties are not studied for AZ91 alloys. There are few papers about the effect of melt temperature on porosity distribution of AM50 alloy and grain size of AM60 alloy. It is suggested that increasing the melt temperature from 682 to 704 °C, increases the gas porosity content of the cast parts due to higher amount of dissolved gas in the liquid magnesium. However, it is also added in the articles that more research on this topic is needed to prove that effect [59]. H. I. Laukli et. al. investigates the effect of casting temperature on grain structures. The specimens are casted at 640, 680, 710 °C. At lower temperatures area fraction of externally solidified crystals are higher and show dendritic structure. At higher temperatures fraction of ESCs are lower and their morphology is elongated dendrites. At low melting temperatures, large undercooling is rapidly established nucleating large number of crystals. Undercooling near to the walls is reduced at higher casting temperatures nucleating fewer crystals. Nucleation and growth of crystals depends on the melt temperature [32]. According to Pitsaris et.al. it was concluded that among several different hpdc process parameters, casting temperature is the most effective parameter on mechanical properties. Increasing metal temperature reduces fraction of ESCs, increases tensile strength, yield stress

and ductility [71]. Knowledge about the effect of melt temperature on microstructure and mechanical properties of AZ91 alloy is not adequate in the literature.

2.19.2 Effect of casting thickness

Effect of casting thickness on microstructure is due to the different solidification rates of different thickness sections. Y. Wei et. al. suggest that with the increase of specimen thickness, UTS should decrease. The microstructure, consisting primary and eutectic phases become coarsen with the relatively low solidificaiton rate in thick sections compared to thinner sections. They also add that this proposition is only true when the specimens are taken from the same casting machine at the same time. In the article it is suggested that more fraction of primary phase means higher UTS [60].

Table 2.5 : Effect of section thickness on grain size, 0.2 % proof strength, and UTS of Mg AZ91 alloy

reference	T_m (°C)	T_{die} (°C)	thickness (mm)	Grain size (μm)	$\sigma_{0.2}$	UTS (MPa)
[24]	650-670	150-200	1.5	3.6	175	235
	650-670	150-200	3	4.7	163	243
	650-670	150-200	6	5.1	164	242
	650-670	150-200	9	8.4	148	228
[61]	630±20	280	1.5	4.8	-	191.6
	630±20	280	3	13.6	-	133.5
	630±20	280	4.5	12.2	-	181.7
[73]	-	-	5	3.9	130-147	188-209
	-	-	10	7.72	122-135	165-190

However, the effect on ductility is not well documented in the literature. Prakash and Regener documented increase in strength and ductility with decreasing section thickness.There are various articles about thickness effect on tensile properties, the results of which are given in table 2.5. The accepted proposition is the increase in mechanical properties by decreasing section thickness. There is only one reported contradiction to this effect by Rodrigo et. al. In their article it is suggested that tensile

strength decreases with decreasing thickness [66]. In a different article it is published that local solidification time effects microstructural evolution of different sections in the same cast part. Microstructural variation can also be seen in different positions also due to externally solidified crystals. Average size of β – $Mg_{17}Al_{12}$ particles decreases 27% in thin castings according to Prakash and Regener, which increases the potential sites for crack initiation [72]. Caceres et. al. proposed that β phase near the surface of the casting part form a fine structure , while at the interior parts coarser β are observed due to relatively lower solification rate. The structure of a hpdc AZ91 can be thought analogus to a composite structure having a ductile Mg matrix reinforced with β phase. Experiments show that composites with smaller reinfrocement cells are stronger than the composites with larger cells [68].

2.19.3 Effect of position

The effect of position on microstructure and mechanical properties are similar to the effect of thickness. It is accepted that microstructures of regions close to the die and central specimens show variations. Smaller grains are obtained at the positions near to the die surface due to higher cooling rate. In the literature position effect on porosity distribution is investigated. In the regions far from the gate amount of porosity increases [52][56]. Effect of position with respect to the distance from the die surface on mechanical properties is investigated and edge specimens are found to have lower grain size and thus higher mechanical properties than specimens from the middle of the cast part in two publications [72][73].

Table 2.6: Effect of position on grain size and mechanical properties [72]

T_m (°C)	T_{die} (°C)	thickness (mm)	position	Grain size (μm)	$\sigma_{0.2}$ (MPa)	UTS (MPa)
680	230	10	edge	5.91	122-131	171-190
680	230	10	middle	8.82	128-135	165-177

2.19.4 Effect of gate velocity

Gate velocity is influenced by velocity of piston, diameter of the shot sleeve, and gate thickness of the die. When the gate velocity is low filling of the die cavity

become a problem. On the other hand if the gate velocity is too high, the liquid entering the die cavity atomizes leading to higher porosity. Porosity distribution is investigated by S. G. Lee et. al. gate velocity increase founded to increase the porosity amount [59]. However N. A. Mahallawy et. al. published that increase in gate velocity has a negligible effect of porosity. Additionally N. A. Mahallawy et. la. increases the gate velocity from 40 to 80 m/s for Mg AM20HP alloy and obtain a slight increase in 0.2 % proof strength. For Mg AM50HP again gate velocity is increased from 40 to 80 m/s and a reasonable increase in 0.2 % proof strength obtained. In the same article it is suggested that 0.2 % proof strength and ductility is not affected by gate velocity [52]. There should be an optimum gate velocity depending on the shot sleeve diameter, fill fraction of the shot sleeve, and geometry of the cast part. This effect should be investigated further by a well prepared experimental setup.

2.19.5 Effect of intensification pressure

The intensification pressure is the pressure applied during the solidification of the cast part. Therefore it is expected that higher the intensification pressure lower the shrinkage porosity. There are few papers in the literature about this study presenting negligible effect of intensification pressure on shrinkage porosity. As the detection of shrinkare porosity is not an easy job, this effect is not well documented in the literature. However UTS increase with higher intensification pressure and negligible effect of intensification pressure on 0.2 % proof strength and ductility is published several times [52][59].

2.20 FEM - casting analysis

Growing needs of the industry such as complex geometies, thin sections, and extereme tolerances urges foundries each day. Hence, construction of a die set is very difficult job. Any fault on the die will result in defected parts, therefore die designs should be checked before construction of the die sets. Also this strategy is easier and cheaper than the trial and error method. Proper finite element method (FEM) packages are in use throughout the foundry industry. This casting analysis softwares are used for the optimization of several processes such as sand casting, investment casting, low pressure die casting, and high pressure die casting. This processes are sub divided into operations namely filling simulation, solidification

analysis, cooling process, and cycling analysis for hpdc can be calculated. Computer aided engineering (CAE) softwares for casting simulation generally consists of computer aided design (CAD) packages, FEM meshers, materials databases, and a postprocessor.

The CAD part of the die design should be imported into the software.The part is then meshed appropriately. Mesh number should not be too small for the reliability of the simulation, and should not be too large for the calculation to finish in appropriate time. The complexity of the cast parts especially in the case of hpdc and lpdc, makes meshing very difficult. After meshing, casting process and general constraints such as gravity constant are defined. Casting and die materials are selected from the software database. Software is started to calculate after input of the casting parameters such as melt and die temperature, filling time, velocities of phases, and intensification pressure. Cooling curve of the material in a specific point, filling vectors of the flowing liquid, air left in the die are some of the results which can be obtained from the casting analysis softwares.

There are various research on the reliability of the casting analyis softwares. The FEM package used in this thesis is “Vulcan simulation software for casting optimization”. M. Chiumenti et. al. published cooling curves and distortion analyisis form Vulcan software and compare them with the real casting situation. From the figure it can be seen that there are very small deviations in temperature from the real case which can be neglected [74].

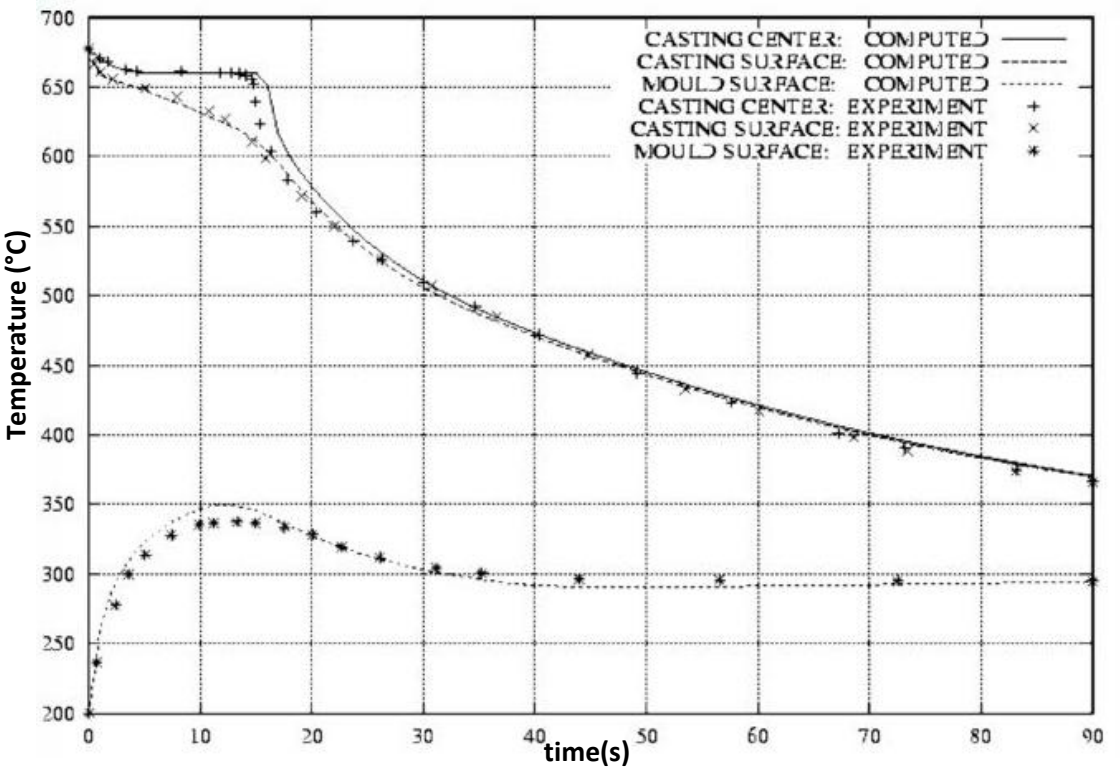

Figure 2.16 : Temperature vs time graph comparison of computed and experimental data [74]

CHAPTER 3

EXPERIMENTAL PROCEDURE

The experimental procedure consists of simulating the high pressure die casting process with different casting variables, manufacturing cast parts, investigating the tensile properties of the cast parts, grain size and porosity measurements by optical microscopy and scanning electron microscopy (SEM). Thesis is concluded with the comparison of tensile properties of Al and Mg parts. The parts are manufactured in the facilities of RUTAŞ Die Casting which is a company with 30 years of aluminium die casting experience. Tensile tests , optical microscopy and SEM observations are carried out in mechanical testing, SEM, and foundary laboratories of METU. The flowchart of experiments and experiment groups can be seen in table 3.3 and table 3.4 respectively.

In the experiments three different dies are used to produce three different cast parts. Magnesium AZ91 alloy is used in all casting processes. Cast parts can be seen throught the figures 3.1, 3.2, and 3.3. Variables whose effects will be investigated are casting temperature, V_1 and V_2 speeds during injection, thickness of the cast parts, and position of the specimen in the die.

All three parts are assembled together after manufacturing to be an electronic device. The first part is the cover of this system, the second is a stand holding the electronic cards , and the third one is the body of a wireless phone. Mass and volume of the cast parts can be seen in table 3.1.

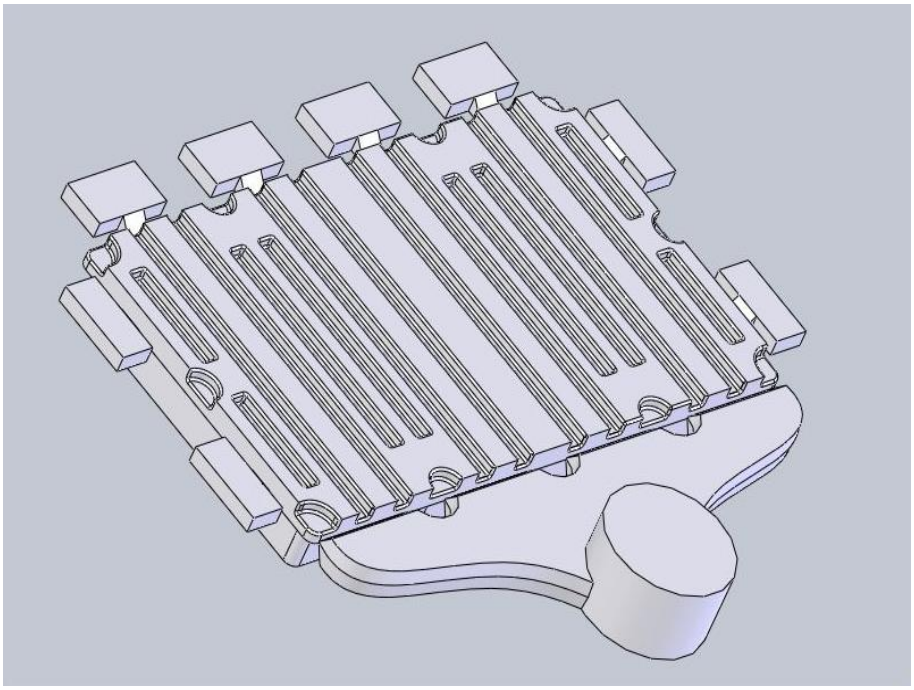

Figure 3.1: CAD of cast part 1

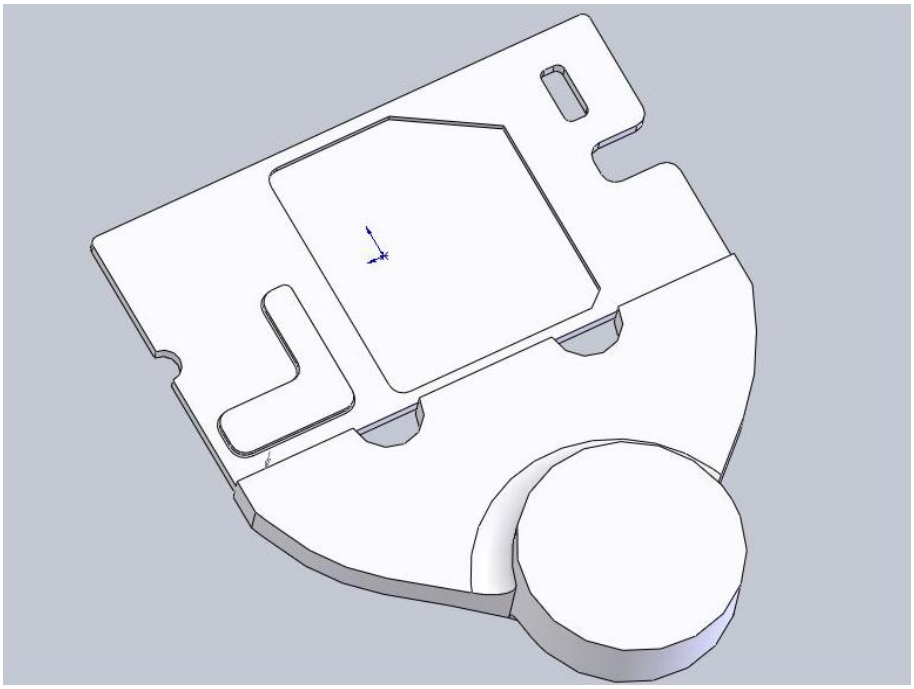

Figure 3.2: CAD of cast part 2

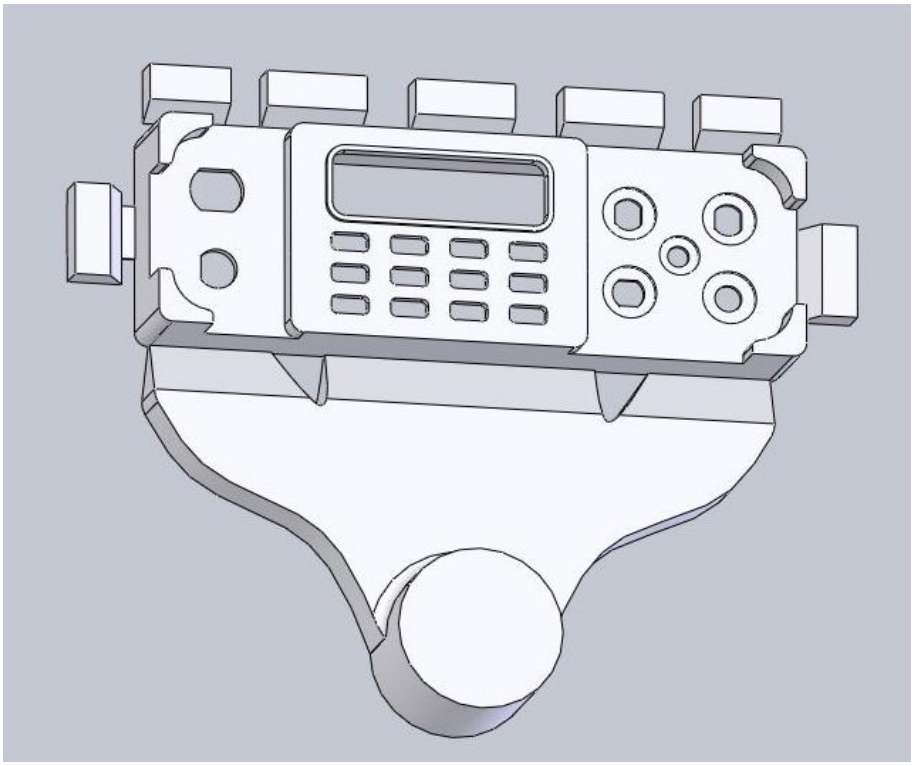

Figure 3.3: CAD of cast part 3

Table 3.1 : Mass and volume of the cast parts

cast part	thickness (mm)	mass (gram)	volume (mm^3)
1	6	930	522 x 10^3
2	2.5	620	347 x 10^3
3	4	800	450 x 10^3

3.1 Raw materials

The materials used in the experiments are the conventional high pressure die casting alloys of aluminium and magnesium. Aluminium alloy is Al A.413 in ASTM standarts or AlSi12Cu in ISO standarts, and magnesium alloy is AZ91 with the compositions shown in table 3.2. These alloys are conventional high pressure die casting alloys.

Table 3.2 : Compositions of the alloys used in the study

Aluminium A.413	
elements	%
Si	10.5 – 13.5
Fe	1.0 max
Cu	1.0 max
Zn	0.2 max
Mn	0.5 max
Mg	0.2 max
Ni	0.1 max
Sn	0.1 max
others	0.25 total
Al	balance

Magnesium AZ91	
elements	%
Al	8.3 – 9.7
Zn	0.3 – 1.0
Mn	0.1 – 0.5
Si	0.1 max
Fe	0.05 max
Cu	0.03 max
Ni	0.002 max
Be	0.002 max
others	0.02 each
Mg	balance

Table 3.3 : Flowchart of experiments

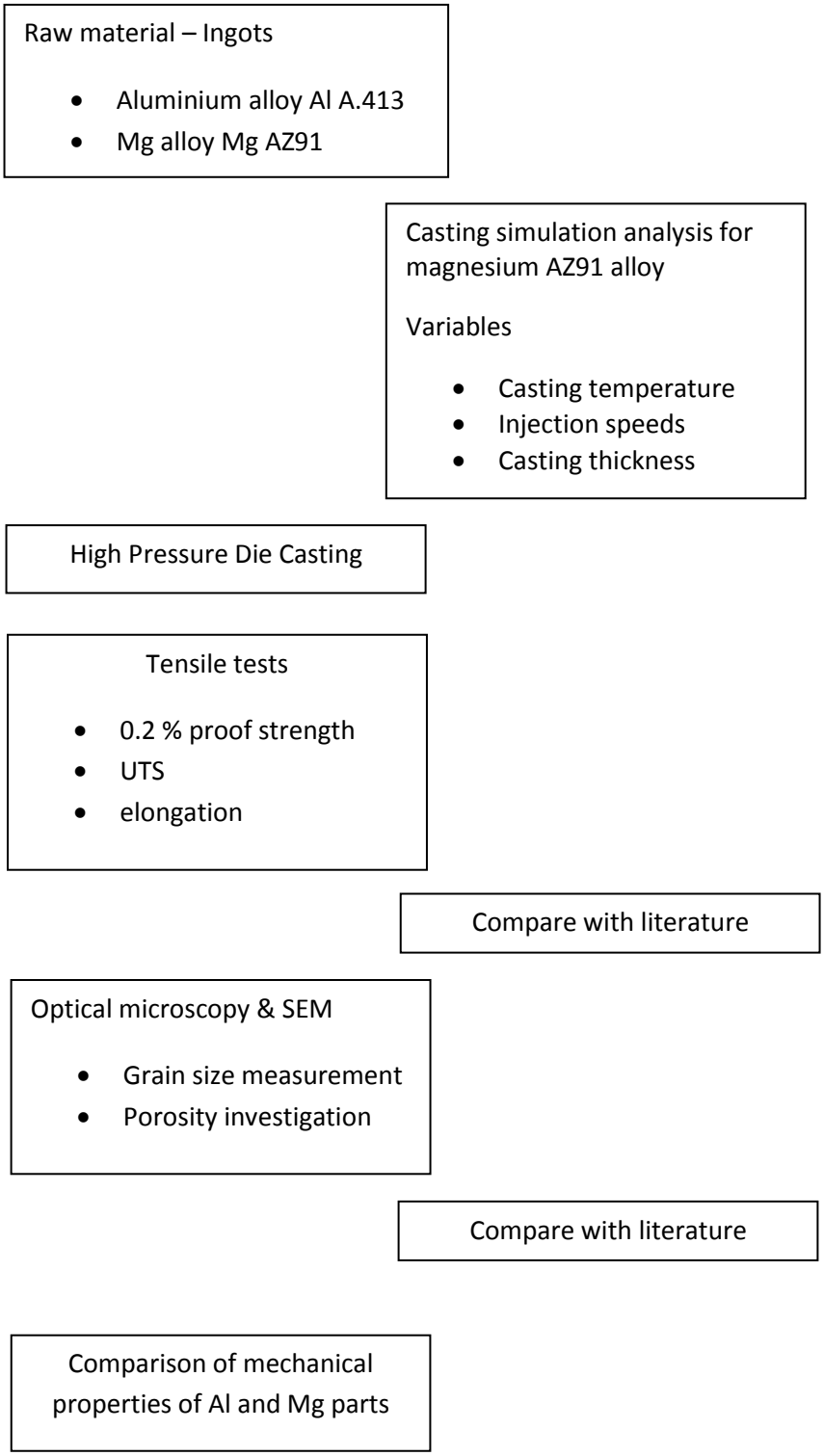

Table 3.4 : Experiment groups

Group 1

- Cast part 1
- Casting T 650 & 670 °C
- Casting simulation analysis
- V_1 = 0.15 m/s, V_2 = 1.5 m/s
- Very low tensile values are obtained
- Optical microscopy & SEM
- No grain size measurement
- No porosity investigation

Group 2

- Cast part 2
- Casting T 685 °C
- Casting simulation analysis
- V_1 = 0. 5 m/s, V_2 = 2.5m/s
- Casting thicknesses of 2 & 4 mm
- Optical microscopy & SEM
- EDS analysis
- Grain size measurement
- Porosity investigation

Group 3

- Cast part 3
- Al A.413 and Mg AZ91 alloys
- Casting T 645 & 675 °C
- Casting simulation analysis
- V_1 = 0.5 m/s, V_2 = 2.5 m/s
- Optical microscopy & SEM
- EDS analysis
- Grain size measurement
- Porosity investigation

3.2 Casting simulation analysis

V_1 and V_2 speeds are first calculated from the equations 2.2 and 2.3 and they are input to the software. The final process variables of Mg high pressure die casting process is determined by the casting simulation software. To run the simulation, computer aided design (CAD) files of the cast parts are imported into the software. Then the imported design file is divided into meshes. Optimum mesh number is 250000 to 350000.

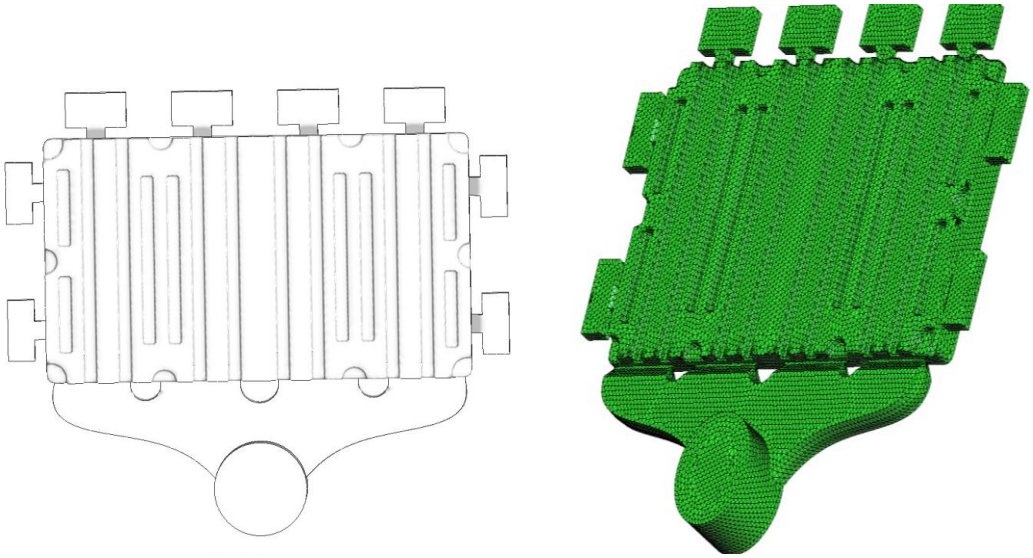

Figure 3.4: Cast part 1 before and after meshing

The problem is defined by selecting High pressure die casting method from the process type tab. Gravity constant, environmental temperature, and gravity direction is entered.

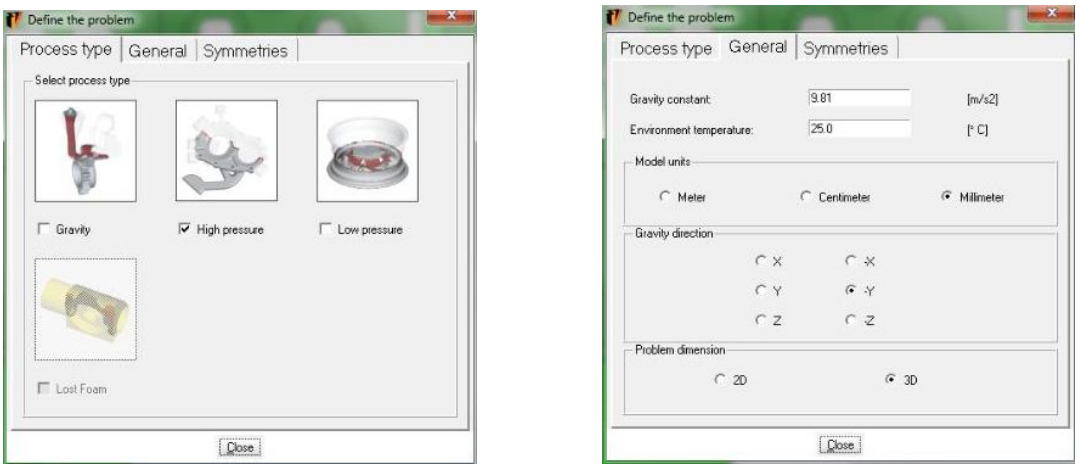

Figure 3.5 : Problem definition in Vulcan Castign Simulation Software

Definition of the problem is followed by definition of foundary components. The part is introduced to the problem, in addition the alloy and the initial temperature of the alloy is input in this section.

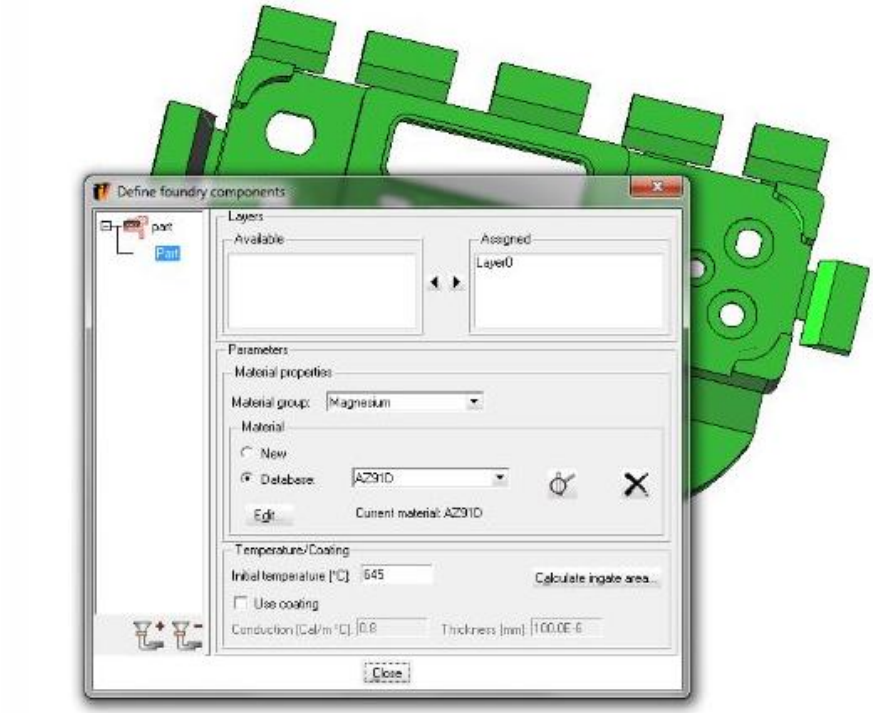

Figure 3.6 : Definition of foundry components in Vulcan Casting Simulation Software

Piston diameter, injection speeds, and mold temperature are entered into the define operations – strategy tab. After entering process parameters, filling time is calculated automatically.

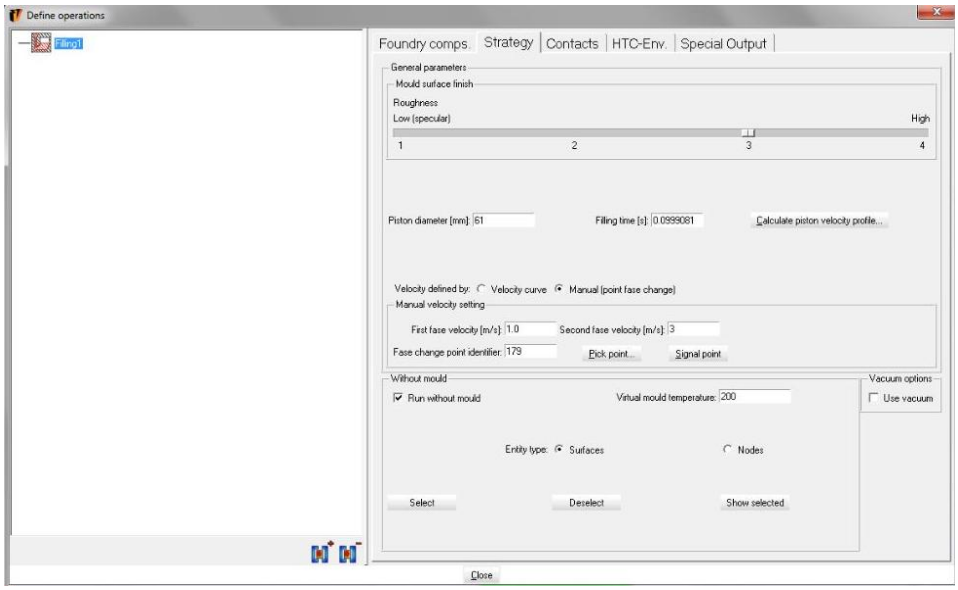

Figure 3.7 : Definition of operation in Vulcan Casting Simulation Software

Calculation is started after defining the process, components, and operation. Calculation time depends on the number of components and number of meshes of each component.

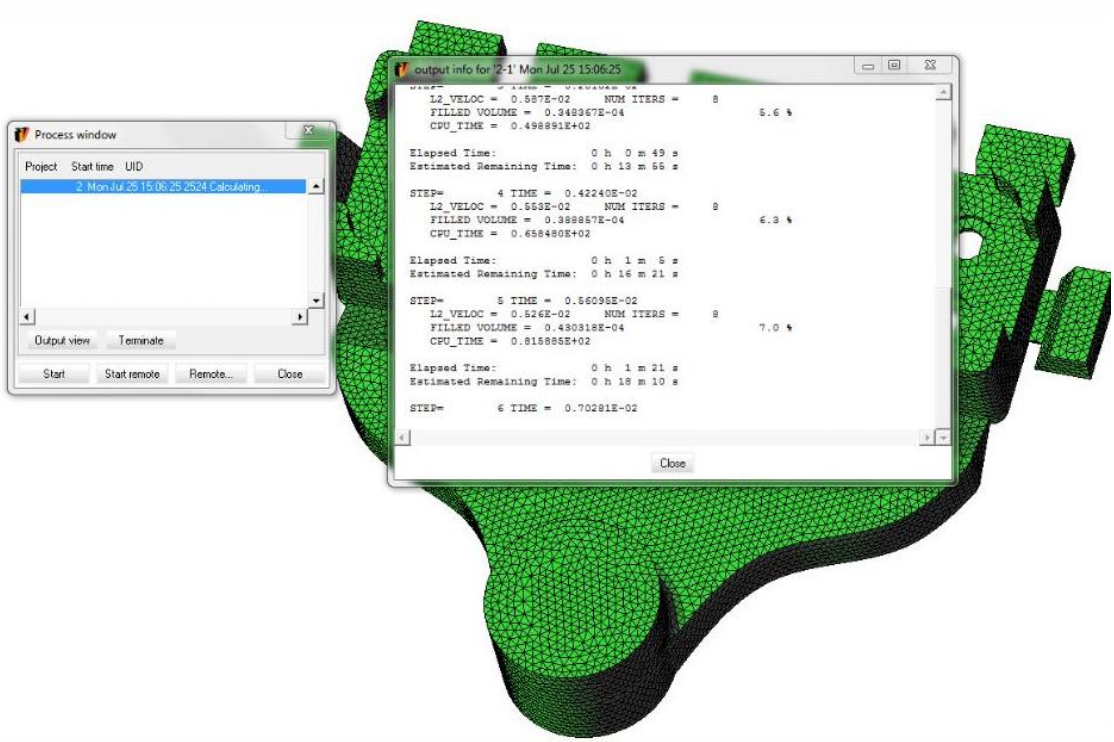

Figure 3.8 : Calculation of the problem in Vulcan Casting Simulation Software

3.3 Manufacturing of the Specimens

In the manufacturing process , Amei AMD350 magnesium dosing furnace and Hidroteknik HTME 400 hpdc machines are used. Amei AMD 350 dosing furnace has a capacity of 350 kg, and can melt the alloy at 50kg/hour rate. Hidroteknik HTME 400 has 400 tons of clamping force capacity, maximum 3.0 m/s piston speed, and maximum 35 MPa injection pressure. Linde SF_6 and N_2 are used as protective gases. High pressure die casting steps are as follows:

1. Magnesium furnace is started 8 hours before the casting process for preheating
2. When the temperature of the furnace reaches 350 °C, protective gas starts to flow

3. As the melt reaches desired temperature, the dosing pump is mounted in its place
4. Die is heated up to 150 - 200 °C
5. Dosing pump parameters are set according to the volume of casting part
6. Casting parameters of the hpdc machine are set
7. Operator closes the die of the hpdc machine
8. Magnesium melt is dosed into the shot sleeve automatically
9. Magnesium melt is injected into the die from the shot sleeve
10. Injected liquid is let to solidify for 5 to 10 seconds with applied intensification pressure
11. Die is opened and part is ejected
12. The runner and overflows are trimmed when the part is cooled to room temperature

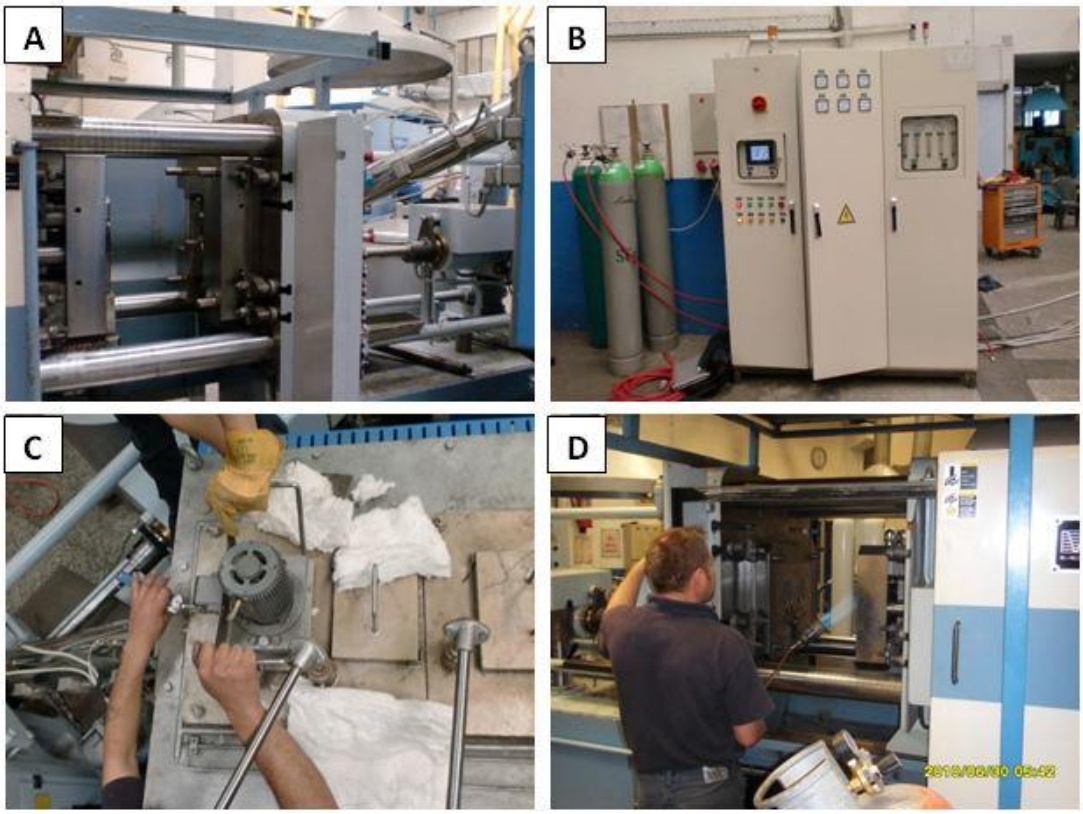

Figure 3.9: a- Die and transfer tube of furnace, 3.9: b- Control panel and protective gases, 3.9: c- Mounting of the dosing pump, 3.9: d- Heating the die

The cover gas used consists of 0.03 % SF_6 as protective gas and 99.97% N_2 as carrier gas. The flow rate of gases are 1 cm^3/min and 3000 cm^3/min respectively.

In the above figures high pressure die casting die can be seen schematically. In figure 3.10-a die is ready for casting process. Magnesium melt is dosed in this position. Figure 3.10-b shows the injection step of the liquid into the die cavity. After cooling the die halves are opened, and the ejector plate ejects the part from the die in figure 3.10-d.

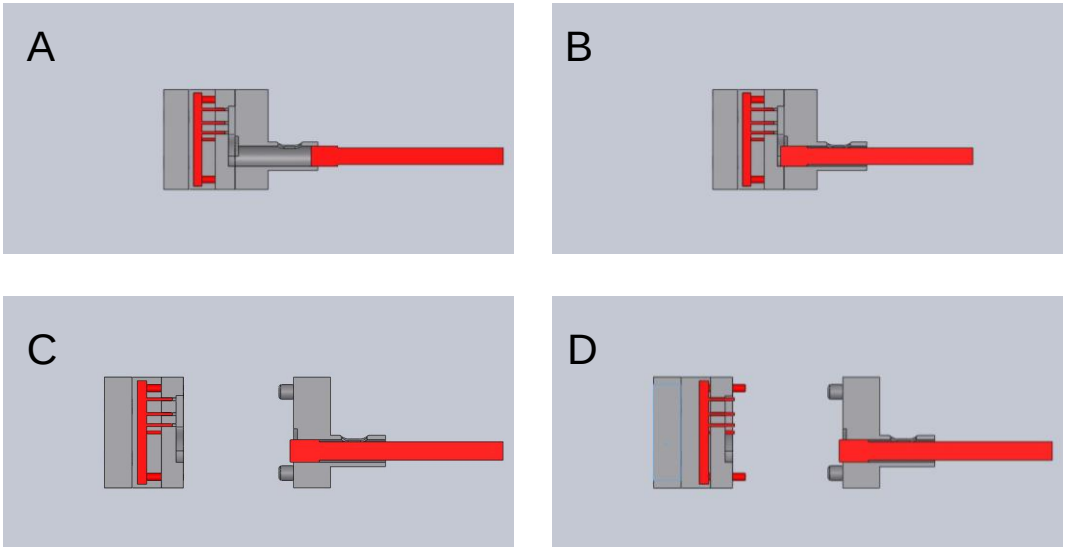

Figure 3.10: (a-d)- Hpdc process steps

The casting parameters used for experimental groups are listed in table 3.5. The parameters are used according the calculation, simulation, and capacity of the hpdc machines. The parameters used for cast part 2 & 3 are high values pushing the limits of hpdc machine. Therefore cast part 1 is manufactured with parameters appropriate for casting Al alloys.Calculation and simulation of parameters will be examined in chapter 4.

Table 3.5 : Casting parameters used in manufacturing

cast part	T_m (°C)	V_1 (m/s)	V_2 (m/s)
1	650	0.15	1.5
1	670	0.15	1.5
2	685	0.5	2.5
3	645	0.5	2.5
3	675	0.5	2.5

3.4 Microstructural Analysis

The specimens are examined by optical and scanning electron microscopy to determine microstructure, grain size, and porosity content. Externally solidified crystals are also observed in some regions of the specimens.

3.4.1 Sample Preparation

Specimens for microstructural analysis are taken various positions from casted parts. Group 1 and group 2 specimens are machined from gate, middle, and overflow (air vent) sections. Group 3 specimens are machined from gate and overflow sections. Group 2 specimens are mounted into bakalite resin, as they are very thin to properly hold. Mounting is done by using Metkon Hydropress 50 mounting machine. The specimens are then grinded from 180 grit to 1200 grit SiC paper by water cooling. Polishing is done on soft polishing coat with 1 μm diamond suspension. No water is used on polishing operation due to low corrosion resistance of magnesium alloys. Grinding and polshing operations are performed on Ontas phaidon grinding-polishing machine. Polished specimens are used for porosity concentration investigation to avoid widening of the pores by etchants. For grain size determination etchants should be used to reveal grain boundaries. Etchant used for magnesium alloy is 2 % Nital (2% nitric acid in alcholol).

3.4.2 Optical Microscopy

SOIF XJF-6A optical microscope is used to investigate the microstructure of the specimens. Porosity content and grain sizes of specimens are measured by the image analysis software Dewinter Materials Plus 4.1. An analyzed image can be seen in figure 3.11 b .

3.4.3 SEM

Detailed microstructural investigation is carried out by SEM. SEM studies are conducted with JEOL JSM6400 scanning electron microscope equipped with NORAN system. The specimens used for optical microscopy are also used for SEM analysis.

3.4.4 EDS Analysis

Integrated EDS system to JEOL JSM6400 scanning electron microscope is used for EDS analysis to detect the elemental compositions of primary Mg grains and eutectic Mg- Al regions.

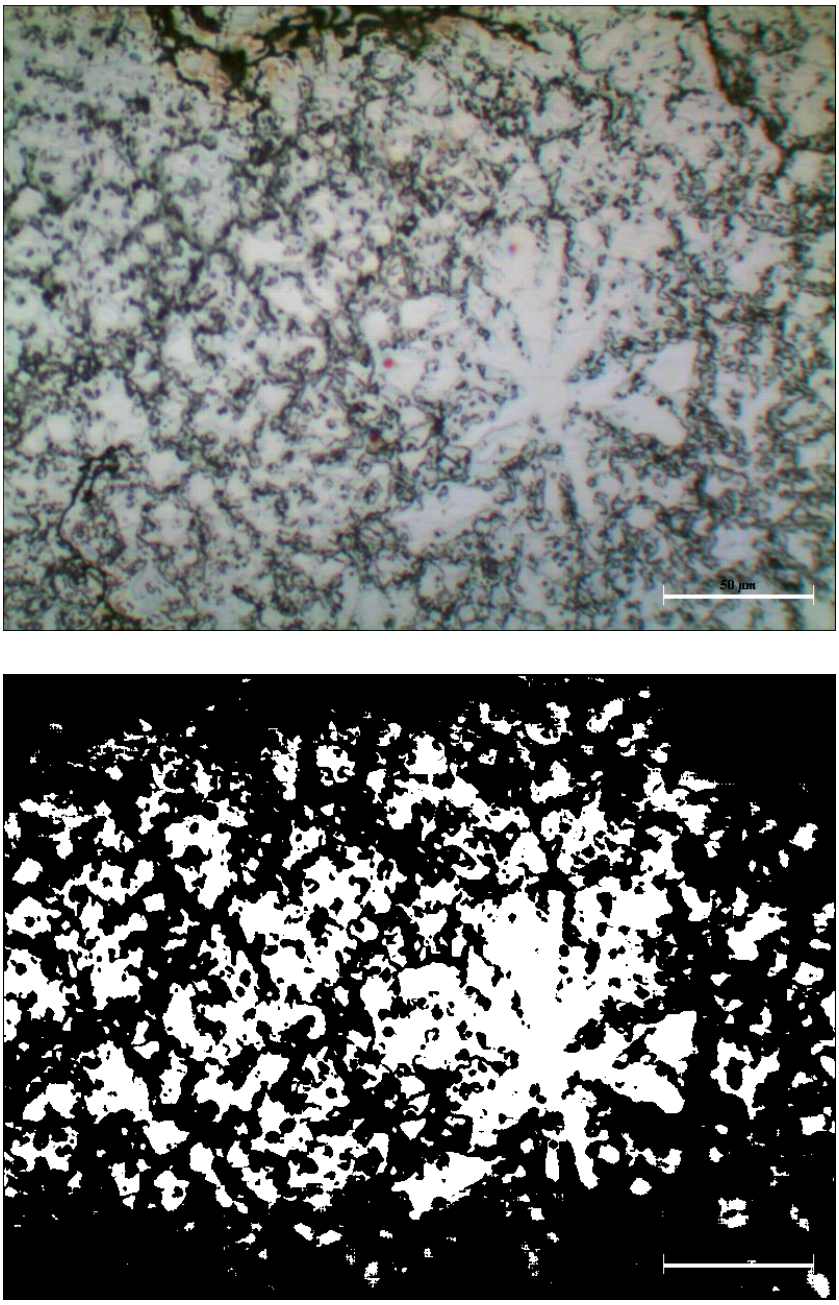

Figure 3.11: a- sample image of gate section of cast part 3 specimen casted at 670°C 400 x magnification 3.11: b- The image after image anayzing

3.5 Mechanical Testing

Tensile tests are conducted to the sample parts machined from specimens. As the geometry of the cast parts are complex, extracting tensile test specimens was not an easy job. The geometry of the specimens are compatible with "Standard test methods for tension testing wrought and cast aluminum and magnesium alloy products" ASTM B 557M – 07. Specimens are machined directly from the manufactured parts in CNC machining centers. 2mm diameter endmill tools are used in operation. Powermill Computer aided manufacturing (CAM) software is used to command CNC machining centers.

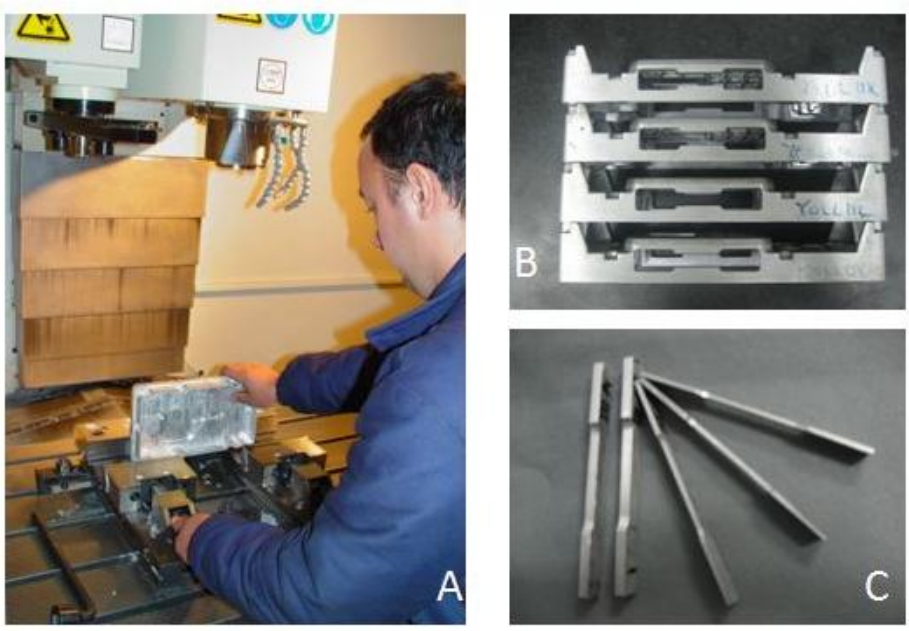

Figure 3.12: a- placing parts onto the table of CNC machine , 3.12: b- machined parts, 3.12: c- extracted specimens

Tensile tests are carried out using INSTRON 5582 universal testing machine. INSTRON 5582 has a load range of 2kN to 100kN which satisfies the predicted maximum load for tensile test specimens. Predicted UTS values are from the literature. [23] [60] Maximum load is calculated using the below formula :

$$F = UTS\ x\ A_0 \tag{3.1}$$

where F is the load in N, UTS is the ultimate tensile strength in MPa, and A_0 is the cross section area of the gage in mm^2 . Speed applied during the tensile test is 1 mm/min. Table 3.6 shows tensile test specimens, and their geometrical parameters. In the table w is the width of the specimens, and t is the thickness .

Table 3.6 : Tensile test samples used in the study

	sample	w x t (mm)	A_0 (mm^2)	Gage length (mm)	predicted max UTS (MPa)	predicted max load (N)
Cast part 1	1a	5.8 x 5.1	29.58	31.5	200	5916
	1b	5.8 x 5.1	29.58	31.5	200	5916
	2a	5.8 x 5.1	29	33.6	200	5800
	2b	5.8 x 5.1	29	33.6	200	5220
Cast part 2	3a	6.0x3.9	23.4	34.3	220	5148
	3b	6.0x2.0	12	34.3	240	2880
	3c	6.0x2.0	12	34.3	240	2880
	3d	6.0x2.0	12	34.3	240	2880
	3e	6.0x3.9	23.4	34.3	220	5148
Cast part 3	1	6.0 x 5.5	33	30	200	6600
	2	6.0 x 5.5	33	30	200	6600
	3	6.0 x 5.5	33	30	200	6600
	4	6.0 x 5.5	33	30	200	6600
	5	6.0 x 5.5	33	30	200	6600
	6	6.0 x 5.5	33	30	200	6600
	7	6.0 x 5.5	33	30	200	6600
	8	6.0 x 5.5	33	30	200	6600
	9	6.0 x 5.5	33	30	200	6600
	10	6.0 x 5.5	33	30	200	6600
	11	6.0 x 5.5	33	30	200	6600
	12	6.0 x 5.5	33	30	200	6600
	13	6.0 x 5.5	33	30	200	6600
	14	6.0 x 5.5	33	30	200	6600
	15	6.0 x 5.5	33	30	200	6600
	16	6.0 x 5.5	33	30	200	6600

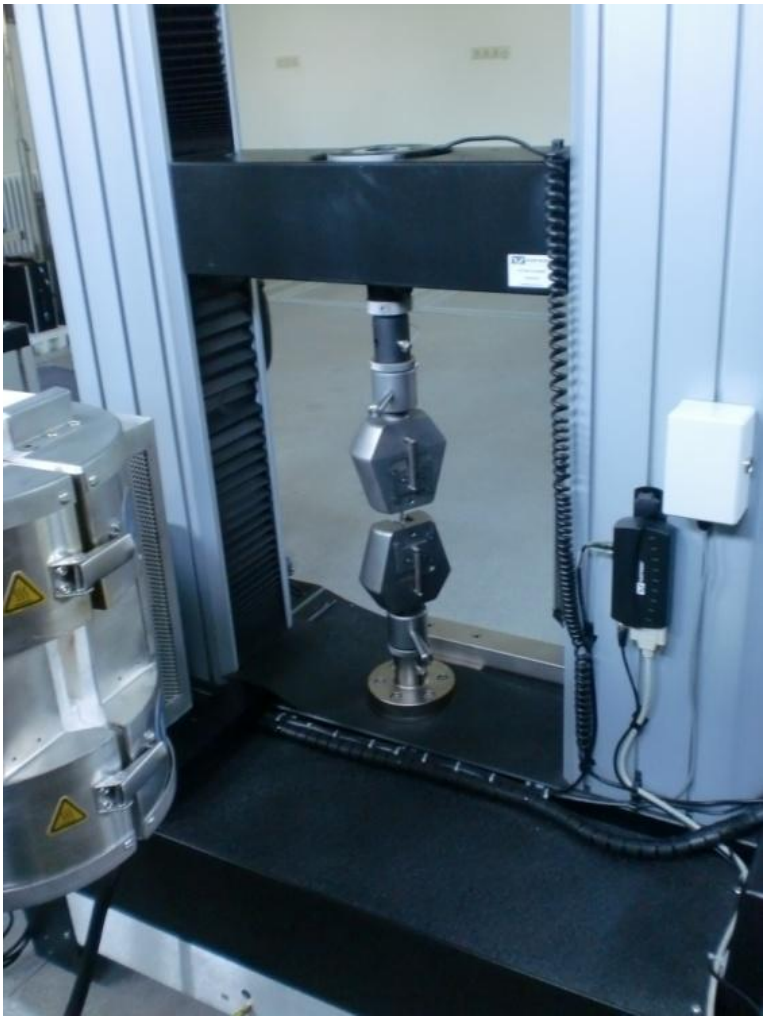

Figure 3.13 : Instron 5582 universal testing machine

CHAPTER 4

RESULTS and DISCUSSION

In this study effects of casting temperature, section thickness, and position in the die on the mechanical properties of hpdc Mg AZ91 alloy are investigated. Microhardness measurements are also conducted to reveal a dependence on yield strength.

4.1 Determination of Filling time, V_1 and V_2 speeds

To determine filling time average thickness of the cast part (t), fraction of solid entering into the die (S), melting temperature (T_m), and fluidty temperature (T_f) of the alloy are need to be known. T_f and S are 500 °C and 20% respectively, which are assumed constant for all casting processes in this study . T_m and t values, and calculated filling times are given in the table.

Table 4.1: Calculated filling times from equation 2.1

cast part	t (mm)	T_m (°C)	t_f (s)
1	4	650	0.068
1	4	670	0.083
2	2	685	0.038
3	2.5	645	0.043
3	2.5	675	0.056

For V_1 and V_2 calculation, fill fraction of the shot sleeve, diameter of the piston, and volume of the casting should be integrated into equations 2.2 and 2.3 Casting of all the parts are carried out in the same hpdc machine with piston diameter of 61 mm and, shot sleeve length of 300 mm. Volume of the shot sleeve is nearly 800 x 10^3 mm^3. Calculated V_1 ,and V_2 speeds can be seen in the table 4.2 .

Table 4.2 : Calculated V_1 ,and V_2 speeds

cast part	T_m (°C)	$v_{casting}$ (mm^3)	$f_{shotsleeve}$	V_1 (m/s)	V_2 (m/s)
1	650	522 x 10^3	0.65	0.314	2.627
1	670	522 x 10^3	0.65	0.314	2.152
2	685	347 x 10^3	0.43	0.512	3.125
3	645	347 x 10^3	0.56	0.395	3.581
3	670	450 x 10^3	0.56	0.395	2.75

4.2 Casting Simulation

As mentioned before, V_1 is the velocity of the piston until the first melt droplets reaches to the die cavity from the shot sleeve. Calculated V_1 values were checked by using the simulation software by selecting V_1 values as 0.15 m/s, 0.5 m/s, and 1.0 m/s. Figures 4.3 (a-c) are taken from the software , showing the left air in the piston by red regions. In figure 4.3: a- velocity of 0.15 m/s is low and a turbulence is occuring in the shot sleeve, encapsulating air in the liquid wave and dragging air into the cast part. In figure 4.3: b- velocity of 1.0 m/s is high, therefore it causes a wave and air is entrapped in the flowing melt in the region where the direction of flow is changing. Optimum slow shot velocity was found to be 0.5 m/s which is very close to the calculated values. By using that parameter, piston forces the liquid to form a wave which does not cause an air entrappment. Therefore there will be very little porosity in the cast part because of air entrappment in the shot sleeve. The porosity related to air in this samples may arise because of the turbulences of liquid flow in the die cavity. Filling analysis can also aid the design of a die. Avoiding turbulences, location of the gating, and location of the overflows can be also be checked after the draft design of the cast part. For example in cast part 3 there is a front encounter of liquid waves which is shown in figure 4.5: h. In that region front encounter cannot be avoided, because of the monitor space in the component. However, possible porosity in the front encounter zone can be eliminated by placing the overflow above or below that region. Correct location of overflow, drag the porosity out of the cast part to the overflow.

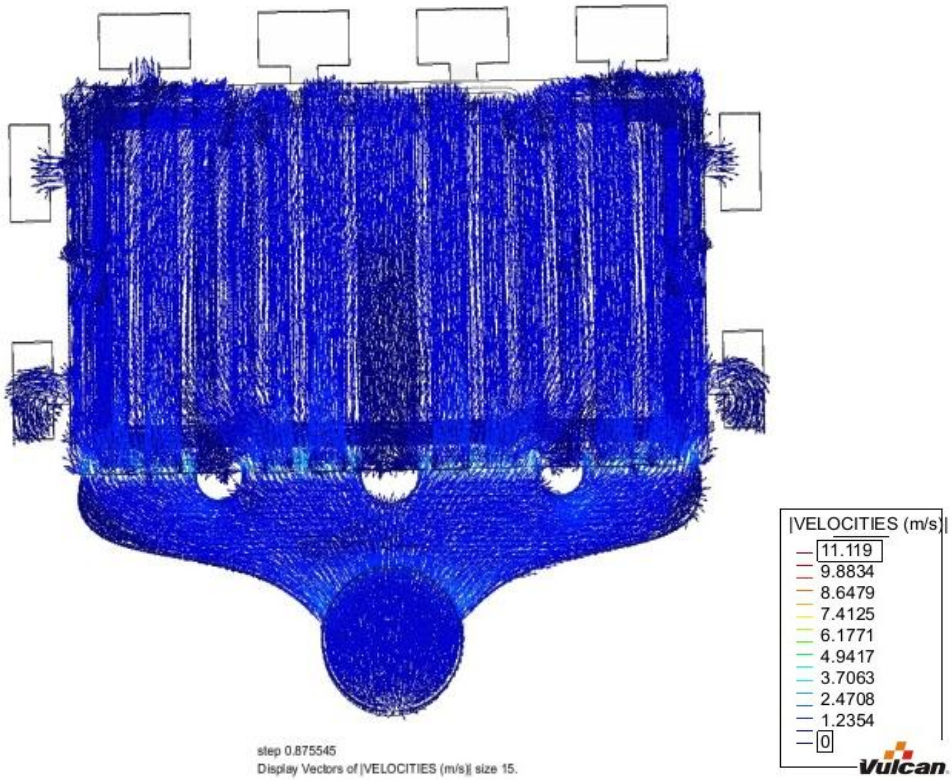

Figure 4.1 : Filling analysis showing vectors of liquid flow

V_2 value must be high not to allow solidification of liquid alloy before filling the cavity properly and it should be as slow as possible not to cause atomization of liquid when entering to the die cavity. Calculated V_2 values are very close to the velocity limit of the hpdc machine, V_2 of cast part 2, and cast part 3 casted at 650ºC are even above the limit. Therefore, slower second phase velocities were needed to be used in manufacturing. V_2 = 2.5 m/s was used in casting processes because simulation with V_2 = 2.5 m/s did not reveal any gas related porosity.

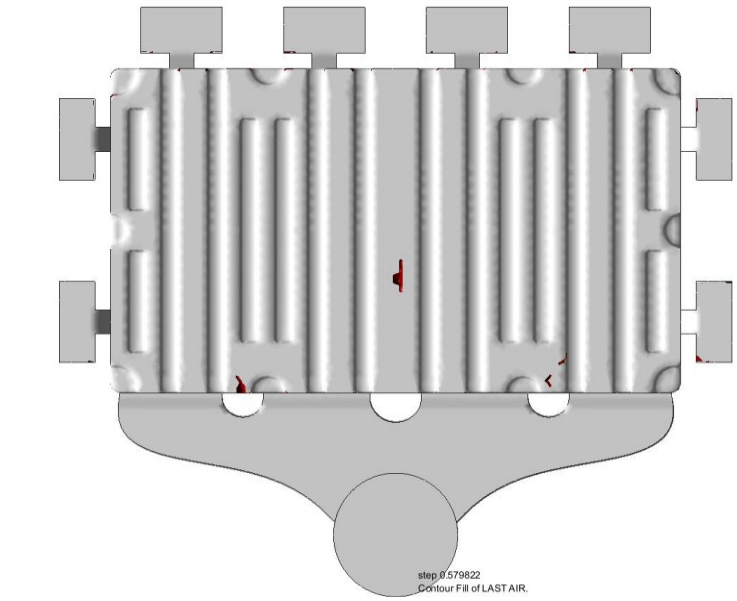

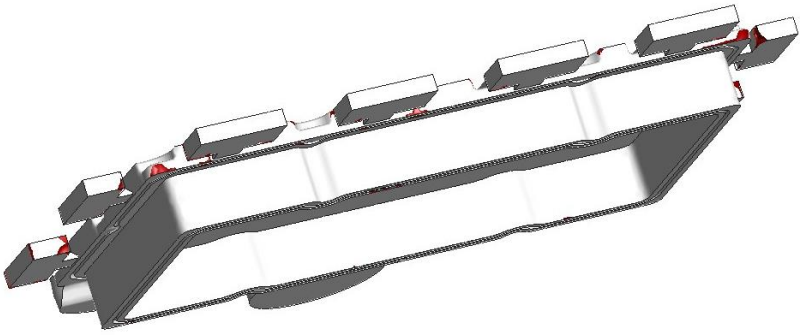

Figure 4.2: cast part 1 simulation results, air left is shown by red regions, Tm=645ºC, V_1=0.15 m/s, V_2=1.5 m/s

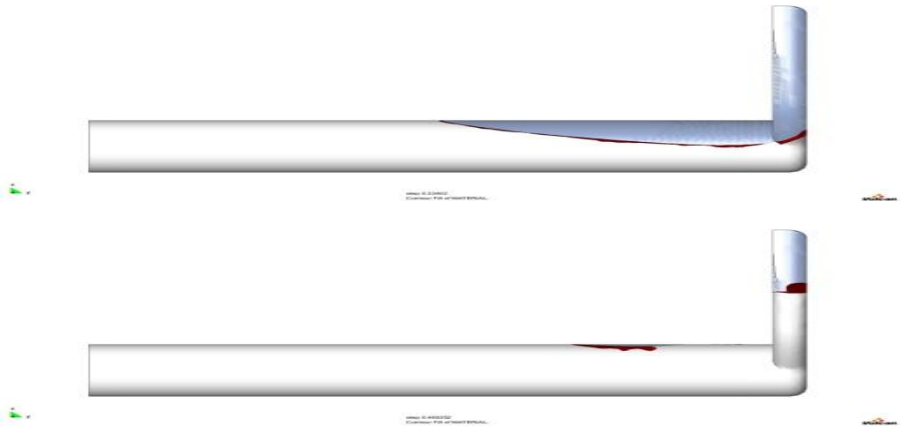

Figure 4.3: a- Flow of liquid in the shot sleeve with V_1 speed 0.15 m/s

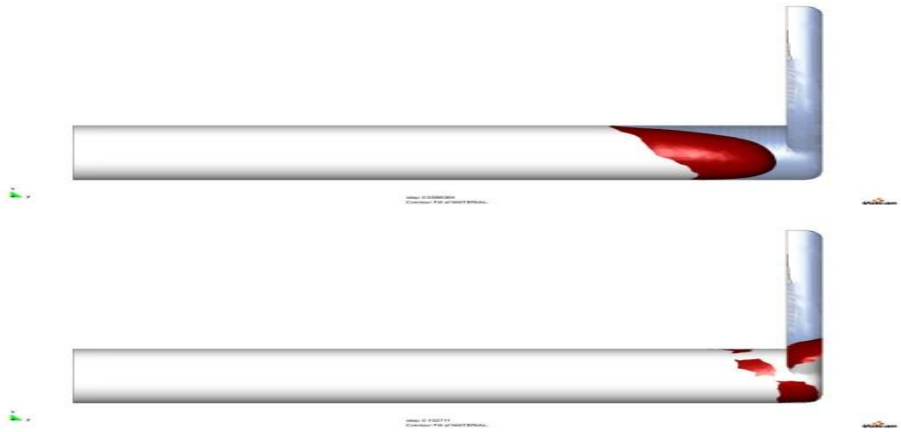

Figure 4.3: b- Flow of liquid in the shot sleeve with V_1 speed 1.0 m/s

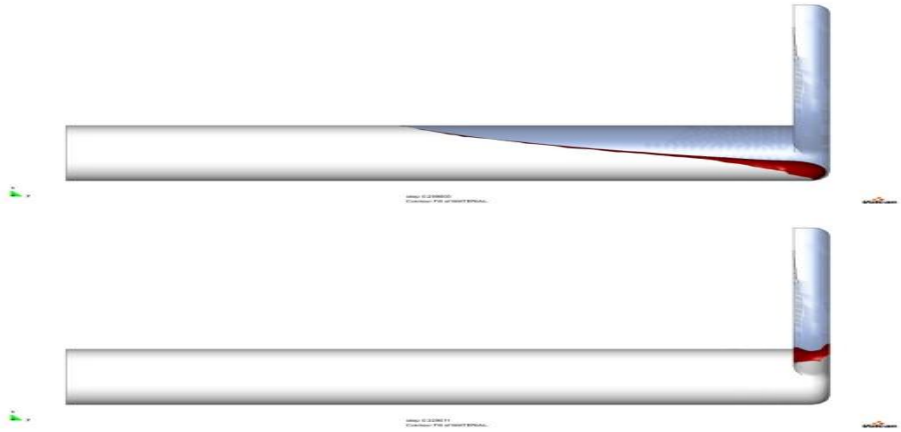

Figure 4.3: c- Flow of liquid in the shot sleeve with V_1 speed 0.5 m/s

V_1=0.15 m/s , and V_2=1.5 m/s values for casting part 1 are not appropriate parameters for casting Mg alloys as seen in table 4.2. However, as the calculated values are pushing the limit of piston speed of the hpdc machine, casting was conducted by slower shot velocities tabulated in table 4.3. It is expected to have large air related porosity in the cast parts according to the simulation. As the superheated liquid comes in contact with relatively cool die, temperature of the liquid immediately decreases. If the section thickness of cast part is small in other words surface area is large, cooling rate is very high which may even lead to unfilling of the die. Therefore if the cast part is small in section thickness, either the melt superheat or the injection speed must be sufficiently high to properly fill the die.

Figure 4.2 shows the possible porosity regions colored in red. The real case can be seen in figure 4.4. A tensile specimen near the gating was machined from the cast part 1 which is casted at 650 ºC. There are large amount of porosity present in the machined zones. As mentioned previously in hpdc parts porosity generally lies inside of the cast part, no porosity can be seen in the surface of the part due to the phenomena called skin layer.

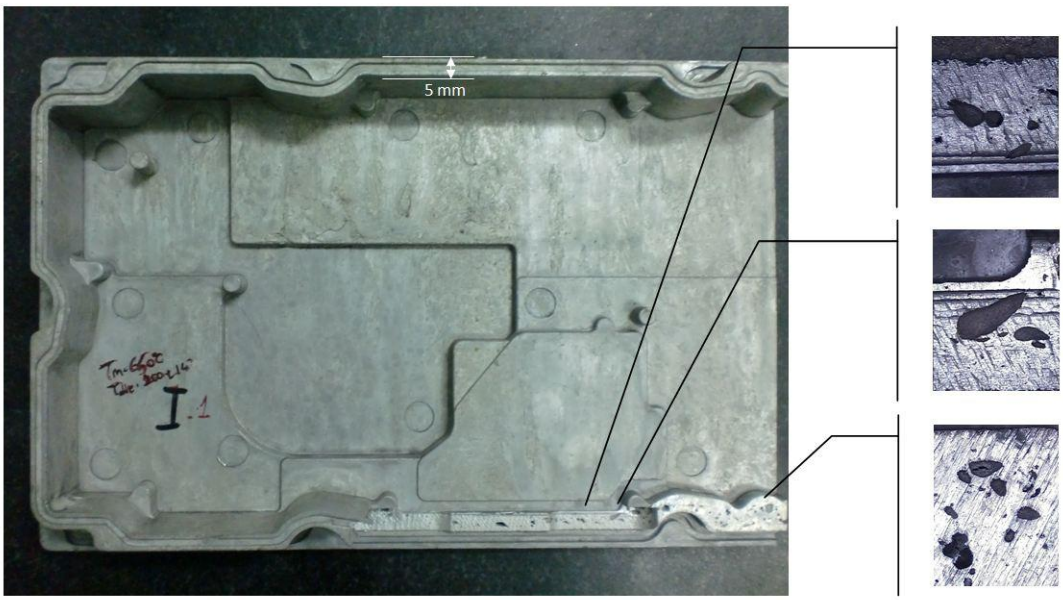

Figure 4.4 : Air porosity in cast part 1 casted at 650 ºC

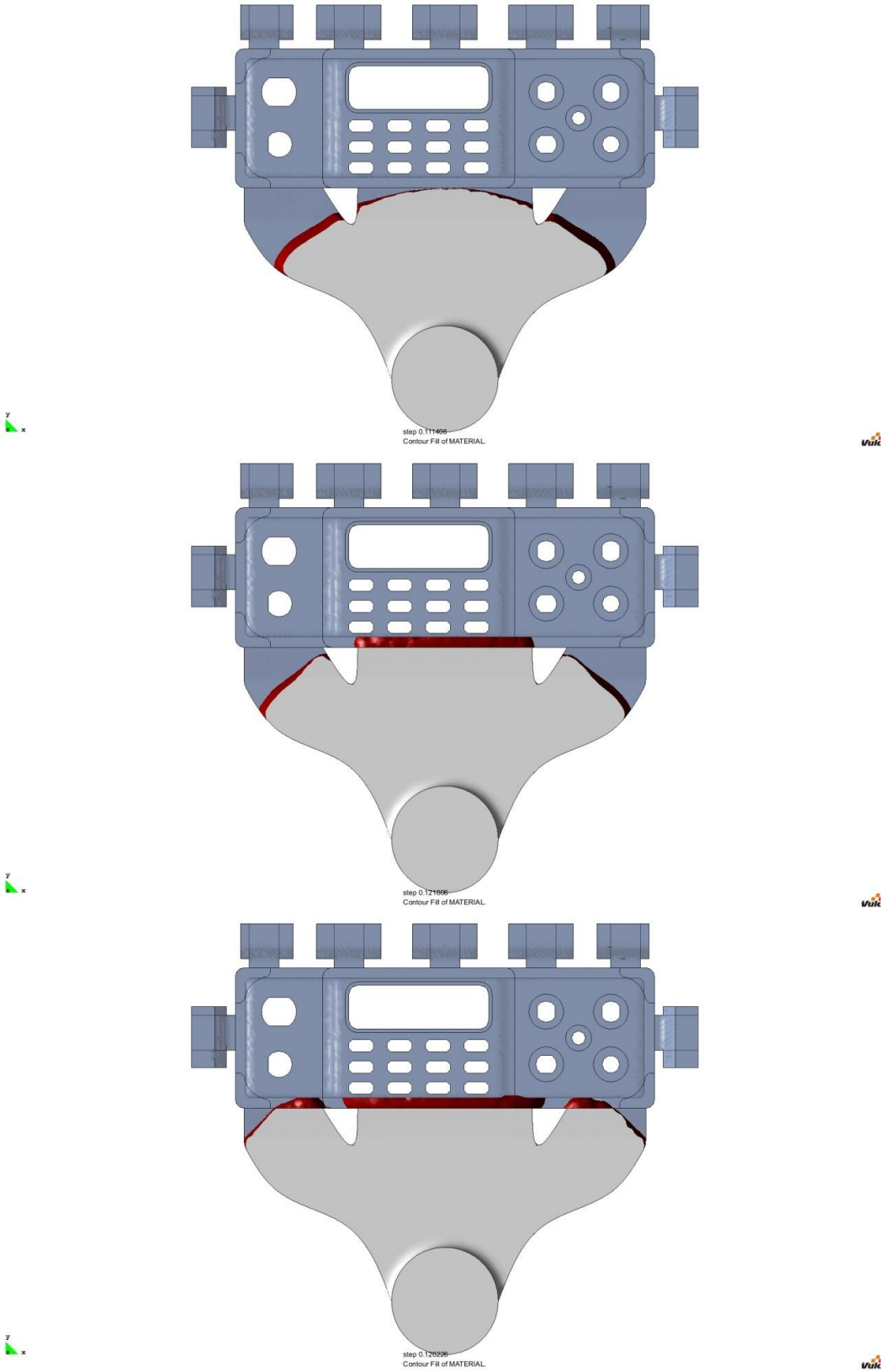

Figure 4.5 : (a-c) Filling simulation of cast part 3, T_m =645 °C, V_1=0.5 m/s, V_2=2.5m/s

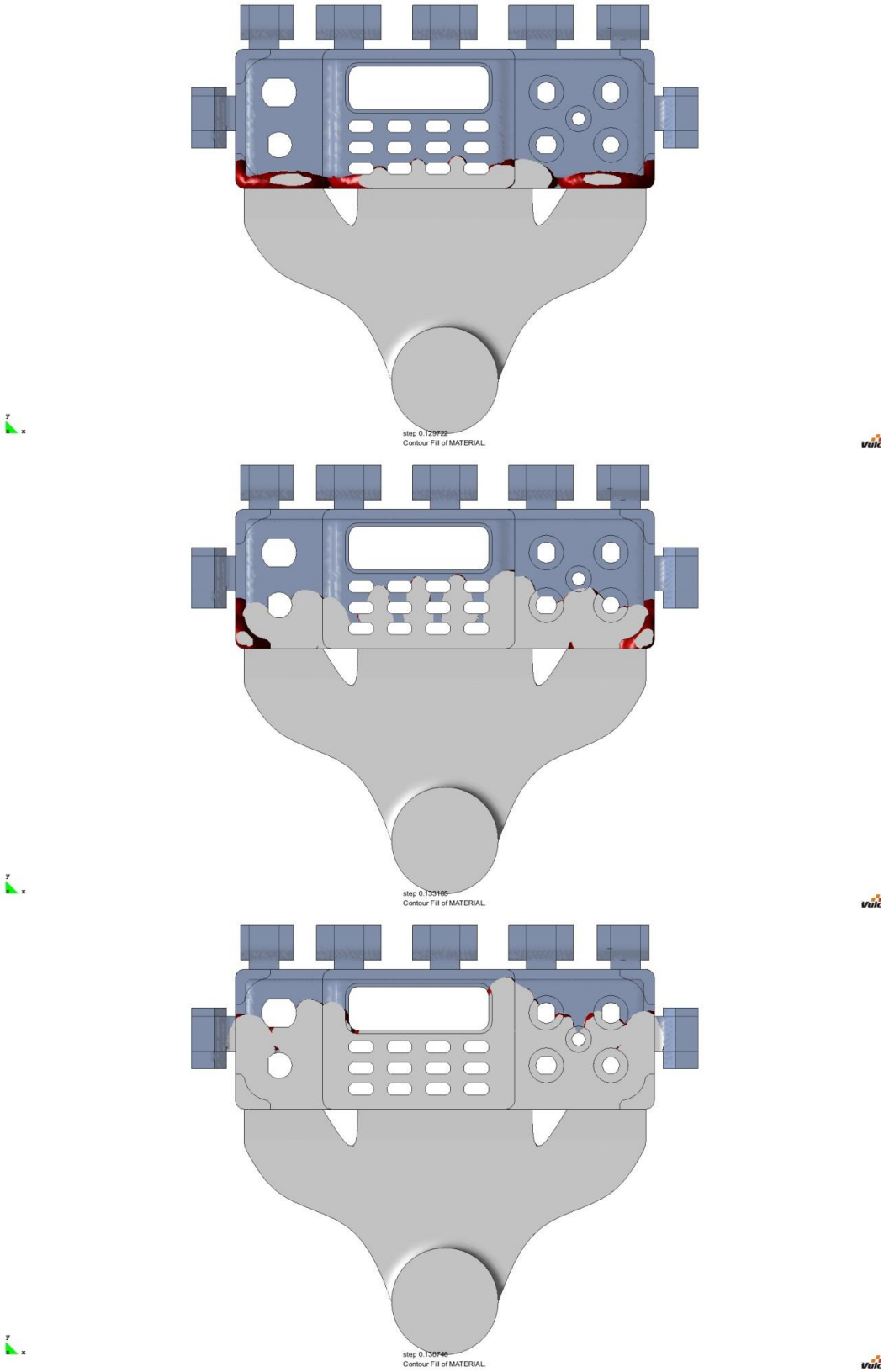

Figure 4.5 : (d-f) Filling simulation of cast part 3, T_m =645 °C, V_1=0.5 m/s, V_2=2.5m/s (contiuned)

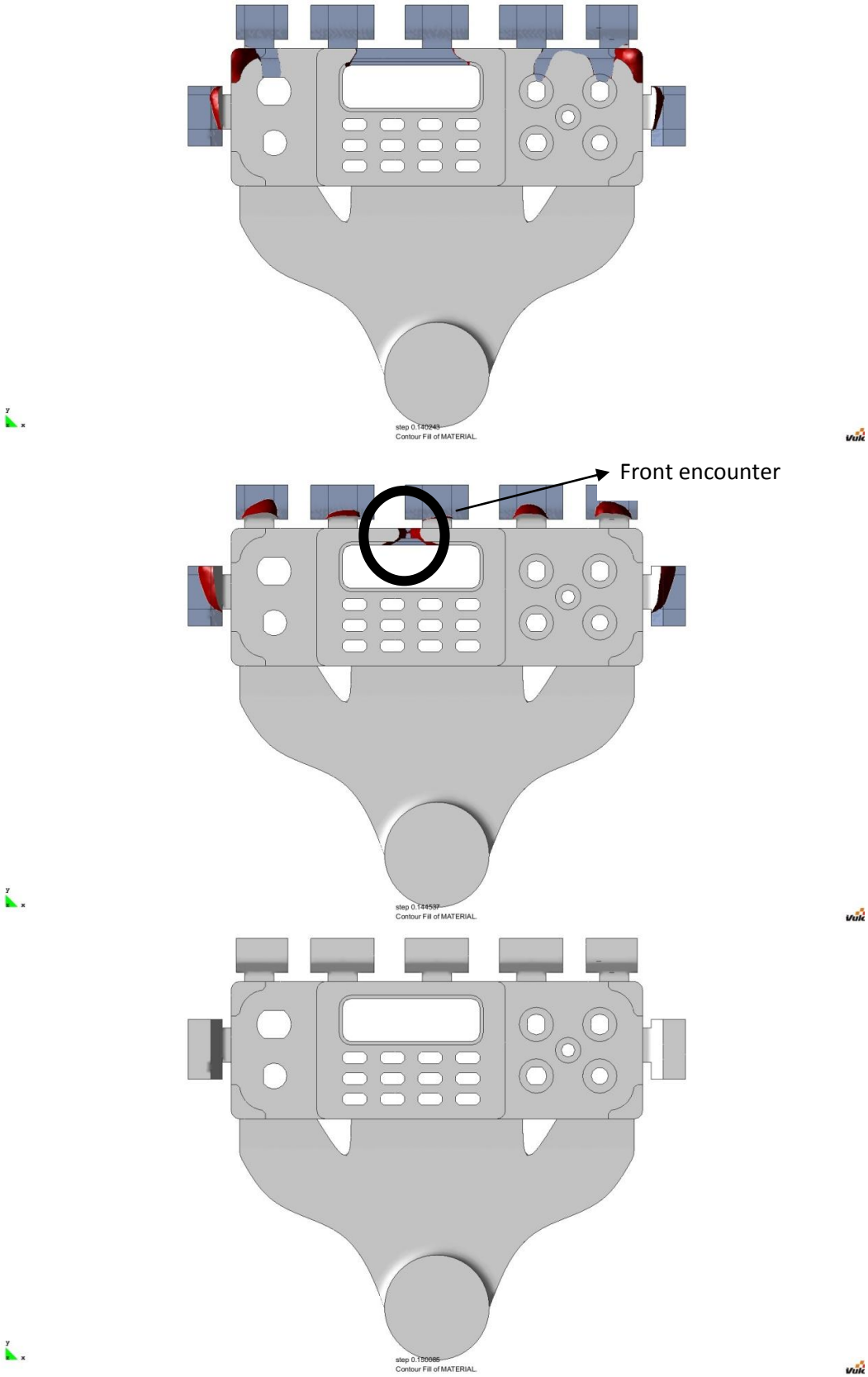

Figure 4.5 : (g-i) Filling simulation of cast part 3, T_m =645 °C, V_1=0.5 m/s, V_2=2.5m/s (contiuned)

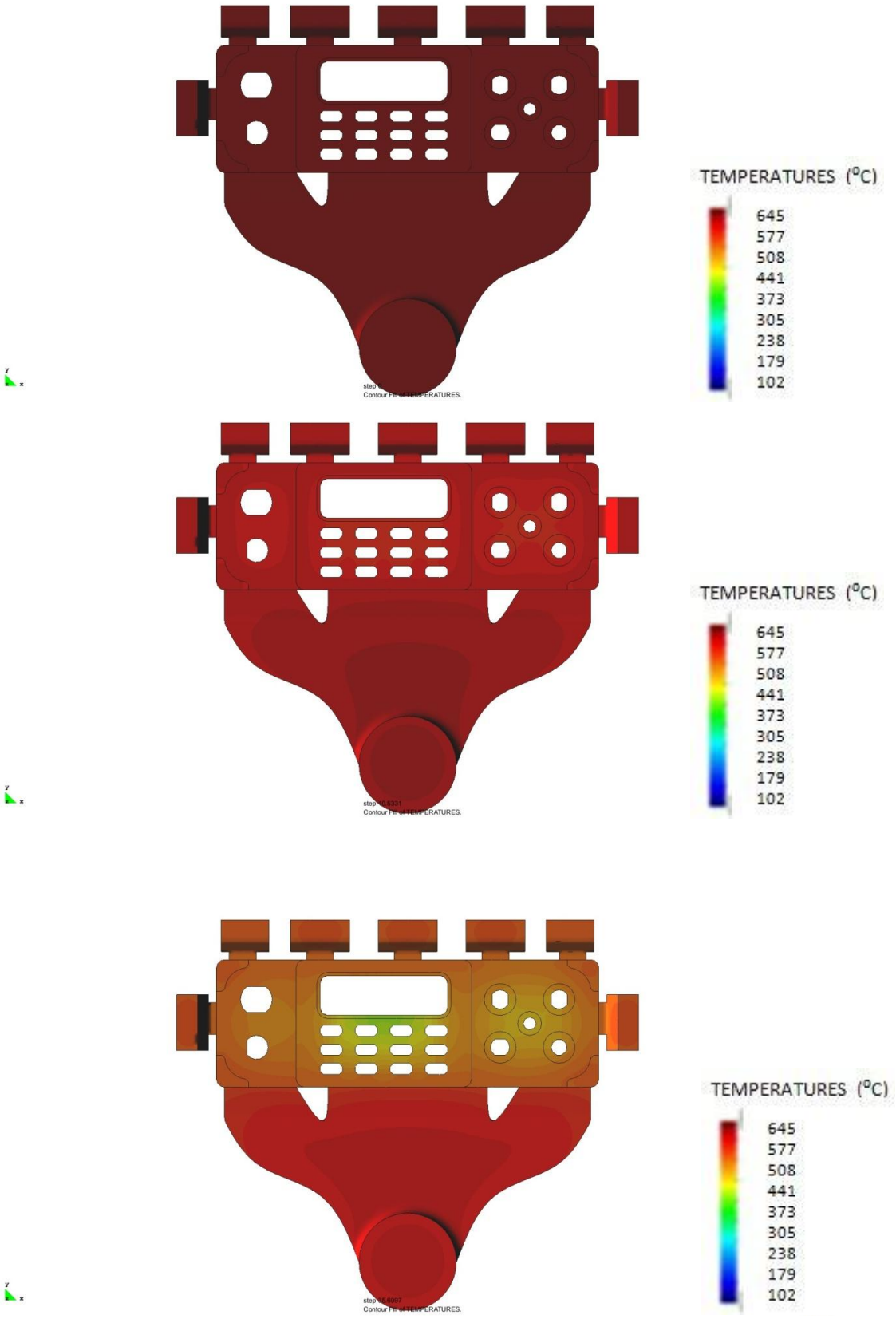

Figure 4.6 : (a-c) Temperature evolution analysis, T_m =645 °C, V_1=0.5 m/s, V_2=2.5m/s

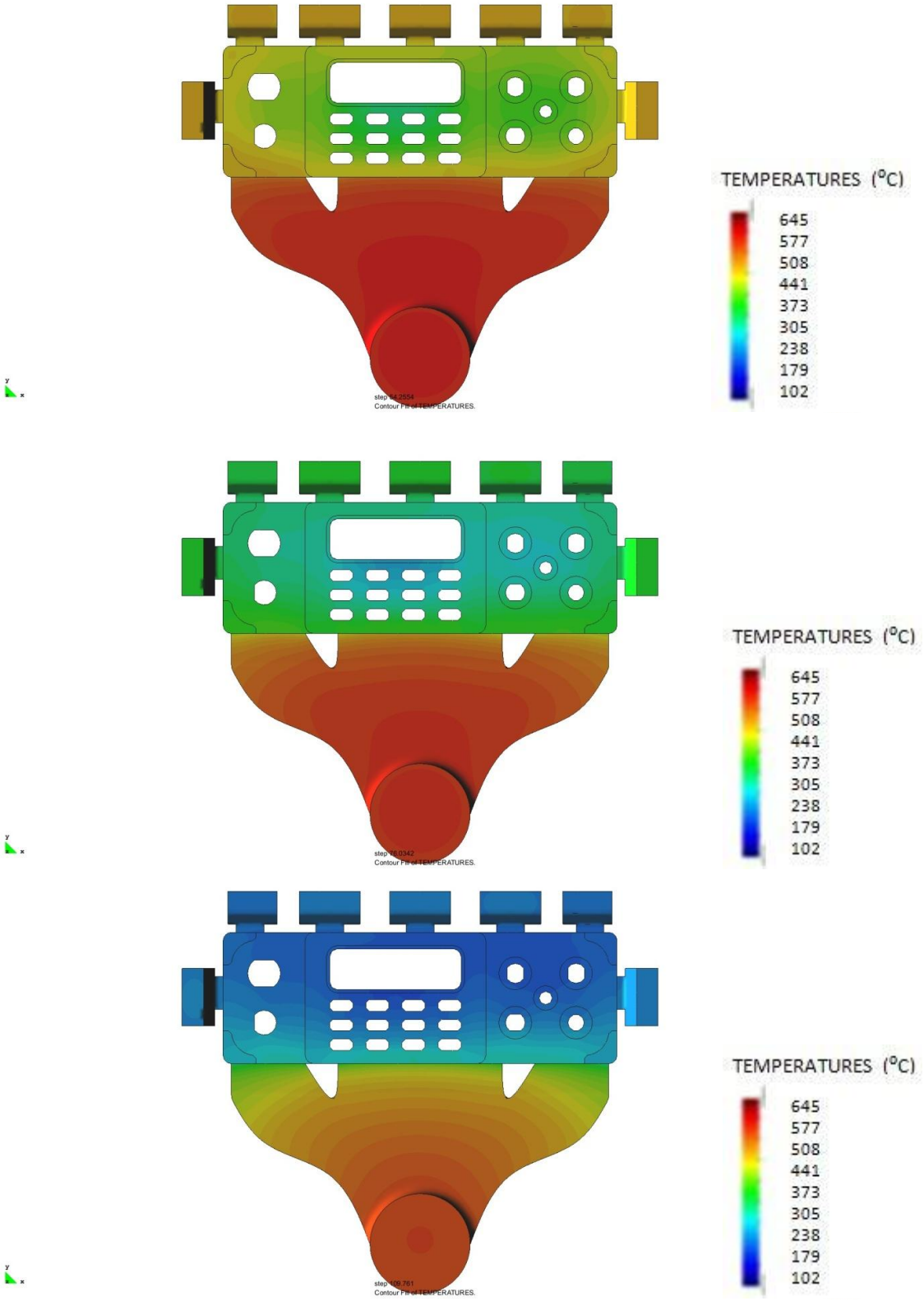

Figure 4.6 : (d-f) Temperature evolution analysis, T_m =645 °C, V_1=0.5 m/s, V_2=2.5m/s (contiuned)

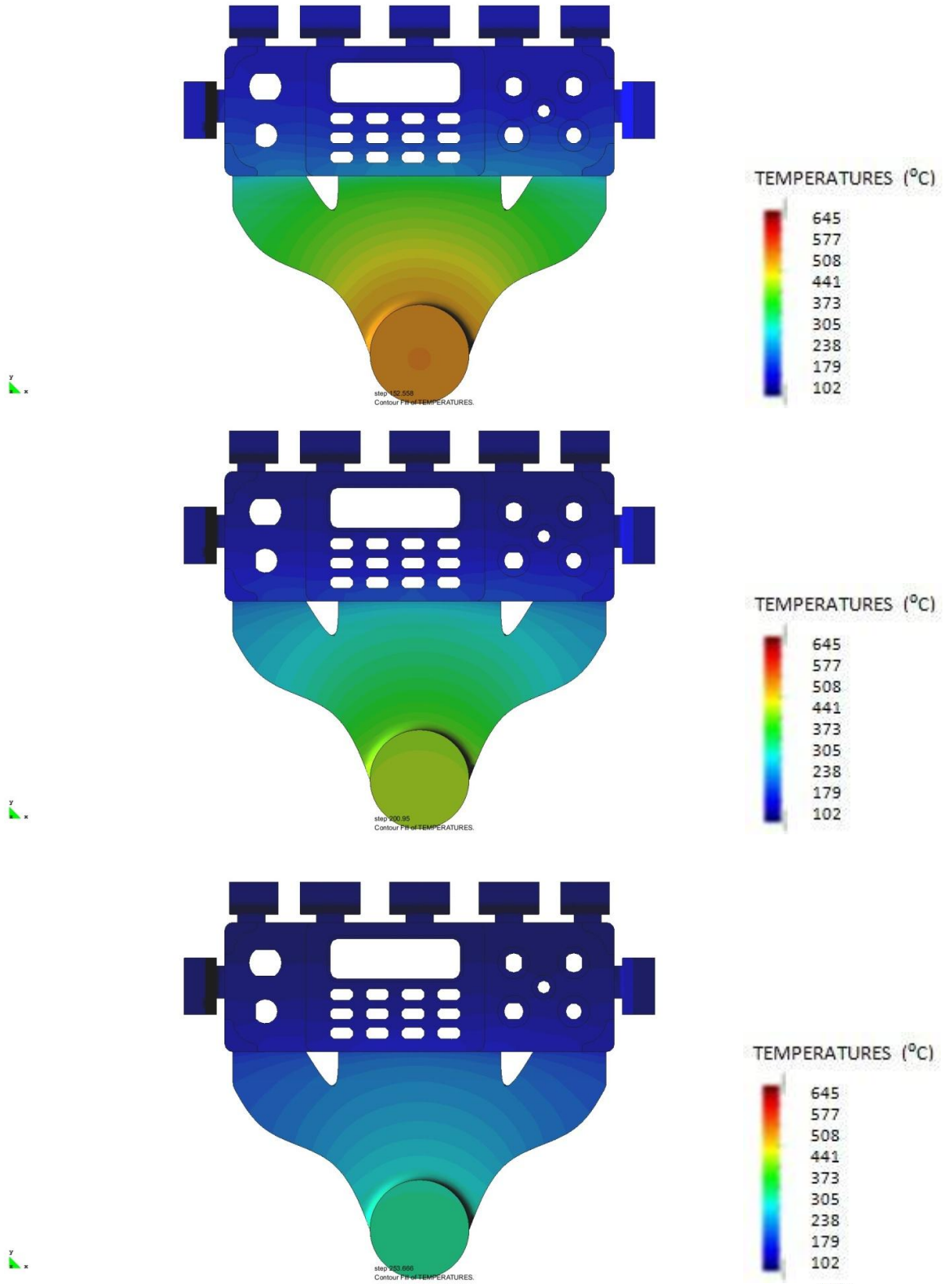

Figure 4.6 : (g-i) Temperature evolution analysis, T_m =645 °C, V_1=0.5 m/s, V_2=2.5m/s (contiuned)

Other than filling analysis, temperature evolution of the melt can be monitored by using the Vulcan casting simulation software. Anticipation of the potential shrinkage regions is possible by following temperature evolution. On the other hand, it is also possible to draw the cooling curves of specified points on the cast part. Cooling curves give an indication of relative grain size, it is suggested that lower cooling rate gives larger sized grains. A temperature evolution analysis can be seen through figures 4.6 : (a-i)

4.3 Manufacturing of the Specimens

Each part is high pressure die casted with the casting parameters shown in table 4.3. Melting temperature of the magnesium alloy should be selected 30 – 90 ºC above the actual melting temperature of the alloy depending on the geometry of the cast part. Selecting low melting temperatures causes problems in filling of the die, if the casting geometry has thin sections. On the other hand, high melting temperatures causes air porosity inside the cast parts. At high temperatures gases are dissolved in magnesium melt, during cooling they form porosity due the decrease in dissolving ability of gases in the magnesium alloy. Melting temperautes of the cast part 1 and 3 are selected very close to each other as their section thicknesses are similar. Cast part 2 has smaller section thickness and melting temperature is higher than other cast parts because of this reason. Tensile strengths of the cast parts are compared in following sections.

Injection speed of the cast part 1 is intentionally selected slow, because the maximum injection speed of the hpdc machine is 3 m/s. At low speeds large amount of porosity is seen in cast part 1 because low injection speeds causes air entrappment and also problems about proper die filling arises. To avoid this problems calculated injection speeds should be used. Calculated injection speeds are very high, but although the limits of the hpdc machine is forced, cast part 2 and 3 are casted at high injections speeds to fill the die cavity properly and avoid large gas porosities related to air entrappment.

Table 4.3 : Casting parameters

cast part	T_m (ºC)	T_{die} (ºC)	V_1 (m/s)	V_2 (m/s)	P_i (MPa)
1	650	200	0.15	1.5	30
1	670	200	0.15	1.5	30
2	685	200	0.5	2.5	30
3	645	200	0.5	2.5	30
3	675	200	0.5	2.5	30

4.4 Microscopy

Microscopy investigation is carried out by both optical microscopy and SEM. Figure 4.7 is a SEM picture of a cast part 3 casted at 645 ºC. The grey areas are primary α-Mg, the darkest areas surrounding whole microstructure are high Al content eutectic α - Mg and the lightest areas are eutectic phase β - $Mg_{17}Al_{12}$.

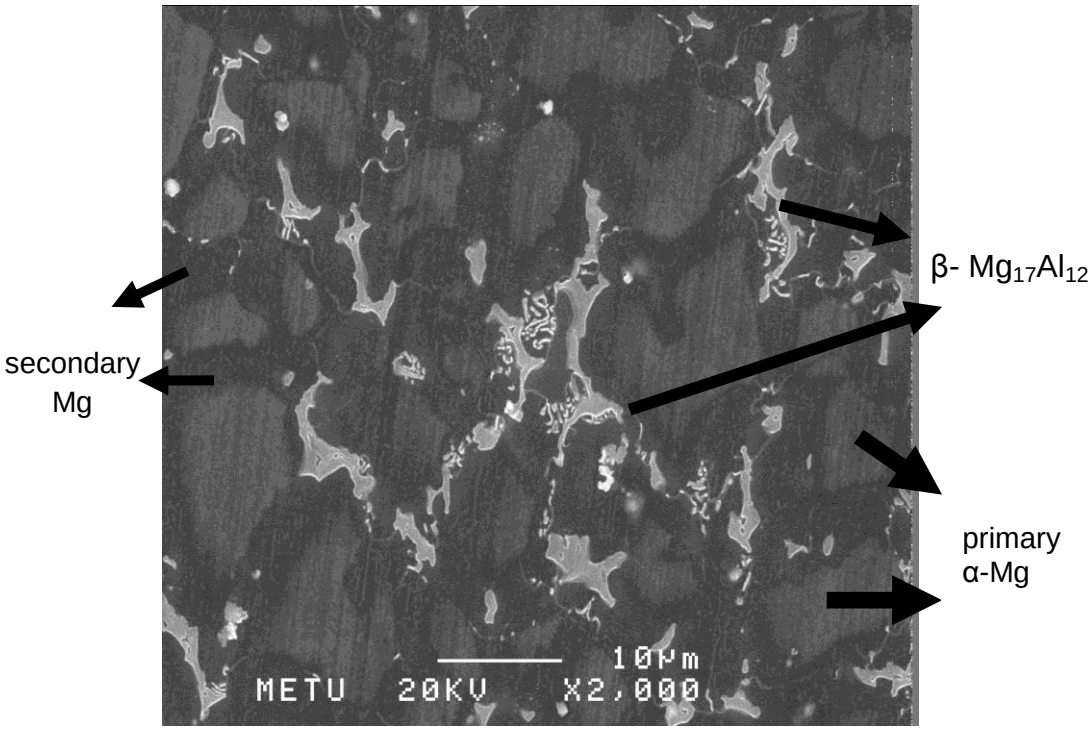

Figure 4.7 : Cast part 3, T_m=645 ºC , SEM 2000X magnification

In figure 4.8 presolidified α- Mg grains can be seen, which form in the shot sleeve. It occurs in all hpdc casting processes. If the shot sleeve temperature is low,

probability to see presolidifed grains, and their sizes increases. The presolidified grains are up to 20 times larger than other grains, which decreases the tensile properties of the cast part if present in large amounts.

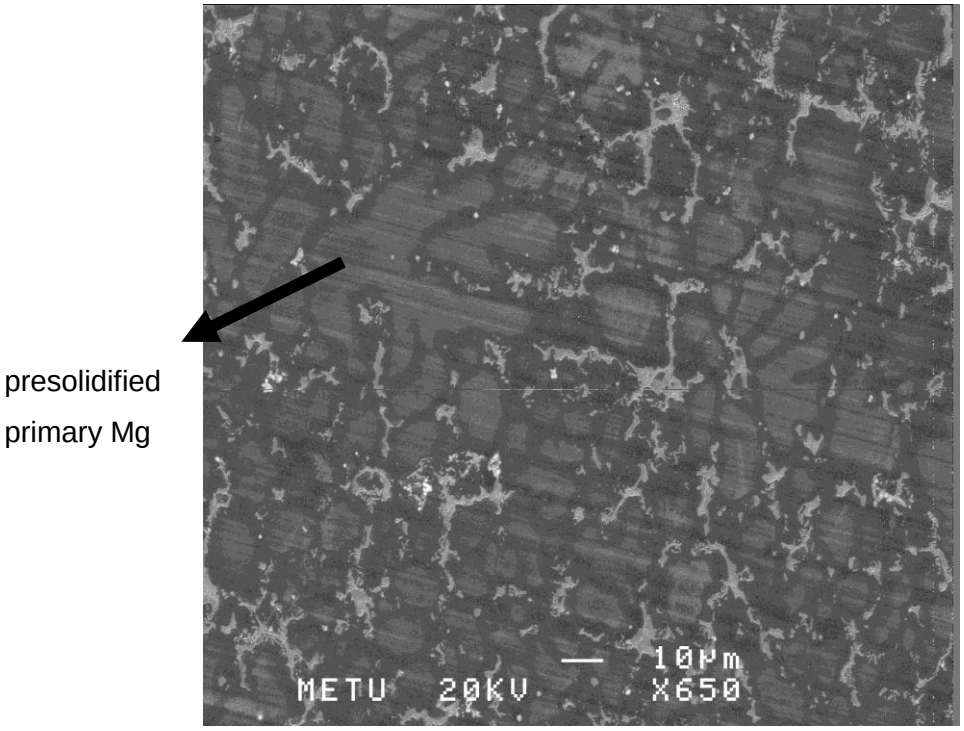

Figure 4.8: Cast part 3, T_m=645 ºC , SEM 650X magnification

Porosity investigation is carried out on the polished optical microscopy pictures. However SEM pictures reveal both gas related pores, and shrinkage related pores. Gas related pores are spherical in shape and generally larger than shrinkage related pores, which have irregular shapes. Shrinkage related pores are formed near the grain boundaries of primary and eutectic phases. Figure 4.10 and 4.11 show SEM pictures of gas pores and shrinkage pores respectively.

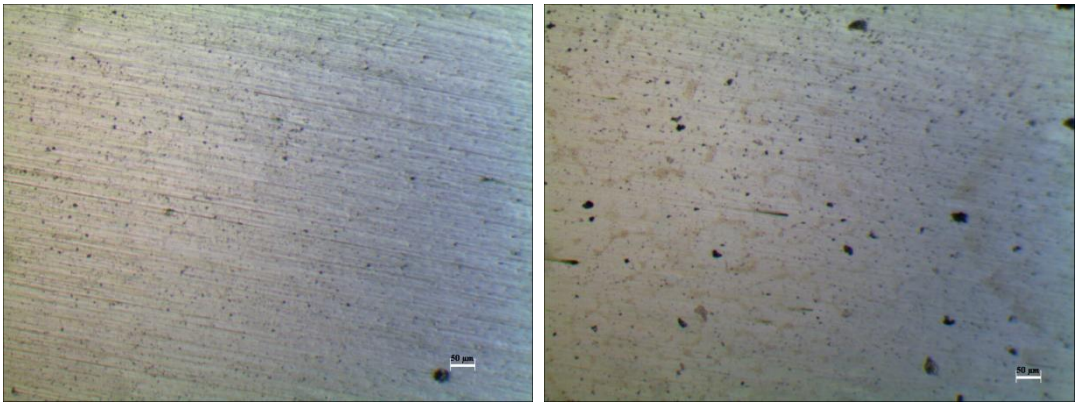

Figure 4.9:a- Cast part 3, T_m= 645 gate section ; 4.9: b- cast part 3 T_m= 645 overflow section, optical microscopy, polished specimens 100x magnification

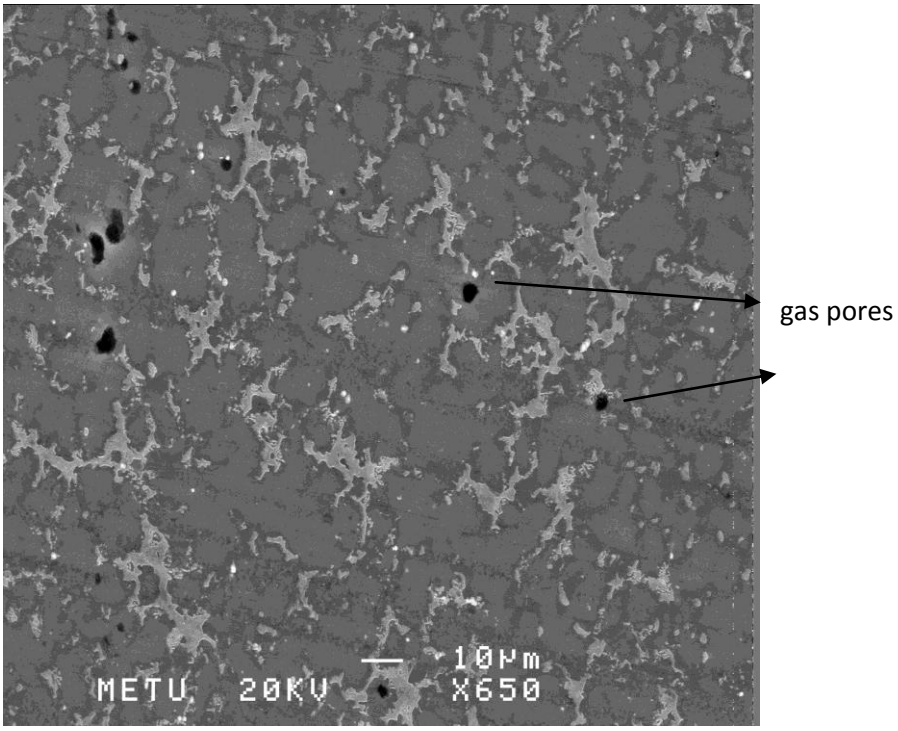

Figure 4.10 : Cast part 3, T_m=675 ºC , SEM 650X magnification

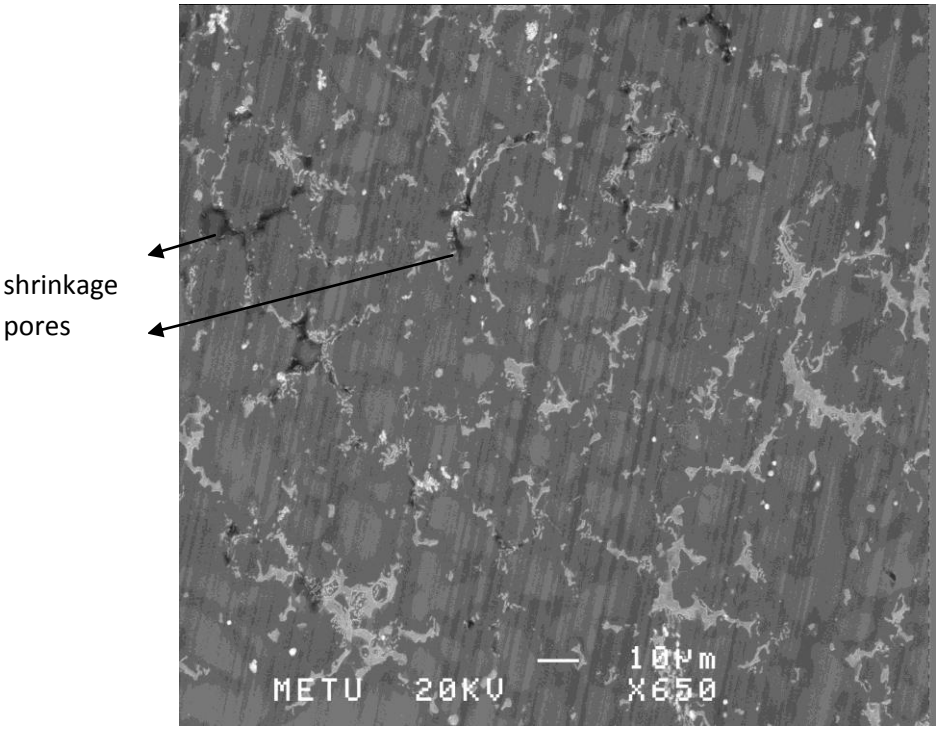

Figure 4.11 : Cast part 3, T_m=645 ºC , SEM 650X magnification

4.5 EDS results

EDS results are taken from the primary Mg and eutectic $Mg_{17}Al_{12}$ regions of cast part 3. Figure 4.12 is the EDS graph for α-Mg region, in that region for 96.03 weight % Mg, there are 3.97 weight % Al present at the α – Mg. In the literature it is suggested that 6 % Al present in α-Mg region, which is slightly higher that 3.97% in that study. Concentration of elements in primary or eutectic zones depend on solidification rate of the alloys. Figure 4.13 is the EDS graph for β- $Mg_{17}Al_{12}$ region. In eutectic zone of the samples of this study, there are 77.66 % Mg, 19.84 % Al, and 2.50 % Zn . In the literature 35 % Al is found to be in the for β- $Mg_{17}Al_{12}$ region which shows a higher Al content.[43] Differences in local solidification rates due to uncontrolled die temperaure or different temperatures of different parts of the die cavity can cause discrepancies to the results in the literature.

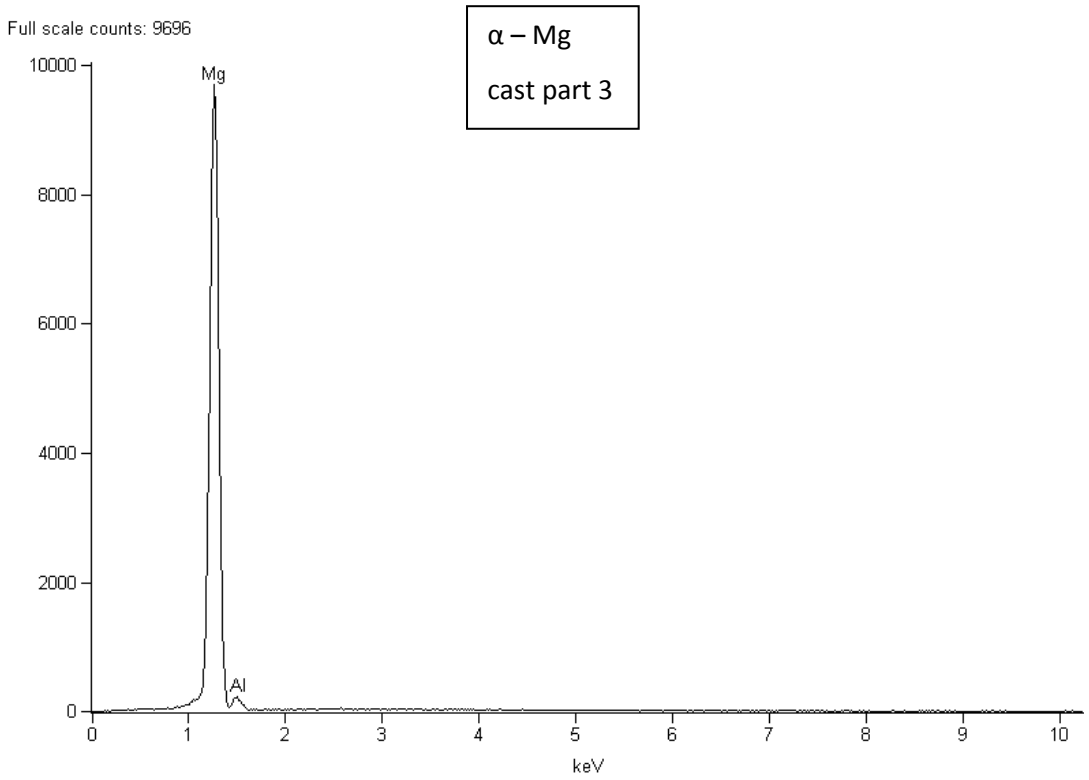

Figure 4.12: EDS graph, α – Mg region , cast part 3

Table 4.4: Compostion table of figure 4.13

Element	*Weight Conc %*	*Atom Conc %*
Mg	96.03	96.41
Al	3.97	3.59

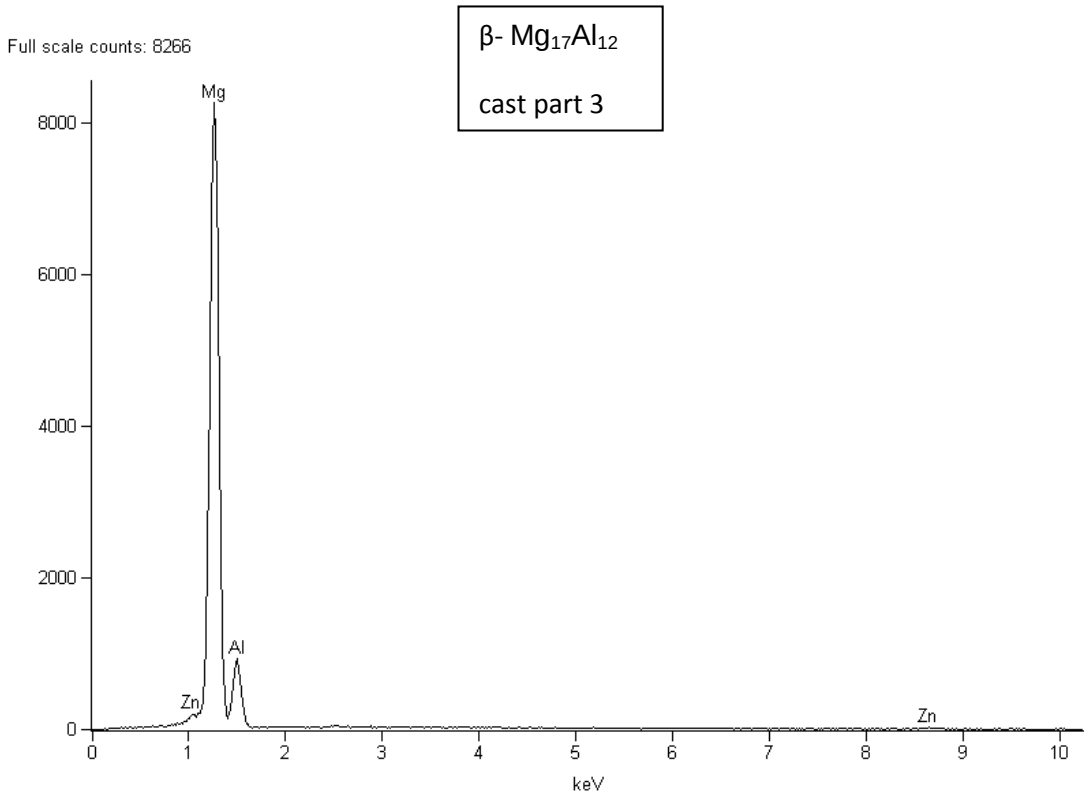

Figure 4.13- EDS graph, β- $Mg_{17}Al_{12}$ region , cast part 3

Table 4.5 : Composition table of figure 4.14

Element	*Weight Conc %*	*Atom Conc %*
Mg	77.66	80.51
Al	19.84	18.52
Zn	2.50	0.96

4.6 Porosity measurements

Porosity contents of the cast part 1 ,2, and 3 were investigated. Porosity contents depending on melting temperature of the alloy and position of the specimen at the die will be clarified. As expected from the casting simulation, cast 1 part has vast amount of porosity in both specimens casted at 650 and 670 ºC.

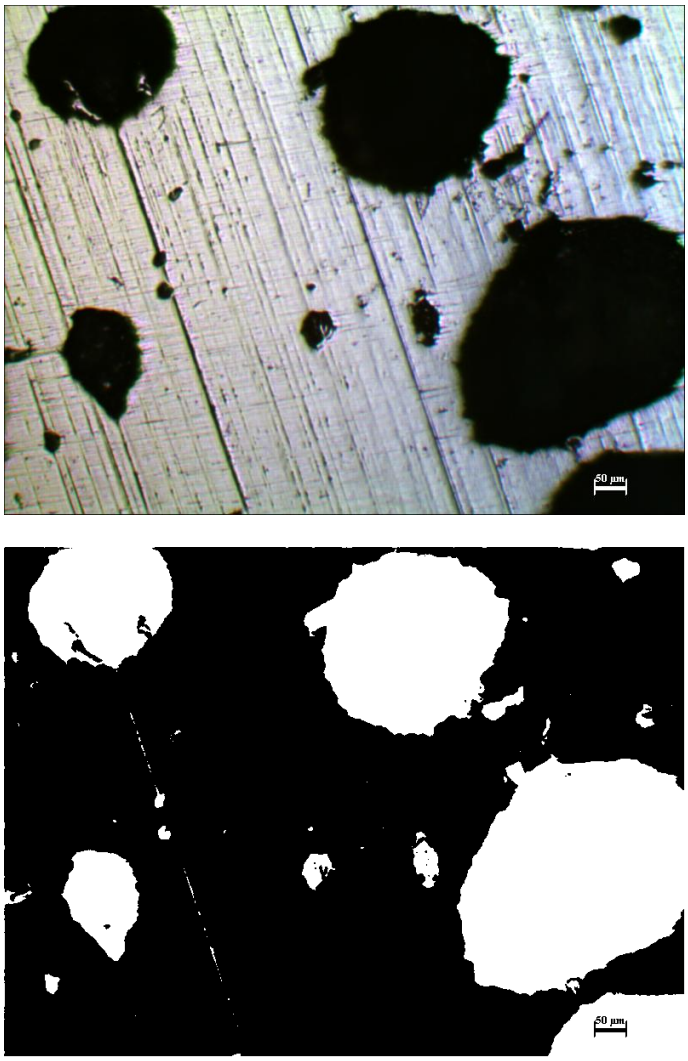

Figure 4.14: a- Cast part 1, T_m =650 ºC, optical microscopy, as polished, 100 X magnification ; 4.15: b- same image, analyzed

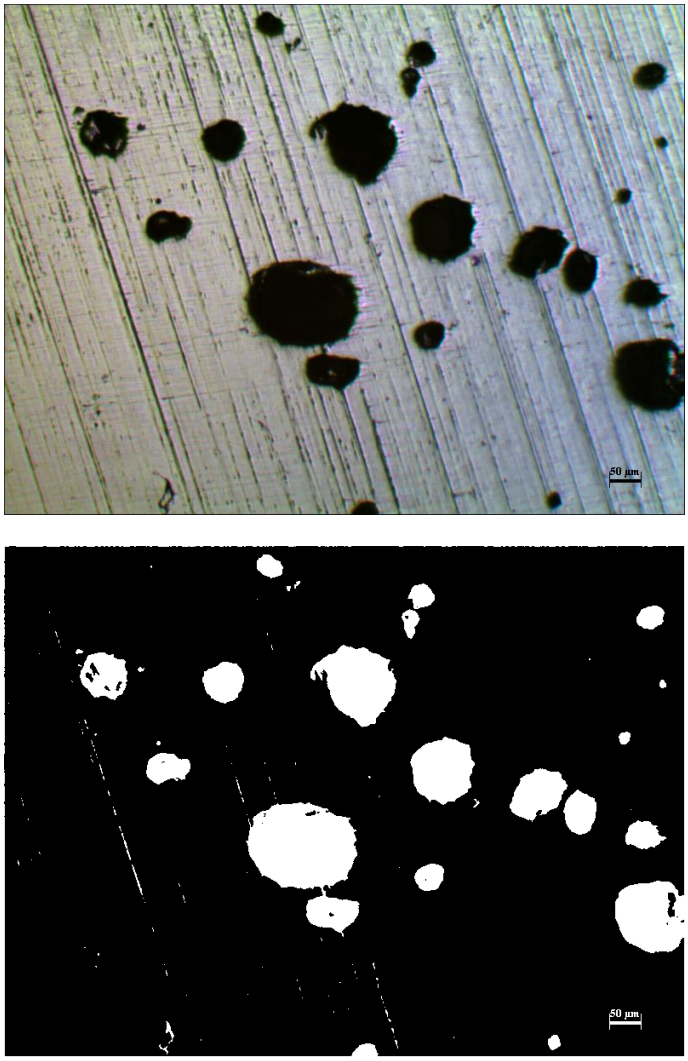

Figure 4.15: a- Cast part 1, 670 ºC,optical microscopy, as polished, 100 X magnification ; 4.16: b- same image, analyzed

It is obivous from the microscopy pictures that amount of porosity is above the acceptable level. But interestingly, porosity level of the specimen casted at 650 ºC is higher than the one casted at 670 ºC . Generally at high temperatures air related porosity is expected to be higher due to high amount of dissolved gases. Therefore it can be said that the porosity in that casting parts are not related to the dissolved gases. The porosity are related to both air entrappment in the shot sleeve, and improper filling of the die cavity due to low injection speeds. As the injection speed is slow, some amount of melt is solidified before complete filling of the die. Thin sections cannot filled at such cases. For cast part 1 it can be said that porosity is decreasing from 40% to 20 % by increasing the melt temperature of the alloy from 650 to 670 ºC. But that proposition is only true for low injection speeds of the plunger which cannot fill the die cavity properly.

Increasing injection speeds for the cast part 2 yielded in good filling of the die cavity, thus decreasing the porosity contents close to the values in the literature. Five samples from 2 and 4 mm sections of the cast part 2 which is casted at 685 ºC were investigated on microscope, and analyzed at the image anaylzing software. Results can be seen in table 4.6. It is clear that the average porosity content is decrasing from 2.53 ± 0.49 % to 2.08 ± 0.45 % with decreasing section thickness, which is expected to increase the mechanical properties of the cast parts.

Increasing injection speeds for the cast part 3 also yielded in good filling of the die cavity. Results can be seen in table 4.7. Three samples for each section were investigated on microscope and average porosity values are published. In contrast to cast part 1, porosity content is increasing with increasing melting temperature. In gate sections average porosity increases from 1.38 ± 0.04% to 2.31 ± 0.39 %, while T_m is increasing from 645 ºC to 675 ºC. In overflow sections, porosity content increases from 2.14 ± 0.05 % to 2.54 ± 0.2 % as T_m is increasing from 645 ºC to 675 ºC. That is the expected result for porosity content depending on temperature of the melt, as the dissolved gases in magnesium melt increases with temperature.

Effect of position on the porosity content is clearly seen from the table. Porosity content of the gate section of specimen casted at 645 ºC is 1.38 ± 0.04 %, while it is 2.14 ± 0.05% in overflow section. Similarly porosity increses from 2.31 ± 0.39 % to 2.54 ± 0.2 % as going far from the gate in specimens casted at 675 ºC. This results is in a good agreement with the reported results suggesting hpdc parts to have inner defects in the regions which are filled last.

Table 4.6 : Porosity contents of cast part 2

	sample #	porosity (%)	average porosity (%)
Mg AZ91 685 °C 2mm section	1	2.26	2.08 ±0.45
	2	2.17	
	3	1.34	
	4	2.1	
	5	2.55	
Mg AZ91 685 °C 4mm section	1	3.14	2.53±0.49
	2	2.28	
	3	2.69	
	4	2.71	
	5	1.84	

Table 4.7 : Porosity contents of cast part 3

	sample #	porosity (%)	average porosity (%)
Mg AZ91 645 °C gate section	1	1.35	1.38±0.04
	2	1.43	
	3	1.37	
Mg AZ91 645 °C overflow section	1	2.17	2.14±0.05
	2	2.17	
	3	2.08	
Mg AZ91 675 °C gate section	1	2.32	2.31±0.39
	2	2.69	
	3	1.91	
Mg AZ91 675 °C overflow section	1	2.69	2.54±0.2
	2	2.62	
	3	2.31	

4. 7 Mechanical Testing

Tensile properties of the magnesium hpdc parts are a function of grain size as mentioned before. Therefore in this section the cooling curves obtained from casting simulation software and grain sizes are first compared, then the results of tensile tests will be studied according to that dependence

As suggested before tensile properties of cast part 1 depend mainly on amount of porosity because of improper filling of the die. The effect of porosity is more significant than the effect of grain size. Therefore cooling curve and grain size investigation were not conducted for this cast part.

Tensile specimens are CNC machined directly from the manufactured part. The specimens from the cast part casted at 650 ºC is numbered as 1. Other specimens from the part casted at 670 ºC is numbered as 2. Specimens close to the gate are symbolized by the letter “a”, and specimens close to the overflows are symbolized by the letter “b”. In figure 4.16 location of the tensile test specimens on the cast part 1 can be seen.

Tensile test results can be seen in table 4.8. It is clear that the cast part 1 casted at higher melting temperatures show higher $\sigma_{0.2}$, UTS, and elongation values. 0.2 % proof strength of samples casted at 650 ºC are 25 MPa lower than the ones casted at 670 ºC. Ultimate tensile strength values show a more significant decrease than 0.2 % proof strength. UTS of samples decreases almost 50 MPa, as T_m decreases from 670 ºC to 650 ºC. Elongation values are higher than expected for such porous parts. It is 3.9 ± 2.40 % for samples casted at 650 ºC, and 5.2 ± 2.51 % for samples are casted at 670 ºC.

For that cast part 1 it can be said that increasing melting temperature of the alloy increases the mechanical properties of the parts. However, $\sigma_{0.2}$ and UTS values are very low compared to the literature. As mentioned before low mechanical properties are associated with the high amount of porosity due to slow injection speeds. Therefore, a general suggestion cannot be made for the effect of T_m on mechanical properties for that sample.

Table 4.8 : Mechanical properties of cast part 1

sample	T_m (°C)	thickness (mm)	$\sigma_{0.2}$ (MPa)	UTS (MPa)	elongation (%)
1a	650	5	82.24	91.14	5.59
1b	650	5	63.55	69.97	2.21
average	650	5	72.9	80.56	3.9
2a	670	5	110.5	147.6	6.98
2b	670	5	85.48	107.48	3.42
average	670	5	97.99	127.54	5.2

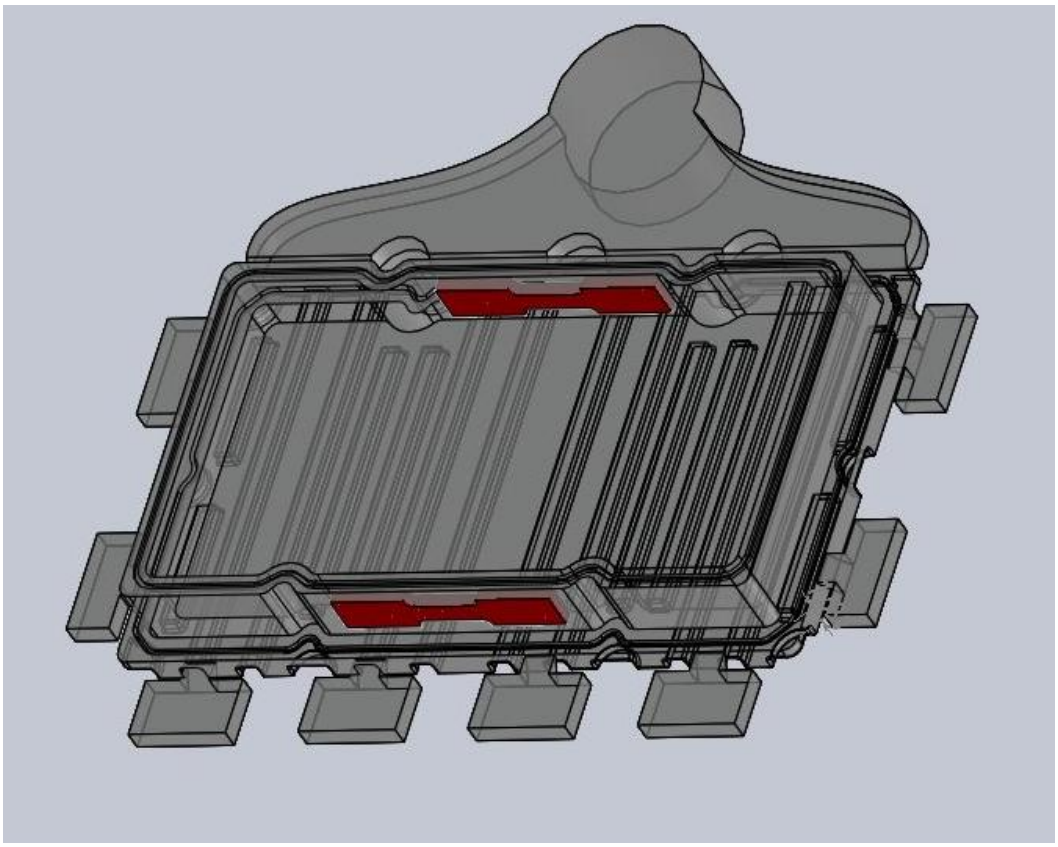

Figure 4.16 : Location of tensile test samples in cast part 1

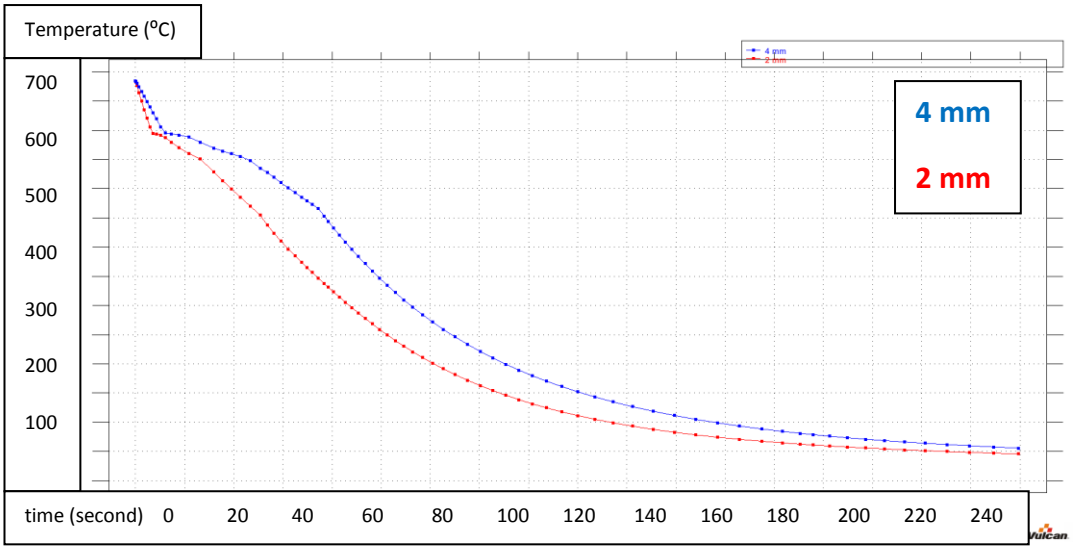

Figure 4.17 : Cooling curve obtained from Vulcan for cast part 2

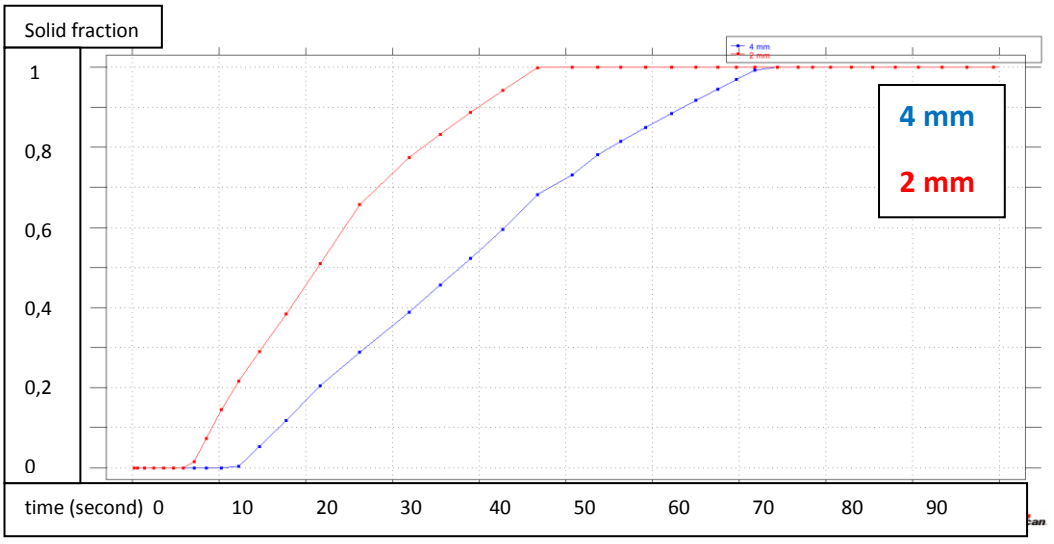

Figure 4.18 : Solid fraction vs time curve obtained from Vulcan for cast part 2

Cooling curve and the solid fraction vs time graphs of cast part 2 which is casted at 685 °C can be seen in the figures 4.18 and 4.19. As seen from the cooling curve 2 mm section is cooling faster than the 4 mm section due to its high surface to volume ratio. Solid fraction vs time graph is in a good agreement with the cooling curve. When the 2 mm section reaches to 100 % solid state, 4 mm section is still 30 % liquid. Solidification of thin region is faster than some thicker region in the same

casting part in the same manufacturing cycle. Therefore grain size of 2 mm section is expected to be smaller that that of 4 mm section. Average grain size of the samples are published in table 4.9. Average grain size of 2 mm section samples are 9.57 ± 0.56 µm whereas, grain size of 4 mm section samples are 12,46 ± 0.74 µm. The grain sizes were found to be as expected and close to the ones in reference [61]. Effect of smaller grain size and lower porosity of 2 mm section samples, makes mechanical properties of 2 mm samples better than that of 4 mm samples.

Table 4.9 : Average grain sizes of samples from cast part 2

section size (mm)	T_m (°C)	average grain size (µm)
2	685	9.57 ± 0.56
4	685	12.46 ± 0.74

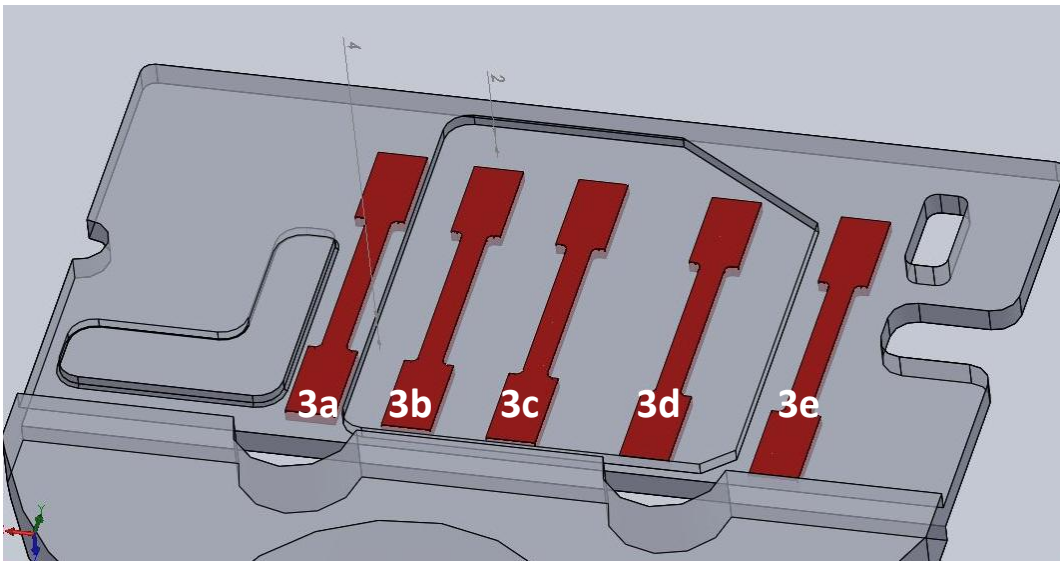

Figure 4.19 : Location of tensile test samples in cast part 2

Tensile test samples are machined from the 2 and 4 mm sections of the cast part 2 directly by CNC machining. Figure 4.19 shows the locations of the tensile test specimens on the cast part. Specimens are represented by 3a to 3e from left to right. 3a and 3e are 4 mm samples, which have 125.26 ± 31.06 MPa average 0.02 proof strength, 173,80 ± 22.45 MPa average ultimate tensile strength, and

6,54 ± 1.53% elongation. On the other hand the average 0.02 proof strength of 2 mm samples are 156.51 ± 47.85 MPa which is almost 30 MPa higher that that of 4 mm samples. UTS of 2 mm samples are 197.70 ± 35.29 MPa, which is also 30 MPa higher. Elongation is 6.02 ± 2.59 % which is decreased from 6.54 ± 1.53 % by decreasing section size. It is expected that increasing section thickness increases the elongation due to enhancing of mechanical properties. That result may arise because location of specimen 3d is just above the bore of the runner and a turbulence may occur in that region which can lower the mechanical properties. Fluid flow in the casting part can be seen in figure 4.20 emphasizing turbulence. Another reason of low mechanical properties of sample 3d may be the local temperature of the die. If the temperature of the die at that point was low during casting then the at this point liquid solidifies and only let fluid flow pass around the solidified zone which also causes turbulence and thus porosity.

From the results it can be said that thickness has a significant effect on $\sigma_{0.2}$, and UTS in the same casting part. As the thickness decreases, 0.2 % proof strength and UTS increases [24][61][73]. Thickness do not play an important role on the amount of elongation.

The grain sizes and mechanical test results are close to the ones in the literature, however there are no studies in the literature which have the same casting parameters with the casting parameters of this study. Taking a result without considering the casting parameters does not make sense for complicated processes like high pressure die casting. Only relative results such as; increasing elongation or decreasing strength when altering a process parameter are meaningful.

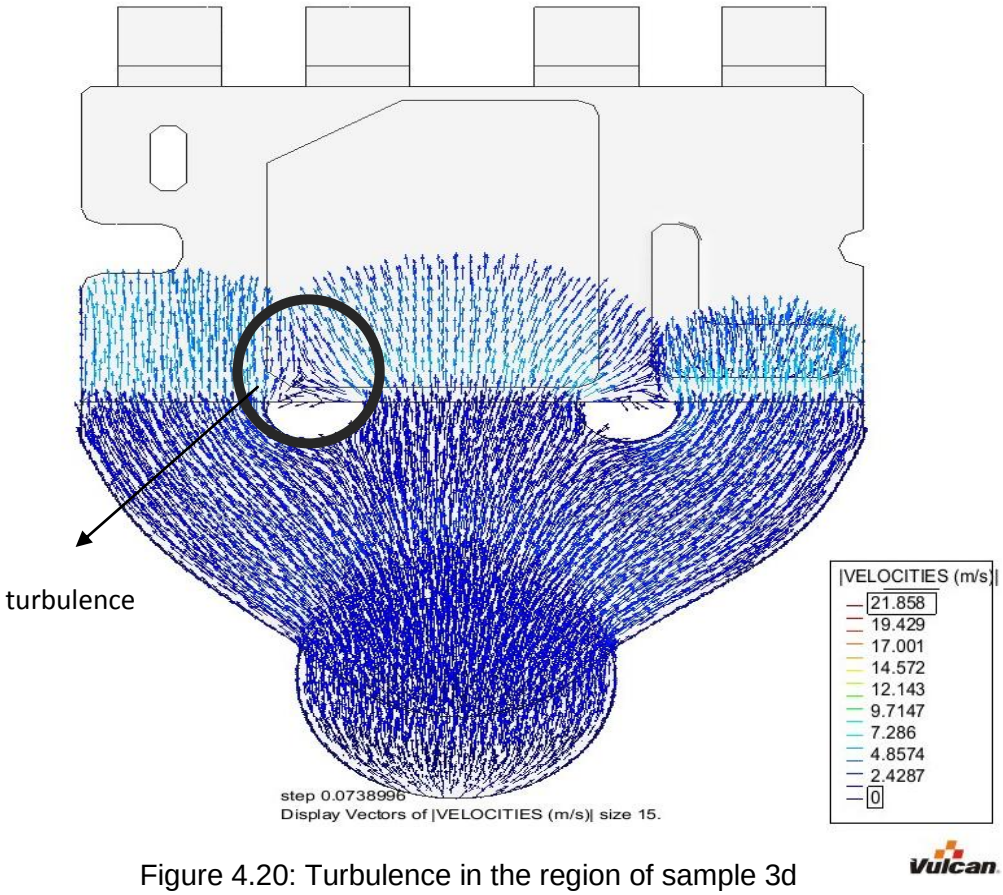

Figure 4.20: Turbulence in the region of sample 3d

Table 4.10 : Mechanical properties of cast part 2

sample	T_m (°C)	thickness (mm)	$\sigma_{0.2}$ (MPa)	UTS (MPa)	elongation (%)
3a	685	4	103.29	157.92	5.46
3e	685	4	147.22	189.67	7.62
average	685	4	125.26	173.8	6.54
3b	685	2	-	212.73	6.83
3c	685	2	190.35	222.98	8.11
3d	685	2	122.68	157.38	3.12
average	685	2	156.51	197.7	6.02

The effect of melting temperature, and position in the die cavity on the mechanical properties are investigated with cast part 3 samples. Tensile test specimens machined from the cast part can be seen in figure 4.21. It is clearly seen from the

cooling curve that the T_m =645 ºC are cooling faster that T_m =675 ºC specimens, which is a straightforward result. Faster cooling will yield to small grain size. Grain sizes are published in table 4.11 for cast part 3. As T_m decreases from 675 ºC to 645 ºC grain size of gate sections decreases from 16.43 ± 0.95 to 13.13 ± 0.84 µm. At the same time grain size of overflow sections decreases from 14.12 ± 1.02 to 11.05 ± 0.77 µm. Porosity investigation for this casting procedure gives low fraction of porosity for T_m 645 ºC. T_m 645 ºC sample with small grain size and lower porosity should have superior mechanical properties when compared to T_m 675 ºC samples.

As expected 0.2 % proof strength and ultimate tensile strength of T_m 675 ºC are lower than T_m 645 ºC samples. Data can be seen in table 4.12. $\sigma_{0.2}$ decreases from 105.65 ± 4.72 to 101.23 ± 4.01 MPa for gate sections, whereas it almost remains constant for overflow sections. A similar behaviour can be seen for UTS values. Increasing T_m form 645 to 675 ºC, decreases UTS from 202.79 ± 14.07 to 180.40 ± 18.87 MPa for gate sections. Whereas it almost remains constant for overflow sections. Elongation values decrease as porosity content increases. Decrease of elongation is due to the notch effect of pores.

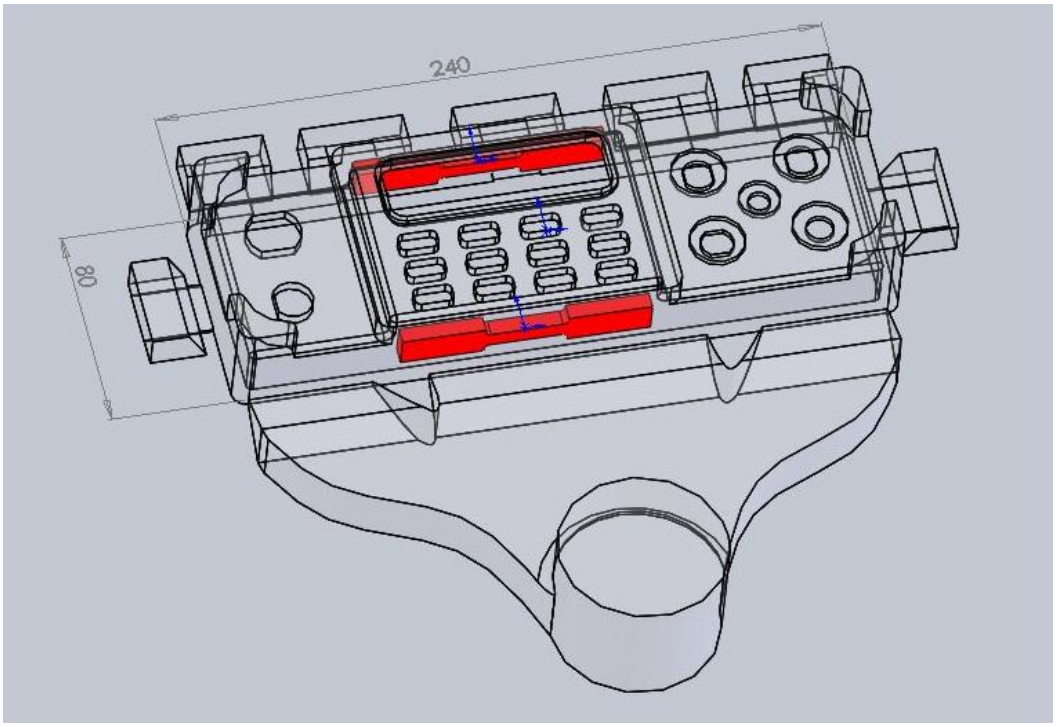

Figure 4.21 : Location of tensile test samples from cast part 3

Position in the die cavity has an effect both on porosity and grain size. The reason of the effect of position on grain size can be interpreted easily from the cooling curve in figure 4.22 In the figure, it is seen that the blue curve being the curve of T_m 675 °C gate section cools slowest, which is followed by the green curve being the curve of T_m 645 °C gate section. There is a slight difference between these two curves. Another slight difference is between the yellow curve of T_m 675 °C overflow and red curve of T_m 645 °C overflow sections. These two groups are separated by a significant amount.

T_m 675 °C gate section has the largest grain size by 16.43 ± 0.95 µm. T_m 675 °C overflow section, and T_m 645 °C gate section has 14.12 ± 1.02 and 13.13± 0.84 µm grain sizes respectively. T_m 645 °C overflow section has the smallest grain size by 11.05 ± 0.77 µm.

According to the cooling curve obtained from casting simulation software, grain size sequence from larger to smaller should be T_m 675 °C gate section, T_m 645 °C gate section, and other two samples with similar grain sizes. However that is not the case, that grain size difference may arise from the uncontrolled die temperature. Die temperature is tried to kept constant at 200 °C by heating the die at every 15 to 20 casting cycles. Correct die temperature control should be done by transferring hot liquid inside the cooling channels of the die set, unfortunatelly the die set do not contain such channels. It can be said that cooling curves obtained from the casting simulation software gives an identication for grain sizes only for the sections or parts manufactured in the same die with the same die temperature.

The most significant effect on mechanical properties is the effect of position in the die cavity. The cooling curve revals the large difference between cooling behaviours of gate and overflow sections. Grain sizes decreases when going far from the gate to overflows. 13.13 ± 0.84 decreases to 11.05 ± 0.77 µm for T_m 645 °C samples on the other hand, 16.43± 0.95 decreases to 14.12 ± 1.02 µm for T_m 675 °C specimens. According to grain sizes it can be said that overflow sections will show higher mechanical properties. However that is not the case, all $\sigma_{0.2}$, UTS, and elongation values decreases in overflow sections. For T_m 645 °C samples $\sigma_{0.2}$, UTS, and elongation values are respectively 96.74 ± 8.44 MPa, 127.95 ± 15.93 MPa, and 2.65 ±0.74 % in overflow sections. At the same casting temperature in gate sections $\sigma_{0.2}$, UTS, and elongation values are respectively 105.65 ± 4.72 MPa, 202.79±14.07MPa, and 9.13± 1.89 %. For overflow sections of T_m 675 °C samples

$\sigma_{0.2}$, UTS, and elongation values are respectively 97.45 ± 4.42 MPa, 129.65±15.97 MPa, and 3,03 ± 0.89 %. Whereas the gate sections have 101.23 ± 4.01 MPa $\sigma_{0.2}$, 180.40 ± 18.87 MPa UTS, and 7.55 ± 2.79 % elongation. Therefore it can be said that the most significant factor effecting mechanical properties is not the grain size, but the porosity content. Increasing the porosity only by small amount detoriates UTS, and elongation of the high pressure die cast parts.

Table 4.11: Average grain sizes of samples from cast part 3

section	T_m (ºC)	average grain size (µm)
gate	645	13.13 ± 0.84
overflow	645	11.05 ± 0.77
gate	675	16.43 ± 0.95
overflow	675	14.12 ± 1.02

Table 4.12: Mechanical properties of cast part 3 from Mg AZ91alloy

sample #	section	T_m (°C)	thickness (mm)	$\sigma_{0.2}$	UTS (MPa)	elongation (%)
5	gate	645	5.5	109.44	209.77	9.33
6	gate	645	5.5	100.36	186.59	7.14
7	gate	645	5.5	107.15	212	10.92
average		645	5.5	105.65	202.79	9.13
8	overflow	645	5.5	91.24	113.52	1.82
9	overflow	645	5.5	106.45	145.05	3.24
10	overflow	645	5.5	92.52	125.29	2.89
average		645	5.5	96.74	127.95	2.65
11	gate	675	5.5	105	167.5	5.37
12	gate	675	5.5	101.67	171.65	6.59
13	gate	675	5.5	97.02	202.06	10.68
average		675	5.5	101.23	180.4	7.55
14	overflow	675	5.5	99.01	137.93	3.34
15	overflow	675	5.5	92.46	111.24	2.02
16	overflow	675	5.5	100.88	139.77	3.72
average		675	5.5	97.45	129.65	3.03

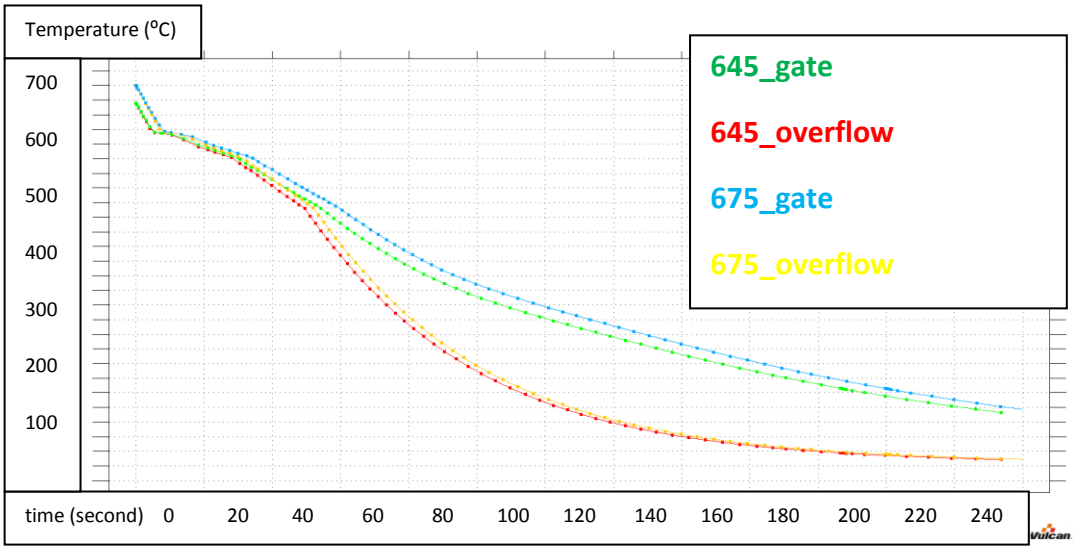

Figure 4.22 : Cooling curve of different sections of T_m 645 °C and T_m 675 °C of cast part 3

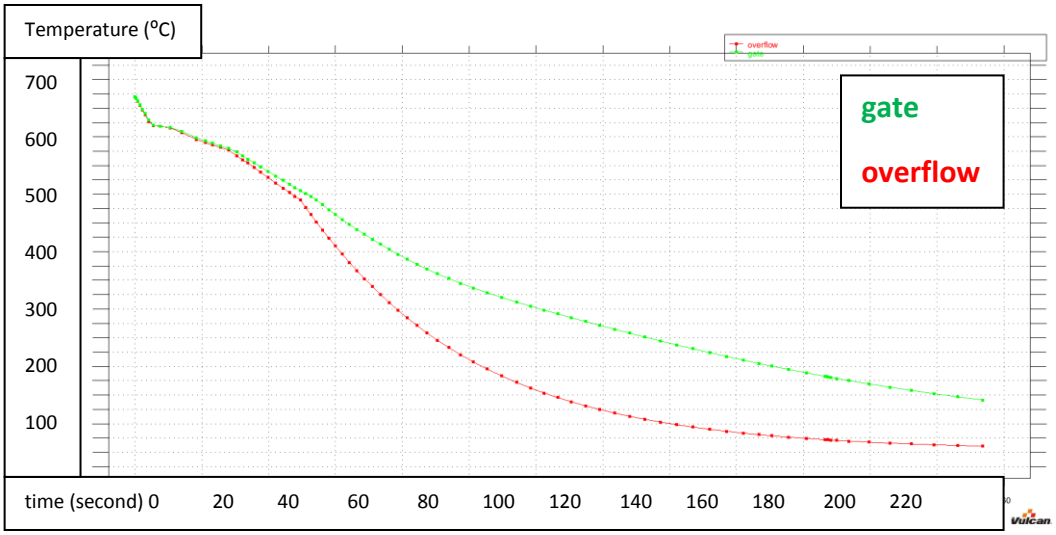

Figure 4.23 : cooling curve of cast part 3, T_m=645 °C

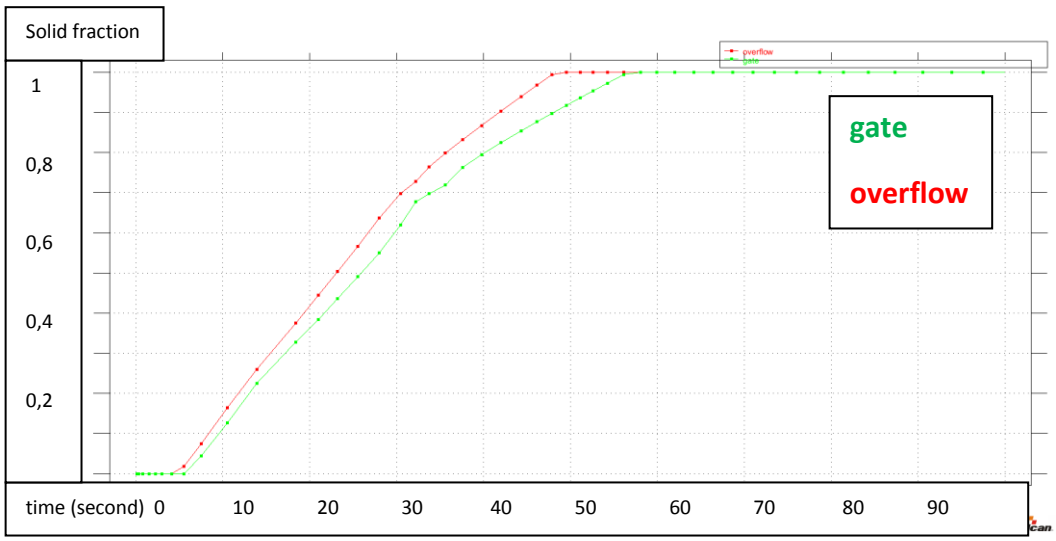

Figure 4.24 : Solid fraction vs time of cast part 3, T_m=645 °C

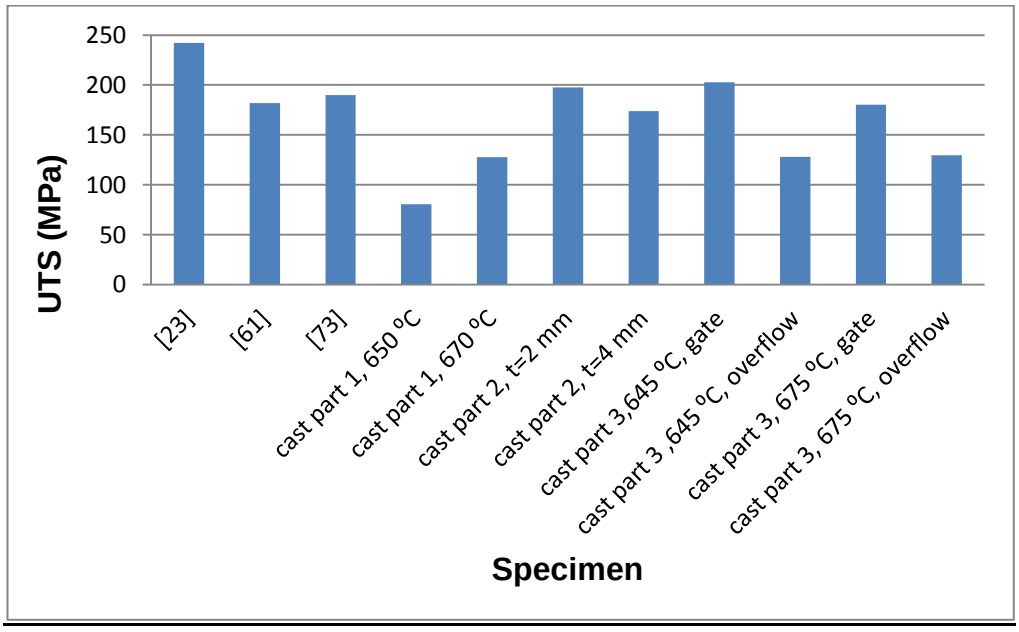

Figure 4.25 : Comparison of UTS with literature data

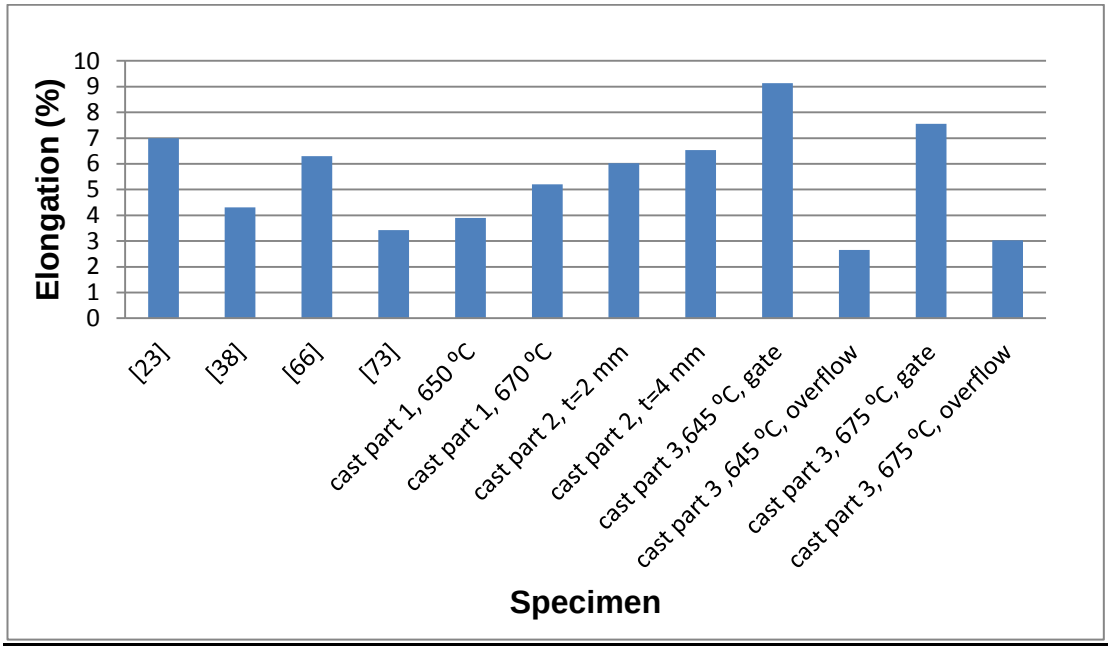

Figure 4.26 : Comparison of elongation with literature data

Figure 4.25 compares the literature data with the UTS values of this study. As thickness of the cast part being a decisive factor on mechanical properties, only the results of thin hpdc parts are taken into account. Thickness of the specimens in references [23], [61], and [73] are 6, 4.5, and 5 mm. Cast part 1 shows very low UTS values, the reasons of which is explained before. UTS of cast part 2 and gate sections of cast part 3 are close to the literature values. UTS of overflow sections are lower thatn 150 MPa. In Figure 4.26 elongation values are compared with the ones in the literature. It should be noted that the elongation values are tabulated without considering the process conditions, and thickness of the specimens as there are not adequate research on elongation of hpdc Mg AZ91 alloys. It can be said that gate sections of cast part 3 specimens reveal the highest elongation values because of the low porosity content near the gate section. On the contrary, overflow section of the same cast parts show the lowest values.

Cast part 3 was also manufactured by using Al alloy A.413 as raw material to compare the mechanical properties of high pressure die cast Al and Mg alloys. Tensile specimens were also machined from the same regions as the Mg samples. It can be seen from the table 4.13 that the effect of position of the specimen inside the die cavity on $\sigma_{0.2}$, and elongation is negligible for Al die casting alloys, only the effect on UTS can be pronounced. UTS of gate section is 212.99±15.89 MPa wheras UTS of overflow section is 195.28±3.66 MPa. Average of gate and overflow sections can assumed to be the UTS of the cast part. Therefore UTS of Al specimen is 204.14±13.89 MPa.

Casting the magnesium alloy with optimum T_m , which is 645 °C for cast part 3, comparable UTS values could be obtained. In today's competing industry weight reduction is a key factor for mobile applications such as automotive, and consumer electronics. 33 % weight reduction $(\frac{\rho_{A:413} - \rho_{AZ91}}{\rho_{A.413}} * 100)$ with comparable mechanical properties can be obtained by casting with magnesium alloys in exchange of aluminium alloys.

Table 4.13: Mechanical properties of cast part 3 from Al A.413 alloy

sample #	section	T_m (°C)	thickness (mm)	$\sigma_{0.2}$ (MPa)	UTS (MPa)	elongation (%)
1	gate	optimum	5.5	123.49	224.23	3.51
2	gate	optimum	5.5	117.25	201.75	3.05
average		optimum	5.5	120.37	212.99	3.28
3	overflow	optimum	5.5	116.11	192.7	2.95
4	overflow	optimum	5.5	113.4	197.87	3.41
average		optimum	5.5	114.75	195.28	3.18

CHAPTER 5

CONCLUSION and SUGGESTIONS

5.1 Conlusions

1. Piston speeds are very determining parameters in filling of the die cavity. In order to obtain proper filling and sound cast parts, piston speeds should be calculated using the equations in the literature and checked by using a casting simulation analysis software. If the piston speeds are low, filling of the die cavity enhances by increasing melt temperature of the alloy. However, low melting temperatures should be used at optimum piston speeds to decrease gas related porosity.

2. Filling simulation of a cast part can reveal many potential defects before machining the die. Turbulences causing surface inhomogenities, improper filling of the die cavity, possible shrinkage porosities can be detected beforehand. Final geometry of the die should be decided using a casting simulation software, which can save both money, and time.

3. The microstructure of the high pressure die cast magnesium AZ91 alloys show a divorced eutectic morphology. Eutectic phase surrounds whole microstructure including primary and eutectic magnesium regions with β - $Mg_{17}Al_{12}$.

4. Position in the die cavity is an effect when considering the amount of porosity. Total porosity of the cast parts increase, as going from the gating to the overflows. Porosity amount is higher in overflow sections than gate sections in the same cast parts. Porosity amount is also affected by thickness of the specimen. Increasing section thickness increases porosity amount. Melt temperature is the other important factor affecting porosity content. Higher melt temperatures increase the porosity amount due to the dissolved gases present in the melt. Melt temperature should be selected 30 to 50 °C above the melting temperature of the alloy.

5. Cooling curves are obtained from Vulcan casting simulation software and they are used to estimate the grain sizes. The grain sizes are small when the solidification rate is high, and large grain sizes can be seen when the solidification rate is low. Cooling curves reveal slower solidification rate in gate sections than overflow sections in the same cast part. Therefore grain sizes are larger in gate sections. Thickness is another key factor determining grain size. Thicker parts solidify slower than thinner parts according to the cooling curves, which yields larger grain size.

6. Mechanical properties of the cast parts are mainly affected by the grain size and porosity content. In order to obtain improved mechanical properties smaller grain size and low porosity content should be satisfied. The results of this thesis also indicate that dependency of mechanical properties to porosity are more dominant than the dependency of grain size.

7. Casting Mg alloys in exchange of Al alloys decrease weight of the sample by 33 %. At the same time UTS of the cast part decreases slightly. Mg alloys can be used to decrease the weight of components which do not carry high loads.

5.2 Suggestions for Future Work

1. Obtained cooling curves from the casting simulation software can be checked by positioning thermocouples to the proper locations of the die cavity.

2. The amount of tensile test samples should be increased for further work. However, it is not always possible to take specimens from mass production parts.

3. Effect of melt temperature can be investigated by choosing four different temperatures which are 15, 30, 60, 90 °C higher than melting temperature of the alloy.

REFERENCES

[1] NADCA, *NADCA Product Specification Standarts for Die Casting*. 2009, pp. 1-44.

[2] A. Hamasaiid, G. Dour, M. Dargusch, T. Loulou, C. Davidson, and G. Savage, "Heat-Transfer Coefficient and In-Cavity Pressure at the Casting-Die Interface during High-Pressure Die Casting of the Magnesium Alloy AZ91D," *Metallurgical and Materials Transactions A*, vol. 39, no. 4, pp. 853-864, Feb. 2008.

[3] B. Andersen, *Die Casting Engineering*, vol. 84. Marcel Dekker, 2005, p. 384.

[4] F. Knell and A. A. Koch, *ASM handbook vol 15. Casting*, vol. 15, no. January. 1992, pp. 1- 1289.

[5] K. Fuchs, "HOT-WORK TOOL STEELS WITH IMPROVED PROPERTIES FOR DIE CASTING APPLICATIONS," *Main*, pp. 17-26.

[6] M. I. Khan, Y. Frayman, and S. Nahavandi, "MODELLING OF POROSITY DEFECTS IN HIGH PRESSURE DIE CASTING WITH A NEURAL NETWORK," *Methodology*, pp. 1-6.

[7] B. Mordike and T. Ebert, "MagnesiumProperties — applications — potential," *Materials Science and Engineering A*, vol. 302, no. 1, pp. 37-45, Apr. 2001.

[8] R. Helenius, O. Lohne, L. Arnberg, and H. I. Laukli, "The heat transfer during filling of a high-pressure die-casting shot sleeve," *Materials Science and Engineering: A*, vol. 413-414, pp. 52-55, Dec. 2005.

[9] M. Sirviö, "Complete Simulation of High Pressure Die Casting Process," pp. 1-7.

[10] A. Fischersworring-bunk, C. Landerl, A. Fent, and J. Wolf, "The New BMW Inline Six-cylinder Composite Mg / Al Crankcase."

[11] T. Altan, B. Lilly, and Y. Yen, "Manufacturing of Dies and Molds," *CIRP Annals - Manufacturing Technology*, vol. 50, no. 2, pp. 404-422, 2001.

[12] X. Niu, "Vacuum assisted high pressure die casting of aluminium alloys," *Journal of Materials Processing Technology*, vol. 105, no. 1-2, pp. 119-127, Sep. 2000.

[13] S. G. Lee, G. R. Patel, a M. Gokhale, a Sreeranganathan, and M. F. Horstemeyer, "Quantitative fractographic analysis of variability in the tensile ductility of high-pressure die-cast AE44 Mg-alloy," *Materials Science and Engineering: A*, vol. 427, no. 1-2, pp. 255-262, Jul. 2006.

[14] E. Gariboldi, F. Bonollo, and M. Rosso, "PROPOSAL OF A CLASSIFICATION OF DEFECTS OF HIGH-PRESSURE DIECAST PRODUCTS," pp. 39-46, 2007.

[15] S. G. Lee and a M. Gokhale, "Formation of gas induced shrinkage porosity in Mg-alloy high-pressure die-castings," *Scripta Materialia*, vol. 55, no. 4, pp. 387-390, Aug. 2006.

[16] M. Kobayashi, Y. Dorce, and H. Toda, "effect of local volume fraction of microporosity on tensile properties in Al-Si-Mg alloys," *Materials Science and Technology*, vol. 26, no. 8, pp. 962 -967, 2010.

[17] S. R. Agnew, K. C. Liu, E. A. Kenik, and S. Vİswanathan, "DIE CAST MAGNESIUM ALLOY AM60B," *Magnesium Technology 2000*, pp. 285 - 290, 2000.

[18] J. R. Brown, *Foseco Non-Ferrous Foundryman's Handbook*. 2004, pp. 1- 295.

[19] R. G. Bowler, "The risk of flourisis in magnesium foundries," *Journal of Industrial Medicine*, vol. 246, no. 4, pp. 111-122, Sep. 1947.

[20] a K. Dahle, "Development of the as-cast microstructure in magnesium–aluminium alloys," *Journal of Light Metals*, vol. 1, no. 1, pp. 61-72, Feb. 2001.

[21] S. Otarawanna, C. M. Gourlay, H. I. Laukli, and a K. Dahle, "Transactions of The Indian Institute of Metals Microstructure formation in high pressure die casting," *Transactions of the Indian Institute of Metals*, vol. 62, no. October, pp. 499-503, 2009.

[22] C. J. Bettles, C. T. Forwood, D. S. Jones, and J. R. Griffiths, "AMC-SC1 : A New Magnesium Alloy Suitable for Powertrain Applications," *High Temperature*, 2003.

[23] E. Aghion, N. Moscovitch, and A. Arnon, "Mechanical Properties of Die-Cast Magnesium Alloy MRI 230D," *Journal of Materials Engineering and Performance*, vol. 18, no. 7, pp. 912-916, Nov. 2008.

[24] M. R. Notis and J. R. Brown, *ASM HANDBOOK VOL 3 Alloy Phase Diagrams*. 1992, pp. 1- 1921.

[25] G. V. Raynor, *The physical metallurgy of magnesium and its alloys*. 1959, pp. 1 - 564.

[26] R. N. Lumley, R. G. O. Donnell, D. R. Gunasegaram, M. Gershenzon, A. C. Yob, and I. J. Polmear, "The role of alloy composition in the heat treatment of aluminium high pressure die castings," *Science And Technology*, vol. 26, pp. 0-9, 2008.

[27] M. C. Flemings, *Solidification Process*, vol. 3, no. 2008. 1974, pp. 1- 705.

[28] W. Kurz and D. J. Fisher, *Fundementals of Solidification*. 1998.

[29] A. Ohno, *Solidification ; The Separation Theory and Its Practical Applications*. Springer-Verlag, 1987.

[30] R. T. Southin, "Transactions of AIME," *Transactions of AIME*, vol. 239, pp. 220 -225, 1966.

[31] B. Chalmers, "a theory on solidification," *J. Australian Institute of Materials*, vol. 8, pp. 255 - 263, 1963.

[32] H. I. Laukli, *High Pressure Die Casting of Aluminium and Magnesium Alloys - Grain Structure and Segregation Characteristics*, no. April. 2004.

[33] W. C. Winegard and B. Chalmers, "a new approach on nucleation," in *Transactions of ASM*, 1954, pp. 1214 - 1224.

[34] D. H. StJohn, a K. Dahle, T. Abbott, and M. D. Nave, "Solidification of cast magnesium alloys," *Magnesium*, no. 55, 2003.

[35] D. H. StJohn, M. A. Qian, M. Easton, P. Cao, and Z. O. Ë. Hildebrand, "Grain Refinement of Magnesium Alloys II . GRAIN REFINEMENT OF MAGNESIUM TECHNICAL STATUS," *Metallurgical and Materials Transactions A*, vol. 36, no. July, pp. 1669-1679, 2005.

[36] M. D. Nave, a K. Dahle, and D. H. StJohn, "Eutectic growth morphologies in Magnesium Aluminium alloys," in *Magnesium Technology 2000*, 2000, pp. 233 - 244.

[37] P. Ebner, "Magnesium Technology 2002 Edited by H . I . Kaplan TMS (The Minerals , Metals & Materials Society), 2002," in *Magnesium Technology 2002*, 2002, pp. 22-28.

[38] D. G. L. Prakash and D. Regener, "Quantitative characterization of Mg17Al12 phase and grain size in HPDC AZ91 magnesium alloy," *Journal of Alloys and Compounds*, vol. 461, no. 1-2, pp. 139-146, Aug. 2008.

[39] G. Song, "Influence of microstructure on the corrosion of diecast AZ91D," *Corrosion Science*, vol. 41, no. 2, pp. 249-273, Feb. 1998.

[40] V. Y. Gertsman, J. Li, S. Xu, J. P. Thomson, and M. Sahoo, “Microstructure and second-phase particles in low- and high-pressure die-cast magnesium alloy AM50,” *Metallurgical and Materials Transactions A*, vol. 36, no. 8, pp. 1989-1997, Aug. 2005.

[41] I. J. Polmear, *Light Alloys : Metallurgy of Light Metals*. J.Wiley & Sons, 1995, p. 362.

[42] J. Cai, G. Ma, Z. Liu, H. Zhang, and Z. Hu, “Influence of rapid solidification on the microstructure of AZ91HP alloy,” *Journal of Alloys and Compounds*, vol. 422, no. 1-2, pp. 92-96, Sep. 2006.

[43] R. Ambat, N. N. Aung, and W. Zhou, “Studies on the in ¯ uence of chloride ion and pH on the corrosion and electrochemical behaviour of AZ91D magnesium alloy,” *Journal of Applied Electrochemistry*, pp. 865-874, 2000.

[44] K. Y. Sohn, S. A. Allison, and J. W. Johns, “Manganese containing inclusions in LPDC AM50 alloys,” in *Magnesium Technology 2000*, no. 815, pp. 50-52.

[45] M. T. Perez Prado and O. A. Ruano, “Texture evolution during annealing of magnesium AZ31 alloy,” *Acta Materialia*, vol. 46, no. 2, pp. 149 - 155, 2002.

[46] W. Baldwin, “Metallography and Microstructures 2004 ASM,” *Managing*, 2004.

[47] E. Aghion and N. Lulu, “The effect of skin characteristics on the environmental behavior of die cast AZ91 magnesium alloy,” *Journal of Materials Science*, vol. 44, no. 16, pp. 4279-4285, Jun. 2009.

[48] W. P. Sequeira, G. L. Dunlop, and M. T. Murray, “Effect of section thickness on mechanical properties high pressure die cast of magnesium alloy AZ91D,” in *Proceedings of the third international magnesium conference*, 1997, pp. 66 - 73.

[49] A. L. Bowles, J. R. Griffiths, and C. J. Davidson, “Ductility and the skin effect in high pressure die cast Mg-Al alloys,” in *TMS annual meeting*, 2001, vol. 67, pp. 161 -168.

[50] Z. W. Chen, “Skin solidification during high pressure die casting of Al-11Si-2Cu-1Fe alloy,” *Materials Science and Engineering A*, vol. 348, no. 2, pp. 145 - 153, 2003.

[51] C. M. Gourlay, a K. Dahle, and H. I. Laukli, “Segregation band formation in Al-Si die castings,” *Metallurgical and Materials Transactions A*, vol. 35, no. 9, pp. 2881-2891, Sep. 2004.

[52] N. A. El-Mahallawy, M. a Taha, E. Pokora, and F. Klein, “On the influence of process variables on the thermal conditions and properties of high pressure

die-cast magnesium alloys," *Journal of Materials Processing Technology*, vol. 73, no. 1-3, pp. 125-138, Jan. 1998.

[53] Z. W. Chen and M. Z. Jahedi, "Die erosion and its effect on soldering formation in high pressure die casting of aluminium alloys," *Materials & Design*, vol. 20, no. 6, pp. 303 - 309, 1999.

[54] W. P. Sequeira, G. L. Dunlop, and M. T. Murray, "effect of section thickness and gate velocity on the microstructure and mechanical properties of high pressure die cast AZ91 alloys," in *TMS annual meeting*, 1997, pp. 169 -183.

[55] C. M. Gourlay, H. I. Laukli, and a K. Dahle, "Defect Band Characteristics in Mg-Al and Al-Si High-Pressure Die Castings," *Metallurgical and Materials Transactions A*, vol. 38, no. 8, pp. 1833-1844, Jul. 2007.

[56] C. D. Lee and K. S. Shin, "Effect of microporosity on the tensile properties of AZ91 magnesium alloy," *Acta Materialia*, vol. 55, no. 13, pp. 4293-4303, Aug. 2007.

[57] J. Weiler, J. Wood, R. Klassen, E. Maire, R. Berkmortel, and G. Wang, "Relationship between internal porosity and fracture strength of die-cast magnesium AM60B alloy," *Materials Science and Engineering A*, vol. 395, no. 1-2, pp. 315-322, Mar. 2005.

[58] D. G. L. Prakash, D. Regener, and W. J. J. Vorster, "Microscopic failure modes of hpdc AZ91HP magnesium alloy under monotonic loading," *Materials Science and Engineering: A*, vol. 488, no. 1-2, pp. 303-310, Aug. 2008.

[59] S. G. Lee, a M. Gokhale, G. R. Patel, and M. Evans, "Effect of process parameters on porosity distributions in high-pressure die-cast AM50 Mg-alloy," *Materials Science and Engineering: A*, vol. 427, no. 1-2, pp. 99-111, Jul. 2006.

[60] Y.-hui Wei, L.-feng Hou, L.-jing Yang, B.-she Xu, M. Kozuka, and H. Ichinose, "Microstructures and properties of die casting components with various thicknesses made of AZ91D alloy," *Journal of Materials Processing Technology*, vol. 209, no. 7, pp. 3278-3284, Apr. 2009.

[61] C. D. Lee, "Tensile properties of high-pressure die-cast AM60 and AZ91 magnesium alloys on microporosity variation," *Journal of Materials Science*, vol. 42, no. 24, pp. 10032-10039, Sep. 2007.

[62] D. G. L. Prakash and D. Regener, "Quantitative Characterization of Pore Arrangement in Pore Bands in Pressure Die Cast AZ91 Magnesium Alloy by Image Processing," *Materials Science Forum*, vol. 514-516, pp. 1477-1482, 2006.

[63] D. G. Leo Prakash and D. Regener, “Micro–macro interactions and effect of section thickness of hpdc AZ91 Mg alloy,” *Journal of Alloys and Compounds*, vol. 464, no. 1-2, pp. 133-137, Sep. 2008.

[64] S. G. Lee, G. R. Patel, a M. Gokhale, a Sreeranganathan, and M. F. Horstemeyer, “Variability in the tensile ductility of high-pressure die-cast AM50 Mg-alloy,” *Scripta Materialia*, vol. 53, no. 7, pp. 851-856, Oct. 2005.

[65] a K. Dahle and D. H. StJohn, “Rheological behaviour of the mushy zone and its effect on the formation of casting defects during solidification,” *Acta Materialia*, vol. 47, no. 1, pp. 31-41, Dec. 1998.

[66] D. Rodrigo, M. T. Murray, and H. Mao, “Effect of section size and microstructural features on the mechanical properties of die cast AZ91D and AM60B magnesium alloy test bars,” in *SAE international Congress, Magnesium session*, 1999.

[67] P. Fu et al., “Low-pressure die casting of magnesium alloy AM50: Response to process parameters,” *Journal of Materials Processing Technology*, vol. 205, no. 1-3, pp. 224-234, Aug. 2008.

[68] C. Caceres, W. Poole, a Bowles, and C. Davidson, “Section thickness, macrohardness and yield strength in high-pressure diecast magnesium alloy AZ91,” *Materials Science and Engineering: A*, vol. 402, no. 1-2, pp. 269-277, Aug. 2005.

[69] C. Caceres, C. Davidson, J. R. Griffiths, and C. Newton, “Effects of solidification rate and ageing on the microstructure and mechanical properties of AZ91 alloy,” *Materials Science and Engineering A*, vol. 325, no. 1-2, pp. 344-355, Feb. 2002.

[70] C. Caceres, J. R. Griffiths, a Pakdel, and C. Davidson, “Microhardness mapping and the hardness-yield strength relationship in high-pressure diecast magnesium alloy AZ91,” *Materials Science and Engineering: A*, vol. 402, no. 1-2, pp. 258-268, Aug. 2005.

[71] C. Pitsaris, T. Abbott, C. Davies, and G. Savage, “Influence of Process Parameters on the Microstructure and Mechanical Properties of Magnesium Die Castings,” in *Magnesium: Proceedings of the 6th International Conference Magnesium Alloys and Their Applications*, 2005, p. chapter 110.

[72] D. G. L. Prakash and D. Regener, “Microstructural Influences on Tensile Properties of hpdc AZ91 Mg Alloy,” *Materials Science*, pp. 9-11.

[73] D. G. Leo Prakash, D. Regener, and W. J. J. Vorster, “Effect of position on the tensile properties in high-pressure die cast Mg alloy,” *Journal of Alloys and Compounds*, vol. 470, no. 1-2, pp. 111-116, Feb. 2009.

[74] M. Chiumenti, C. Agelet de Saracibar, and M. Cervera, “On the Numerical Modeling of the Thermomechanical Contact for Metal Casting Analysis,” *Journal of Heat Transfer*, vol. 130, no. 6, p. 061301, 2008.